MEDICAL UNIVERSITY OF VIENNA

Lymphotoxin Beta Receptor Deficiency Expands the Spectrum of NF-κB Related Inborn Errors of Immunity

Doctoral thesis at the Medical University of Vienna
for obtaining the academic degree

Doctor of Philosophy

Submitted by

Dr. med. Univ. Bernhard Ransmayr

Supervisor:
Prof. Dr. med. Kaan Boztug, MBA

St. Anna Children's Cancer Research Institute (CCRI)
Zimmermannplatz 10, 1090 Vienna, Austria
Medical University of Vienna, Department of Pediatrics and Adolescent Medicine, Vienna, Austria
CeMM Research Center for Molecular Medicine of the Austrian Academy of Sciences, Vienna, Austria

Vienna, August 2025

DECLARATION

This doctoral thesis is based on a primary research article authored by the candidate and published during the course of the doctoral studies. The thesis centers on this publication, which appeared in *Science Immunology* on November 22, 2024, and is included in Chapter 2. The publication resulted from a collaborative effort involving multiple laboratories. Most of the data presented was generated by the author of this thesis in the laboratory of Prof. Kaan Boztug, initially located at the CeMM Research Center for Molecular Medicine of the Austrian Academy of Sciences and later relocated to the St. Anna Children's Cancer Research Institute (CCRI). The individual contributions from the candidate and the co-authors are detailed in the publication.

In addition, the thesis includes contextual and interpretative sections that reference and integrate findings from a broad body of related scientific literature. All chapters of the thesis were written by the author, with critical input and guidance provided by Prof. Kaan Boztug. The thesis does not contain any AI-generated text. Grammarly was used throughout the thesis for grammar and spelling correction.

TABLE OF CONTENTS

LIST OF FIGURES

ABSTRACT

Genetic immune disorders often lead to severe infections and immune dysfunction early in childhood, which, due to their complexity, rarity, and often need for clinical intervention, pose a significant challenge for patients, families, and physicians. Yet, studying the immune dysregulation in these patients enables us to identify critical components and mechanisms of the human immune response, thereby enriching our understanding of immunity in both health and disease and subsequently increasing our chances of developing improved therapies for these and other, more common, conditions.

In this study, we investigated three patients from two families with a novel genetic defect impacting the secondary lymphoid organ (SLO) compartment, resulting in a distinct inborn error of immunity. We identified biallelic loss-of-function mutations in *LTBR* encoding the lymphotoxin beta receptor (LTβR), primarily expressed on stromal cells. We show that LTβR signaling is crucial for SLO development in humans, as evident by the functional hyposplenism, absent tonsils, and complete lymph node aplasia in these patients. SLOs create specialized microenvironments where stromal and immune cells interact to initiate adaptive immune responses and promote B-cell differentiation. Subsequently, LTβR-deficient patients had hypogammaglobulinemia and diminished memory B cells, which collectively led to recurrent infections.

Furthermore, we have shown that B-cell differentiation in an ex vivo co-culture system was intact, implying that the observed B-cell defects were not intrinsic in nature and instead resulted from LTβR-dependent stromal cell interaction signaling critical for SLO formation. This is of particular significance, as it suggests that these patients are unlikely to benefit from hematopoietic stem cell transplantation, a common yet high-risk therapeutic approach for individuals with inborn errors of immunity. Instead, these patients benefit from the early initiation of immunoglobulin replacement therapy and antibiotic prophylaxis.

Recent studies have shown that the activation of LTβR signaling could have a positive effect on the outcome in various types of cancers, while the opposite seems to be the case in autoimmune diseases. The results from our study are therefore also significant for the development of pharmacological therapies in these common forms of disease.

ZUSAMMENFASSUNG

Angeborene Störungen der Immunität führen oft bereits im frühen Kindesalter zu schwerwiegenden Infektionen und Immunfehlfunktionen und stellen durch ihre Komplexität, Seltenheit und meist frühzeitig notwendigen klinischen Intervention eine große Herausforderung für Betroffene, Angehörige und Ärzte dar. Die Erforschung dieser Patienten ermöglicht es uns jedoch auch, die wichtigsten Komponenten und Mechanismen der menschlichen Immunantwort zu identifizieren. Dadurch verbessert sich unser Verständnis der Immunität in Gesundheit und Krankheit, was wiederum unsere Chancen erhöht, bessere Therapien für diese sowie auch für andere, häufigere Erkrankungen zu entwickeln.

In dieser Studie beschreiben wir drei Patienten von zwei Familien mit einem neuartigen genetischen Defekt, der die sekundären lymphatischen Organe (SLOs) beeinträchtigt und dadurch einen angeborenen Immunfehler verursacht. Wir konnten eine homozygote Mutation mit Funktionsverlust im *LTBR*-Gen nachweisen, welches den Lymphotoxin-Beta-Rezeptor (LTβR) kodiert, der hauptsächlich auf Stromazellen exprimiert wird. Unsere Ergebnisse zeigen, dass LTβR-Signale essenziell für die Entwicklung von SLOs beim Menschen sind, wie die funktionelle Hyposplenie, das Fehlen von Tonsillen und die vollständige Lymphknotenaplasie dieser Patienten verdeutlichen. SLOs bilden spezialisierte Mikroumgebungen, in denen Stromazellen und Immunzellen interagieren, um adaptive Immunantworten und die B-Zell-Differenzierung zu fördern. Folglich wiesen diese LTβR-defizienten Patienten eine Hypogammaglobulinämie und reduzierte Memory-B-Zellen auf, was zu wiederkehrenden Infektionen führte.

Wir konnten in einem neu entwickelten Zellkultursystem nachweisen, dass der Defekt in der B-Zell-Differenzierung nicht intrinsisch, sondern durch fehlende LTβR-abhängige Signale von Stromazellen bedingt ist, die für die SLO-Bildung entscheidend sind. Dies ist insofern von Bedeutung, da diese Ergebnisse darauf hindeuten, dass diese Patienten von einer hämatopoetischen Stammzelltransplantation – einer etablierten, jedoch risikoreichen Therapieform für angeborene Immunfehler – vermutlich nicht profitieren würden. Stattdessen profitieren diese Patienten von der frühen Initiierung der Immunglobulinsubstitution sowie antibiotischer Prophylaxe.

Aktuelle Studien zeigen, dass die Aktivierung des LTβR-Signalwegs bei verschiedenen Tumoren einen positiven Einfluss auf die Prognose haben kann, während sie bei Autoimmunerkrankungen negative Effekte zeigt. Unser Forschungsbeitrag ist daher auch für das Verständnis dieses Signalwegs bei häufigeren Erkrankungen von großer Bedeutung und könnte die Entwicklung neuer pharmakologischer Therapien maßgeblich unterstützen.

PUBLICATIONS ARISING FROM THIS THESIS

Bernhard Ransmayr, Sevgi Köstel Bal, Marini Thian, Michael Svaton, Cheryl van de Wetering, Christoph Hafemeister, Anna Segarra-Roca, Jana Block, Alexandra Frohne, Ana Krolo, Melek Yorgun Altunbas, Sevgi Bilgic-Eltan, Ayça Kıykım, Omer Aydiner, Selin Kesim, Sabahat Inanir, Elif Karakoc-Aydiner, Ahmet Ozen, Ümran Aba, Aylin Çomak, Gökçen Dilşa Tuğcu, Robert Pazdzior, Bettina Huber, Matthias Farlik, Stefan Kubicek, Horst von Bernuth, Ingrid Simonitsch-Klupp, Marta Rizzi, Florian Halbritter, Alexei V. Tumanov, Michael J. Kraakman, Ayşe Metin, Irinka Castanon, Baran Erman, Safa Baris, Kaan Boztug. **LTβR deficiency causes lymph node aplasia and impaired B cell differentiation**. *Sci Immunol*. 2024 Nov 22;9(101):eadq8796. doi: 10.1126/sciimmunol.adq8796. Epub 2024 Nov 22. PMID: 39576873.

ABBREVIATIONS

ADA	adenosine deaminase
AICD	activation-induced cell death
AIRE	autoimmune regulator
APC	antigen presenting cell
BAFF	B cell-activating factor
BCR	B-cell receptor
BLNK	B-cell linker
BTK	Bruton tyrosine kinase
CBC	complete blood count
CGD	chronic granulomatous disease
CTLA-4	Cytotoxic T-Lymphocyte–Associated Protein 4
DAMP	damage-associated molecular pattern
DC	dendritic cell
DcR-3	decoy receptor 3
DHR	dihydrorhodamine
G-CSF	granulocyte colony-stimulating factor
GC	Germinal center
GOF	gain-of-function
GvHD	graft-versus-host disease
GWAS	genome-wide association studies
HDR	homology-directed repair
HIES	Hyper-IgE syndrome
HLA	human leukocyte antigen
HSCT	hematopoietic stem cell transplantation
HSPC	hematopoietic stem and progenitor cell
HVEM	herpesvirus entry mediator
IBD	inflammatory bowel disease
IEI	inborn error of immunity
IFN	interferon
Ig	immunoglobulin
IgRT	immunoglobulin replacement therapy
IUIS	International Union of Immunological Societies
IVIG	intravenous immunoglobulins
JAK	Janus kinase
LAT	linker for the activation of T cells
LCK	lymphocyte cell-specific protein tyrosine kinase
LIGHT	homologous to lymphotoxin, exhibits inducible expression and competes with HSV glycoprotein D for binding to herpesvirus entry mediator, a receptor expressed on T-lymphocytes
LOF	loss-of-function
LTi	lymphoid tissue-inducer
LTβR	lymphotoxin beta receptor
MAC	membrane attack complex
MALT	mucosa-associated lymphoid tissue

MAMP microorganism-associated molecular pattern
Mreg regulatory macrophage
mTEC medullary thymic epithelial cell
MG myasthenia gravis
MHC major histocompatibility complex
MS multiple sclerosis
NALT nasopharyngeal-associated lymphoid tissue
NBT nitroblue tetrazolium
NEMO nuclear factor kappa B essential modulator
NET neutrophil extracellular trap
NFKB nuclear factor kappa B
NGS next-generation sequencing
NIK nuclear factor kappa Binducing kinase
NK natural killer cell
NLS nuclear localization signals
PD-1 programmed Cell Death Protein 1
PID Primary Immunodeficiencies
PRR pattern recognition receptor
RANK receptor activator of nuclear factor κB
RHD Rel Homology Domain
RIP1 protein kinase receptor-interacting serine/threonine-protein kinase 1
SCID severe combined immunodeficiency
SIN self-inactivating
SLE systemic lupus erythematosus
SLO secondary lymphoid organs
STAT signal transducer and activator of transcription
SYK spleen associated tyrosine kinase
TAD transactivation domain
TCR T-cell receptor
TFH T follicular helper cell
TLO tertiary lymphoid organ
TL1A tumor necrosis factor like ligand 1A
TLR toll-like receptor
TLS tertiary lymphoid structure
TNF tumor necrosis factor
TRA tissue-restricted antigen
TRAF tumor necrosis factor receptor associated factor
Treg regulatory T cell
WAS Wiskott-Aldrich syndrome
WES whole-exome sequencing
WGS whole-genome sequencing
XLA X-linked agammaglobulinemia
ZAP-70 Zeta-chain-associated protein kinase 70

ACKNOWLEDGMENTS

Foremost, I would like to thank the patients and their families and treating clinicians, who put their trust in us and enabled our work and this study in the first place. Furthermore, I would like to thank my supervisor, Kaan Boztug, for always encouraging me to “think big” and outside the box and giving me the resources and freedom to pursue these ideas. But most importantly, I thank him for putting together a research group made up of such amazing and wonderful people and allowing me to join and be part of it.

The past and present members of this lab, especially Wojtek, Theresa, Ana, Raúl, Ali, Anna, Juri, Artem, Christina, Sarah, Rico, Yirun, Hena, Sören, Claudia, and Jana, have made my years as a PhD student one of the most memorable and rewarding periods of my life. I would like to specifically thank Sevgi, whose unwavering support as a friend, colleague, project partner, and mentor has been invaluable. Mike, who taught me so much, most importantly, to believe in myself, and who helped me not to lose my focus. Cheryl has been an amazing project partner who managed to make me laugh even during the most stressful times. Michael and Irinka who came to the rescue to help overcome the last and most difficult challenges at the final stage of the project. All of you made coming to the lab something I looked forward to every day, and I will always look back on this time with great fondness.

I would also like to thank Anita and Giulio, who created the unique and stimulating atmosphere that can only be found at CeMM. Particularly, the initial months of PhD training, which included courses, seminars, and events, have been eye-opening. But most importantly, it allowed me to truly get to know the amazing people from my PhD cohort, many of whom became close friends, especially Ben, Daria, Justine, Andreas, Anna, and Christina. A special shoutout to Matthew, who always had our backs and was someone we could always count on.

This project could not have been finished without the help of many internal and external collaborators, but I would like to thank specifically Marta Rizzi, Alexei Tumanov, Safa Baris, Christoph Hafemeister, and Robert Pazdzior. I was fortunate to be supported by a fantastic PhD committee made up of Michael Sixt and Johannes Schmid, who encouraged me and my ideas from the very beginning of this journey.

Finally, I would like to thank all my friends and family, and my partner. I could always rely on your support as well as your forgiveness on occasions when I appeared late or had to cancel plans altogether because something in the lab had not worked the way I intended (and hoped for). Without you, I would never have had the perseverance and energy to get through the challenging times that are part of every PhD.

1. INTRODUCTION

1.1 Inborn Errors of Immunity (IEI)

1.1.1 Identification of patients with IEI

Inborn Errors of Immunity (IEIs), previously known as Primary Immunodeficiencies (PIDs), are genetic disorders that result in a severely impaired immune system. These conditions can manifest as immunodeficiency, autoinflammation, autoimmunity, or a combination thereof. Because of the importance of the functional immune system for survival, these defects are inherently rare. Although each individual genetic defect affects only a small number of people, the cumulative number of identified defects, along with advances in early diagnostics and therapeutic options, contributes to a growingly recognized patient population. Recent estimates suggest that 6 out of every 10,000 people in the US suffer from an IEI (Rider *et al*, 2024). This amounts to approximately 200,000 affected individuals in the US alone. Moreover, other studies report prevalence rates ranging from 1 in 5,000 to as high as 1 in 1,000 (Tangye *et al*, 2020), with some authors even proposing figures as high as 1 in 500 (Akalu & Bogunovic, 2024).

In addition to the severity of the disease, the diagnosis can be challenging and time-consuming, yet early diagnosis and treatment initiation are critical in preventing long-lasting effects. Chronic inflammation caused by immune dysregulation or recurrent infections can result in a generalized failure to thrive or organ-specific defects such as bronchiectasis, a reduced function of the lungs due to permanent dilatation of bronchi following repeated infections and inflammation (Barker, 2002). While increased susceptibility to infections is the best known symptom, more than 30% of cases with IEI initially present with other manifestations, including autoimmunity, hyperinflammation, lymphoproliferation, and malignancy (Figure 1) (Thalhammer *et al*, 2021). To increase awareness of the broader clinical spectrum of these disorders, the International Union of Immunological Societies (IUIS) replaced the original classification Primary Immunodeficiencies (PID) with Inborn Errors of Immunity (IEI) (Bousfiha *et al*, 2013).

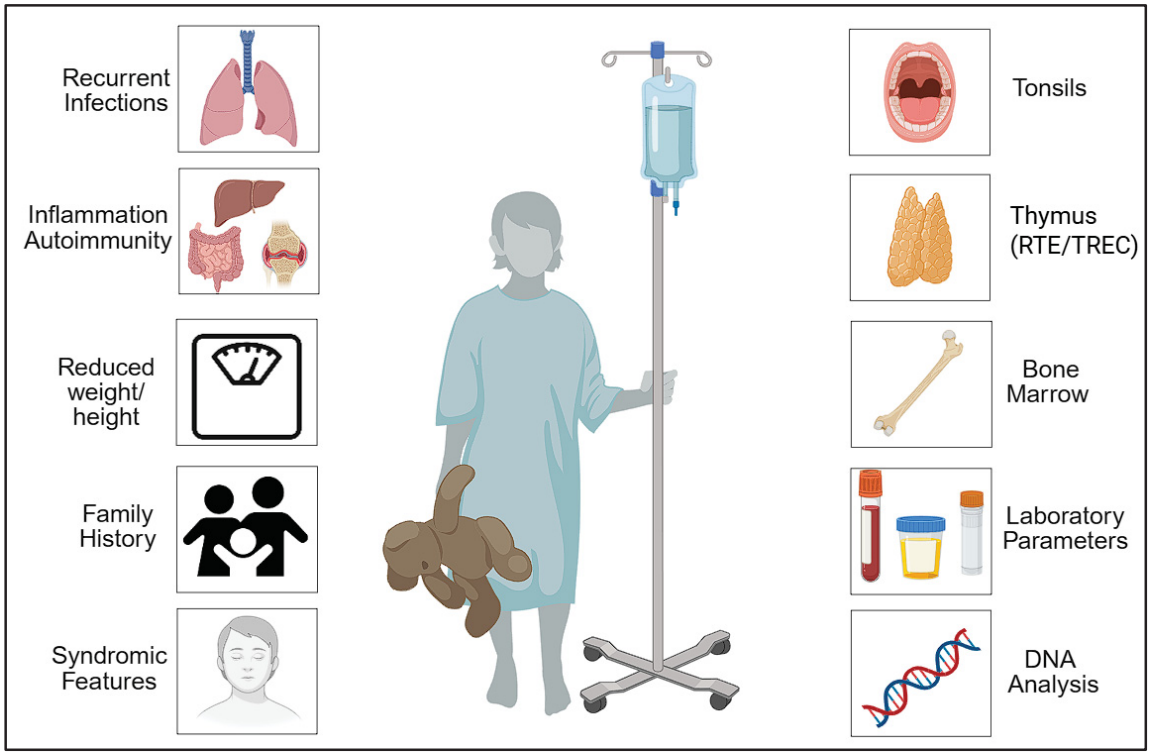

Figure 1. Simplified overview summarizing typical signs of IEI and the core steps of the diagnostic process

Schematic illustration of typical clinical presentations in IEI patients alongside key initial diagnostic evaluations. Patients present with recurrent infections, autoinflammation, autoimmunity, or any combination of these conditions. The severity of the disease and the typical early onset negatively can cause a significant drop in growth percentiles. A positive family history and syndromic features are additional risk factors for an underlying genetic disease. Investigative steps include examination of the lymphoid organs, including measurement of thymic output with Recent thymic emigrants (RTE) and T-cell receptor excision circles (TRECs), followed by assessment of laboratory parameters. While a diagnosis of IEI can often be suspected based on clinical and laboratory findings, DNA-based testing provides the molecular confirmation necessary for a conclusive diagnosis in many cases. Figure created with BioRender.com.

Thanks to rapid advancements in sequencing technologies and analysis, high-throughput techniques such as whole-exome sequencing (WES) (Ng *et al*, 2009) and whole-genome

sequencing (WGS) (Wheeler *et al*, 2008) now enable the comprehensive analysis of a patient's entire coding or even non-coding genomic regions. Additionally, it has become more reasonable and economically feasible to include family members in the sequencing process. Despite these advances, the sequencing process is still not error-free and requires manual control to reduce the likelihood of wrongfully annotated genes as well as to account for areas with limited read depth resolution or alignment artifacts (Goldstein *et al*, 2013).

The correct interpretation of genetic findings requires the combined effort and close collaboration of clinicians, geneticists, and immunologists to put the molecular data in the clinical and immunological context. Although the number of identified disease-causing gene mutations continues to grow rapidly, many variants detected in patients with IEI remain of uncertain significance. These often include previously unreported variants or variants occurring in genes for which no disease-associated mutations have yet been described (Grumach & Goudouris, 2021). Diagnostic decisions can be further complicated by the existence of gene mutations with incomplete penetrance or even more complicated cases such as somatic mosaicism, where the mutation is not the result of a germline mutation, but arises during embryonic or later development (Gruber *et al*, 2020). These cases require additional testing and research efforts in order to correctly diagnose the patient, optimize treatment, and provide genetic counseling to the family.

1.1.2 The research value of studying IEIs

IEIs pose significant challenges for patients, their families, and medical professionals due to their complexity and severity. Yet, they also serve as invaluable models for unraveling the fundamental workings of the human immune system. While inbred mice have long been hailed as the "Rosetta Stone" of modern immunology, they come with notable limitations, such as the inability to capture the genetic diversity and varied microbial exposures found in human populations (Medetgul-Ernar & Davis, 2022). Moreover, given the longer lifespan, delayed sexual maturation, and lower reproductive output of humans compared to mice, it is reasonable to expect that the demands on the immune system—and consequently its functions—differ between the two species. In addition to anatomical differences, a study comparing the transcription profiles of human and mouse immune cell types identified 169 genes with significantly different expression

levels between corresponding cell lineages (Shay *et al*, 2013), not even factoring in posttranslational modifications or non-immunological tissues contributing via cytokines and chemokines (Medetgul-Ernar & Davis, 2022). These discrepancies likely contribute to the low translational success rates in drug development, where only about 10–15% of investigational drugs entering Phase I clinical trials eventually secure FDA approval (Hay *et al*, 2014; Wong *et al*, 2019).

Nevertheless, early breakthroughs in immunology were predominantly derived from mouse studies, especially after the introduction of inbred mouse strains in the 1950s, which provided a controlled environment to elucidate fundamental immune mechanisms. Examples for these most fundamental discoveries related to the immune system were the discovery of the essential role of the thymus in lymphocyte development (Miller, 1961) or the mechanism by which T cells are activated through the major histocompatibility complex (MHC) (Zinkernagel & Doherty, 1974; Medetgul-Ernar & Davis, 2022).

In contrast, analogous insights into human immune function emerged much later, with physicians becoming more aware of the existence of IEI. One of the first widely known human cases was David Vetter, who was born in 1971 and would become famously known as the “bubble boy”. He suffered from an undiagnosed severe combined immunodeficiency (SCID), an especially severe IEI, that requires early diagnosis and HSCT or complete isolation (Rennie, 1985). Finally, in 1985, the first genetic cause of an IEI could be identified in the form of adenosine deaminase deficiency (ADA) (Bonthron *et al*, 1985). Whereas by 2000, fewer than 100 different IEIs had been genetically characterized, this number rapidly increased due to advances in next-generation sequencing (Tangye *et al*, 2022). In 2024, following rapidly decreasing costs, coupled with significant improvements in bioanalytical techniques and our overall understanding of the immune system, more than 555 genetic causes for IEI, attributed to mutations in 504 different genes, have been identified (Poli *et al*, 2025).

Insights gained from studying IEIs have not only improved the quality of life and life expectancy of these patients but also had a direct and dramatic impact on the treatment of much more common causes of disease. Studies of patients with mutations in genes encoding for checkpoint inhibitors such as Cytotoxic T-Lymphocyte–Associated Protein 4 (CTLA-4) (Kuehn *et al*, 2014) and Programmed Cell Death Protein 1 (PD-1) (Ogishi *et al*, 2021) improved our understanding of these

proteins and their regulation, and therefore helped us to predict eventual side effects of inhibiting these proteins in cancer patients. Together with the progress made in gene therapy, these advancements clearly demonstrate the importance of continued research in IEI.

1.2 Organization and effector functions of the immune system

1.2.1 Classifications and functions of the immune system

The main role of the immune system is to keep and restore homeostasis by removing harmful pathogens, mutated or dysfunctional and dead cells, and by supporting wound healing. In order to fulfil these functions, the immune system is equipped with an array of mechanisms, functions, and activity patterns that enable it to mount rapid as well as long-lasting responses. This requires a finely tuned and coordinated system that is highly regulated with multiple checkpoints and feedback loops, ensuring context-dependent immune reactions while preventing excessive inflammation, as seen in autoinflammatory, autoimmune, and allergic diseases.

The immune system is traditionally divided into an innate part providing rapid and non-specific responses, as well as adaptive immunity, which requires more time to respond, but is capable of mounting stronger and more specific responses to particular pathogens, coupled with the capacity for memory (Figure 2). While this simplistic view makes it easier to understand, in reality, there is an intense crossover between the components of this system (Iwasaki & Medzhitov, 2015). Not only is the adaptive immune response dependent on the "time" that the innate immune system provides by slowing down pathogen spread, but it is even more reliant on the innate immune system to be activated by innate antigen-presenting cells (APCs). Both branches of the immune system utilize and depend intensively on fine-tuning and communication using cytokines and chemokines (Murphy & Weaver, 2016). Moreover, our growing understanding of immune mechanisms has shown that cells traditionally categorized as part of the innate response are capable of functions attributed to the adaptive immune response. Innate immune cells, such as natural killer (NK) cells (Kleinnijenhuis *et al*, 2014) or monocytes and macrophages (Kleinnijenhuis *et al*, 2012), can also be “trained” to adapt – a concept achieved through epigenetic and metabolic reprogramming and known as trained immunity (Ochando *et al*, 2023). On the other hand, subtypes of B and T lymphocytes have been identified that display innate-like characteristics and have since been described as part of the innate immune system. For example, B-1 B cells can produce antibodies without previous activation of T cells (Murphy & Weaver, 2016), and are capable of phagocytosis (Parra *et al*, 2012), while γδ T cells can directly bind to antigens, making them independent of MHC presentation (Morita *et al*, 1995). These examples highlight that the traditional division between innate and adaptive immunity, while conceptually useful,

does not fully reflect biological reality, as many cells and mechanisms operate in the space between and connect both parts of the immune system.

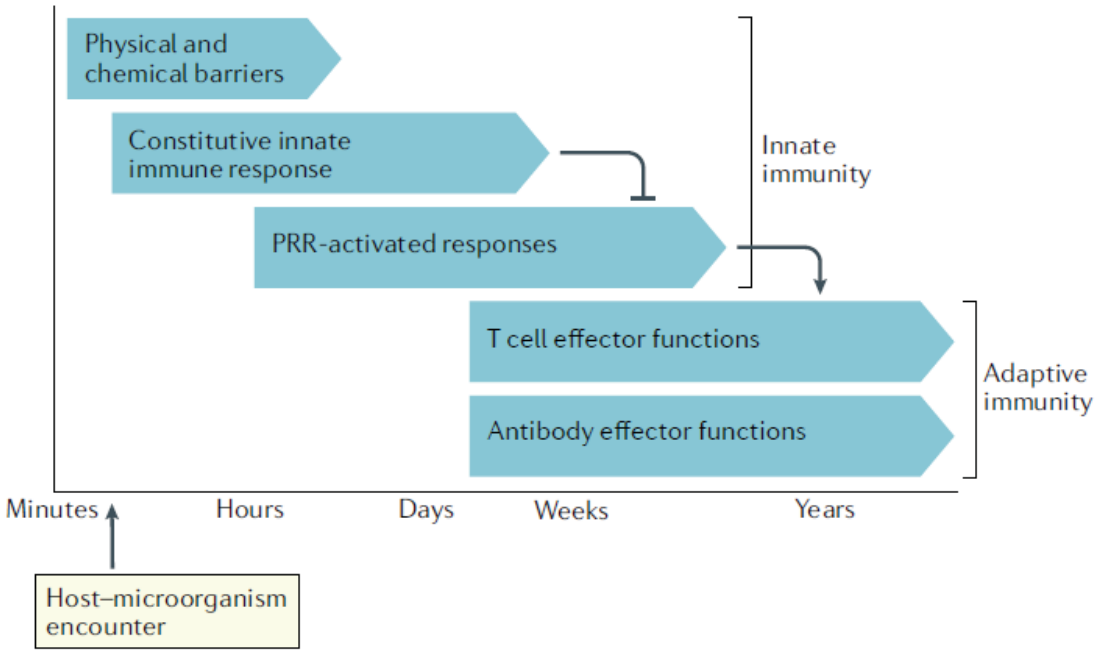

Figure 2. Timeline and mechanisms of the immune response

A simplified overview of the different layers of the immune response and their temporal sequence following exposure to pathogenic microorganisms. The first layer of defense consists of physical and chemical barriers, such as the epithelial surfaces, mucosal secretions, and antimicrobial peptides. Upon breach of these barriers, components of the innate immune system sense and respond to various danger-associated molecular patterns. If these initial mechanisms fail to contain the pathogen and the signal exceeds the threshold required to activate pattern recognition receptor (PRR)-mediated pathways, an inflammatory response is initiated. This subsequently leads to the activation of the adaptive immune system, culminating in a pathogen-specific immune response orchestrated by T cells and plasma cell–derived antibodies. Figure adapted from (Paludan *et al*, 2021) *and used with permission of Springer Nature BV conveyed through Copyright Clearance Center, Inc.*

1.2.2 Innate Immunity

The parts of the innate immune system can be broadly categorized into physical and chemical barriers and a soluble and cellular component. Physical barriers are created by epithelial cells of the skin and the respiratory, urogenital, and gastrointestinal tract. Epithelial cells are held together by tight junctions, which impose a physical barrier between the internal milieu of the body and the external world that contains pathogens. Mucosal epithelial cells produce the viscous fluid mucus, which prevents microorganisms from adhering to the epithelium. The importance of its contribution to the immune system is evident in cystic fibrosis, where a genetic defect affects mucus production, resulting in decreased expulsion of microorganisms in the respiratory tract (Riordan *et al*, 1989). Three important classes of antimicrobial peptides (AMPs) in mammals are defensins, cathelicidins, and histatins. These are small proteins that act directly microbicidally against a broad spectrum of pathogens. Defensins and cathelicidins are mostly produced by epithelial cells and neutrophils, whereas histatins are produced by cells in salivary glands. Epithelial cells can also produce lactoferrin, which binds and sequesters iron that is required for bacterial growth (Wozniak *et al*, 2024). Other examples of chemical barriers are the low pH level in the stomach created by parietal cells, fatty acids on the skin produced by sebocytes and keratinocytes, and lysozyme, an enzyme secreted by salivary glands, tears, and mucosal epithelial cells, which degrades bacterial cell walls (Murphy & Weaver, 2016).

The soluble component of the innate immune system is known as the complement system, a collection of more than 50 soluble proteins present in blood and other body fluids. Upon detection and binding of pathogens via certain surface motifs known as microorganism-associated molecular pattern (MAMP) and damage-associated molecular pattern (DAMP) recognition, respectively, the complement system is activated as a cascade of protein interactions and proteolytic reactions. One of the key functions of the complement system is opsonization, the binding of pathogens, marking them for destruction by phagocytes (Ricklin *et al*, 2010). Following their cleavage and activation, some complement proteins can act as chemoattractants and recruit immune effector cells to sites of infection and inflammatory damage (Ricklin *et al*, 2010). It also has an effect on the adaptive immunity by stimulating lymphocyte activation and proliferation, as well as promoting antigen presentation (Carroll &

Isenman, 2012). Finally, it can also kill pathogens directly by assembly of the multiprotein, cell membrane-perforating complex termed membrane attack complex (MAC) (Mastellos *et al*, 2024).

Cells of the innate immune system include eosinophils, basophils, neutrophils, monocytes, macrophages, NK cells, and dendritic cells (DCs). Unlike lymphocytes, these cells do not undergo somatic recombination to enhance pathogen recognition but instead rely on the detection of signals associated with danger to host homeostasis. These signals include conserved molecular structures on microbes, termed pathogen-associated molecular patterns (PAMPs), or damage-associated molecular patterns (DAMPs) released by endogenous host cells. The receptors that recognize these features are pattern recognition receptors (PRRs) and can be classified into four main groups on the basis of their cellular localization and their function: free receptors in the serum, membrane-bound phagocytic and signaling receptors, and cytoplasmic signaling receptors (Iwasaki & Medzhitov, 2015).

The main function of the innate immune system is to provide an immediate response that contains pathogens to prevent them from spreading and to initiate additional immune mechanisms. It also plays a critical role in alerting and recruiting other immune cells, including those of the adaptive immune system, thereby buying time until a more specific and long-lasting response can be generated. To do so, cells of the innate immune system have a plethora of different functions and mechanisms at their disposal. If the pathogen has been opsonized by either complement proteins or antibodies, phagocytes such as neutrophils, monocytes, macrophages, mast cells and DCs can ingest the target and kill it using different mechanisms, such as respiratory burst, a process that includes the production of reactive oxygen-containing molecules, hence also termed oxygen-dependent intracellular killing (Brown, 2024). Cells can also utilize toxic substances for extracellular killing. NK cells eliminate pathogens through degranulation of cytotoxic molecules such as perforin and granzymes (Voskoboinik *et al*, 2015), whereas neutrophils release antimicrobial proteins and enzymes such as defensins and myeloperoxidase, or immobilizing DNA-containing neutrophil extracellular traps (NETs) (Zhang *et al*, 2024). In order to escalate the immune response, innate immune cells recruit additional immune cells via the release of chemokines, produce cytokines that activate immune cells as well as induce proliferation and differentiation, and, importantly, initiate the adaptive immune response through antigen-presentation. Following phagocytosis, macrophages and DCs can

process and present peptides from microbial proteins on their surface using major histocompatibility complex (MHC) molecules. Once these peptide-MHC complexes are recognized by $CD4^+$ T-helper cells or $CD8^+$ cytotoxic T cells, the adaptive immune response is mounted, leading to clonal expansion, effector cell differentiation and activation, and the establishment of immunological memory (Murphy & Weaver, 2016).

1.2.3 Adaptive Immunity

In contrast to the innate immune response, the adaptive response is characterized by a delayed but highly specific response to the pathogen. Moreover, the adaptive immune system has the capacity to learn from previous encounters and develop a long-lasting immune memory that enables a faster and more robust response upon subsequent exposure to the same pathogen (Murphy & Weaver, 2016). In order to develop their ability to recognize a vast array of different antigens, B and T lymphocytes have to undergo several maturation and differentiation steps (Figure 3). Both originate from common lymphoid progenitor stem cells located in the bone marrow, which themselves derive from the multipotent hematopoietic stem cells (Kumar *et al*, 2018). Immature precursor T cells have to migrate to the thymus, where they undergo V(D)J recombination, the mechanism by which variable (V), diversity (D), and joining (J) gene segments are rearranged to generate a diverse repertoire of antigen receptors (Nikolich-Zugich *et al*, 2004). Some of the key enzymes involved in this process are recombination activating genes 1 and 2 (RAG1/2), Artemis, and DNA ligase IV (LIG4), for which germline mutations have been described that result in a complete absence of functional lymphocytes and severe combined immunodeficiency (SCID) (de Villartay *et al*, 2003). Following this rearrangement, T cells are positively selected for the development of a functional T cell receptor (TCR) that is capable of binding to MHC molecules presenting self-antigens. T cells that are not capable of forming functional TCR-MHC contacts don't receive vital survival signals and go into apoptosis. During this stage, it is also decided whether T cells become $CD4^+$ helper T-cells or $CD8^+$ cytotoxic T cells. To prevent autoimmune reactions by self-reactive T cells, positively selected T cells have to undergo the process of negative selection, where T cells that bind too strongly to self-antigen are eliminated via apoptosis or differentiate to become T-regulatory (Treg) cells (Hogquist *et al*, 2005). The mature naïve T cells can then exit the thymus and go into circulation (Kumar *et al*, 2018).

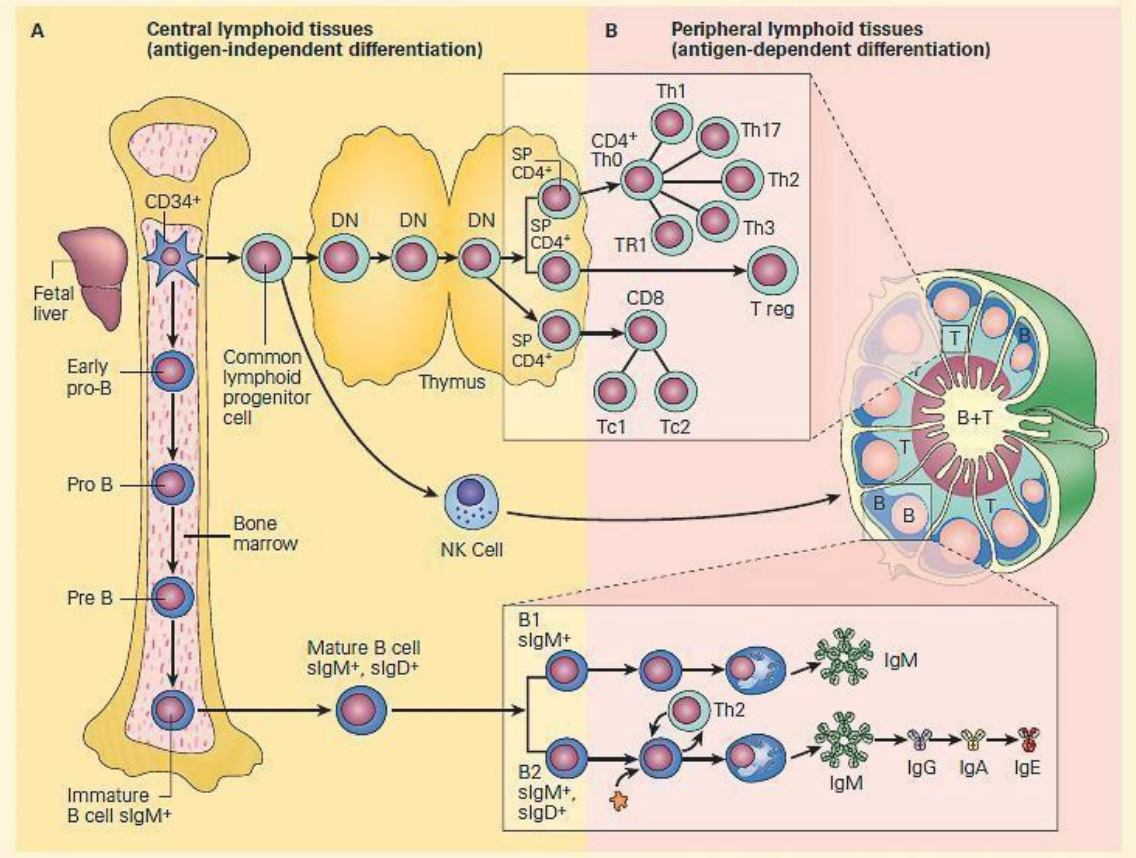

Figure 3. Lymphocyte biogenesis

Lymphocytes are derived from CD34 $^{+}$ hematopoietic stem and progenitor cells, which reside in the fetal liver during embryogenesis and in the bone marrow after birth. Lineage commitment occurs following the common lymphoid progenitor (CLP) stage. While B lymphocytes mature and perform V(D)J recombination in the bone marrow, T cells migrate to the thymus, where they undergo selection processes to eliminate autoreactive clones and develop into CD4 $^{+}$ or CD8 $^{+}$ single-positive T cells. Although V(D)J recombination occurs earlier during thymic development, the final stages of functional differentiation for both T and B cells take place in secondary lymphoid organs, particularly during immune activation. In these sites, T cells differentiate into specialized effector subsets, while B cells undergo class-switch recombination, somatic hypermutation, and differentiation into memory B cells or antibody-secreting plasma cells. Figure adapted from (Stiehm, 2012) *and used with permission of Springer Nature BV conveyed through Copyright Clearance Center, Inc.*

Using the same recombinase system and core enzymes as T cells, B cells also undergo the process of V(D)J recombination, but whereas T cells rearrange T-cell receptor genes, the B cells rearrange immunoglobulin genes to generate a diverse B cell receptor (BCR) repertoire (Pieper *et al*, 2013). Immunoglobulin gene rearrangement occurs in a stepwise manner during B-cell development. In the pro-B cell stage, the D and J gene segments of the heavy chain locus recombine first, followed by the joining of a V segment to the DJ complex. If the rearrangement is successful, a functional μ heavy chain is produced. This μ chain pairs with a surrogate light chain, composed of VpreB and λ5, to form the pre-B cell receptor (pre-BCR). Expression of the pre-BCR on the cell surface signals successful heavy chain rearrangement and allows the cell to progress to the pre-B stage, where light chain rearrangement takes place and, if successful, leads to surface expression of a complete IgM receptor (Murphy & Weaver, 2016).

Similar to the selection of T cells, these B cell precursors have to be tested to ensure that this enormous diversity of antibody specificities does not result in autoreactivity. The first selection step is after the differentiation into the pre-B stage to ensure productively rearranged heavy chain gene segments. This not only provides the cell with survival signals but also shuts down the enzyme machinery catalyzing the rearrangement to prevent the expression of 2 H-chains with different specificities by the same cell. Once IgM production has been established, the B cells are tested for autoreactivity. If the newly expressed receptor binds too strongly to antigen expressed in the bone marrow, the B cell can undergo additional gene rearrangements to replace the autoreactive receptor with a new receptor that is not self-reactive. If this mechanism, termed receptor editing, is successful, the B cell continues with its normal development. If the receptor remains autoreactive and no additional light chain V and K gene segments are available for recombination, the cells are undergoing clonal deletion, meaning being subjected to cell death via apoptosis (Pieper *et al*, 2013).

After leaving the bone marrow, immature B lymphocytes migrate to the spleen, where they complete their maturation through two distinct transitional stages, called T1 and T2. T1 B cells are almost exclusively present in the spleen due to their inability to recirculate. Once these cells have entered the B follicles in the spleen and acquired cell surface IgD and CD23, they are termed T2 B cells. These cells are now able to recirculate and can further differentiate into mature follicular or marginal zone B cells. This differentiation is dependent on the survival and differentiation signal

B cell–activating factor (BAFF) and B cell receptor (BCR) signaling, with the strength of BCR signaling acting as a key determinant: weak BCR signals promote marginal zone B cell development, intermediate signals favor follicular B cell differentiation, and strong signals induce apoptosis. Marginal zone B cells are retained in the spleen and have the ability of self-renewal, whereas follicular B cells recirculate through the bloodstream and the secondary lymphoid organs (Pillai & Cariappa, 2009).

1.2.4 Secondary lymphoid organs

Together with the lymph nodes and mucosa-associated lymphoid tissue (MALT), the spleen constitutes one of the secondary lymphoid organs (SLOs). Historically, the spleen was often viewed as a dispensable organ, mainly involved in filtering blood and recycling erythrocytes (Mebius & Kraal, 2005). Following traumatic injury, the spleen could rupture and, as one of the most vascularized organs in the body result in life-threatening internal bleeding, with the removal of the spleen often being the only therapeutic option (Uranues & Kilic, 2008). Long-term studies of soldiers subjected to splenectomy following injury in the Second World War contributed to our improved understanding and acknowledgment of the immunological functions of the spleen. These patients suffered an increased susceptibility to infections, especially caused by encapsulated bacteria such as *Haemophilus influenzae*, *Streptococcus pneumoniae,* and *Neisseria meningitidis* (Robinette & Fraumeni, 1977). A similar vulnerability has been observed in patients with congenital asplenia (Mahlaoui *et al*, 2011) or in whom splenectomy was performed as a treatment for other underlying diseases such as idiopathic thrombocytopenic purpura or thalassemia (Pedersen, 1983).

Nowadays, it has become abundantly clear that SLOs are critical for the initiation of adaptive immunity (van de Pavert & Mebius, 2010). While antigens introduced directly into the bloodstream are picked up by APCs in the spleen, pathogens located in other tissues are either drained via lymphatic vessels or taken up by APCs, which then migrate to the nearest draining lymph node (Banchereau & Steinman, 1998). The immense diversity of lymphocytes naturally results in very low precursor frequencies for individual antigen responding lymphocytes. The SLOs provide a confined environment in which APCs can encounter lymphocytes that respond to the presented antigen (Gretz *et al*, 1997). Once an APC carrying an antigen and expressing co-stimulatory

molecules has engaged with a naïve T cell that recognizes the presented antigen, the T cell becomes activated, resulting in differentiation and proliferation in a process termed priming. Naïve $CD8^+$ T cells differentiate into cytotoxic T cells, whereas $CD4^+$ T cells can differentiate into various types of effector cells that differ by the secretion of a set of cytokines. One of these subtypes are the T follicular helper (T_{FH}) cells, which are specialized for interacting with B cells to provide help for affinity maturation, differentiation, and class-switching in the course of the Germinal Center (GC) reaction and thereafter (Itano & Jenkins, 2003).

1.2.5 The Germinal Center Reaction

In the absence of infection, resting B cells are found in B cell follicles located between the T cell zone and the capsule in lymph nodes or between the T cell zone and the marginal zone in the spleen (reviewed in Victora & Nussenzweig, 2022). Following antigen delivery to SLOs, these are usually picked up and presented by macrophages residing in the subcapsular sinus of the lymph nodes (Banchereau & Steinman, 1998). There they are picked up by B cells, which migrate back to the B cell follicles and present them to follicular dendritic cells (FDCs), a specific subset of stromal cells that provide the network required to maintain the B cell follicles and which are able of trapping the antigen on its cell surface to be accessible by B cells and DCs (Heesters *et al*, 2014). Activated helper T cells differentiate and either leave the lymph node or migrate to the border of the B cell follicle to engage with the activated B cells (Garside *et al*, 1998). ICOSL secreted by B cells completes differentiation of T cells into T_{FH} cells, which in return provide B cells with CD40L and IL-21, which together with BAFF secreted by FDCs, DCs, and stromal cells are essential for B cell survival, proliferation, and differentiation (Denton & Linterman, 2017).

While some activated B cells stay near the medullary area of SLOs where they proliferate rapidly and differentiate into short-lived plasmablasts that secrete IgM antibodies that offer some immediate protection against the infection, other migrate back to the B cell follicle in the outer cortex of the lymph node and initiate the germinal center (GC) reaction (Chan *et al*, 2009). Here, the B cells undergo additional processes in order to produce antibodies more effectively in eliminating infections (Chan *et al*, 2009). During the process of somatic hypermutation (SHM) random mutations are introduced into the V regions of the immunoglobulin genes, a mechanism mediated by an enzyme termed activation-induced cytidine deaminase (AID), which is only

expressed by B cells in the GC (Revy *et al*, 2000). While the majority of these changes result in a reduction of affinity or unstable immunoglobulins, some increase the affinity to the antigen presented by TFH cells (Stebegg *et al*, 2018). These B cells receive additional pro-survival and proliferation-inducing signals, whereas B cells with reduced affinity undergo apoptosis (Stebegg *et al*, 2018). AID also induces mutations in switch regions of immunoglobulin genes (Muramatsu *et al*, 2000). This results in the class-switch of produced antibodies from the IgM and IgD isotypes to the IgG, IgA, and IgE isotypes. These differ in their ability for tissue penetration and effector functions (Stebegg *et al*, 2018). In the final stage of the germinal center process, the most adapted B cells differentiate into antibody-secreting plasma cells and memory B cells, which provide long-term protection against subsequent infections of the same pathogen (Akkaya *et al*, 2020). This marvelous process that mimics evolution in a rapid immunological setting requires the close interaction of various cell types and, therefore, the microenvironment provided by the SLOs (Denton & Linterman, 2017).

1.3 Nuclear factor kappa-light-chain-enhancer of activated B cells (NF-κB)

1.3.1 The NF-κB signaling pathway

The mammalian Nuclear factor kappa-light-chain-enhancer of activated B cells (NF-κB) family consists of five members, namely NF-κB1 (p105/p50), NF-κB2 (p100/p52), p65 (RelA), V-Rel reticuloendotheliosis viral oncogene homolog B (RelB), and c-Rel (Zhang *et al*, 2017). All members of the NF-κB family are constantly expressed in the cell in the form of preformed, but inactive protein dimers, allowing for rapid activation following upstream signaling. These proteins form various hetero- or homo-dimer complexes that act as major transcription factors (Murphy & Weaver, 2016). The pathway can be activated by various signals ranging from direct ligand-receptor interactions to less specific signals such as DNA damage following ionizing radiation (Basu *et al*, 1998; Fitzgerald *et al*, 2007).

NF-κB is a central regulator of cellular responses, playing a crucial role in immune homeostasis, cell survival, and proliferation. Due to its involvement in these fundamental processes, NF-κB is also critically implicated in various diseases. As a result, since its discovery in 1986, it has become one of the most extensively studied signaling pathways (Sen & Baltimore, 1986; May, 2006). The NF-κB pathway can be separated into a rapid but transient canonical pathway, involving the NF-κB1/p105 protein, and a slow but persistent non-canonical (or alternative) pathway centered around NF-κB2/p100. NF-κB1/p105 and NF-κB2/p100 are the inhibitory precursors of their partially processed and active forms, p50 and p52, respectively, which then form homo-dimers or hetero-dimers with the other members of the NF-κB family, p65/RelA, RelB, and c-Rel. The Rel proteins are suppressed by inhibitory proteins of the IκB family (typically IκBα), which bind and mask the nuclear localization signals (NLS) on the Rel proteins, thus deterring their translocation into the nucleus. In contrast, p105 and p100 are not inhibited by IκB proteins but lack the transactivation domain (TAD) of the other NF-κB family members, thereby preventing their activity to induce gene transcription (Fliegauf *et al*, 2022). Both p105 and p100 contain ankyrin repeats that interact with the Rel Homology Domain (RHD) of all NF-κB subunits, including their active forms p50 and p52. This interaction prevents these subunits from binding DNA motifs and initiating transcription, thereby functioning similarly to the inhibitory IκB proteins. In most cell types, p105 and p100 undergo continuous limited proteasomal processing, which selectively removes their C-terminal inhibitory region containing the ankyrin repeats. As a result, they exist in

both an inhibitory and an active form simultaneously. For NF-κB activation, inhibitory IκB proteins must be removed from RelA, RelB, and c-Rel to free them for nuclear translocation. In contrast, p105 and p100 must be either fully degraded or partially processed, releasing both their active forms, p50 and p52, as well as their bound Rel proteins, allowing them to participate in transcriptional regulation (Beinke & Ley, 2004; Liu *et al*, 2017).

The canonical pathway can be activated by a range of cytokine receptors, pattern recognition receptors (PRRs), members of the TNF receptor (TNFR) superfamily, as well as T-cell receptor (TCR) and B-cell receptor (BCR), and various stress agents (Figure 4) (Liu *et al*, 2017). These receptors activate the canonical NF-κB pathway through multiple distinct mechanisms, depending on the type of receptor, the stimulus, and the cellular context, but they all converge on the activation of the IκB kinase (IKK) complex (Guo *et al*, 2024).

This trimeric complex comprises the two catalytic subunits IKKα and IKKβ and the regulatory subunit IKKγ, also known as NF-κB essential modulator (NEMO). Following activation, the IKK complex phosphorylates the inhibitory IκB proteins, resulting in their ubiquitin-dependent proteasomal degradation. Additionally, it phosphorylates p105, leading to its partial degradation and subsequent release of bound NF-κB dimers comprised of the heterodimers RelA/p50, c-Rel/p50, and the homo-dimer p50/p50, whereas the latter still lacks the TAD and is therefore not transcriptionally active on its own. The release of the bound dimers by either p105 or IκB degradation enables the translocation of the NF-κB dimers into the nucleus, where they activate the transcription of numerous target genes (Guo *et al*, 2024).

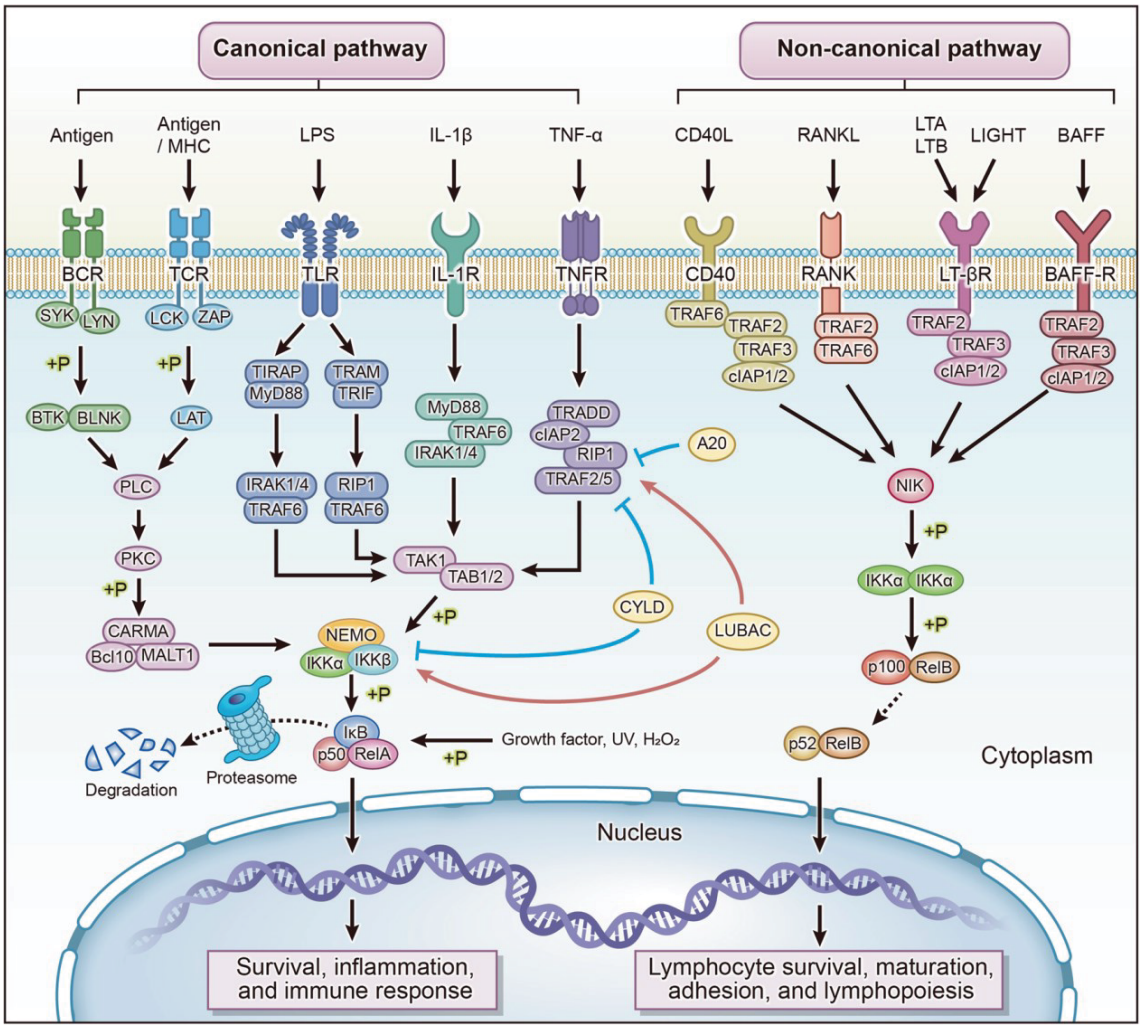

Figure 4. The canonical and non-canonical NF-κB pathway

The canonical and non-canonical NF-κB pathways are activated by a range of stimuli, including cytokines, pathogen-associated molecular patterns such as lipopolysaccharide (LPS), and antigens. To allow for rapid initiation, members of the NF-κB family involved in canonical signaling are sequestered in the cytosol through binding by inhibitors of the IκB protein family. Upon upstream signaling, the suppressing IκB proteins are phosphorylated, ubiquitinated, and subsequently degraded, releasing the bound NF-κB dimers, which then translocate into the nucleus to initiate transcription. In contrast, the non-canonical NF-κB pathway centers on the processing of the NF-κB precursor protein p100. Under homeostatic conditions, this pathway is kept inactive through continuous degradation of NIK (NF-κB-inducing kinase). Following

receptor engagement, NIK becomes stabilized and activates IKKα, which phosphorylates p100, triggering its partial proteasomal processing into the transcriptionally active subunit p52. Similar to the canonical pathway, these processed NF-κB proteins form dimers and translocate to the nucleus, where they function as key transcriptional regulators. Not depicted here are the numerous points of cross-talk and regulatory interactions between components of the canonical and non-canonical NF-κB pathways. Figure adapted from (Guo *et al*, 2024) *and used with permission of Springer Nature BV conveyed through Copyright Clearance Center, Inc.*

1.3.2 Effects of canonical NF-κB signaling

NF-κB activation can be triggered by a diverse array of signals, including extrinsic factors such as cytokines, microbial components, and carcinogens like UV light and heavy metals, as well as intrinsic stressors like DNA damage, hypoxia, cellular stress, and oncogene activation. As a key transcription factor, canonical NF-κB regulates a wide range of genes involved in metabolic processes and the maintenance of cellular homeostasis that enable cells to adapt to environmental changes and stress-related challenges. The effects of NF-κB activation are highly pleiotropic and depend on the cellular context and type, but predominantly influence processes related to inflammation, immune function, cell survival, and proliferation (Aqdas & Sung, 2023).

In innate immune cells, dendritic cells and certain types of epithelial cells, NF-κB signaling not only induces the production of pro-inflammatory cytokines such as TNF-α and IL-1β (Cao *et al*, 1996; Suwara *et al*, 2014), but thereby also initiates the formation and activation of the NLR family pyrin domain containing (NLRP) inflammasomes (Bauernfeind *et al*, 2009). These intracellular multi-protein complexes are formed in response to PAMP and DAMP activation. Once activated, inflammasomes perpetuate the inflammatory response by producing additional pro-inflammatory cytokines and by initiating pyroptosis through the activation of pore-forming proteins. Pyroptosis is a highly inflammatory form of cell death that results in the release of even more cytokines and DAMP molecules such as HMGB-1, ATP, and DNA in order to recruit and activate more immune cells, further intensifying the inflammatory cascade (Bauernfeind *et al*, 2009).

Canonical NF-κB signaling has been shown to be a key driver of cell differentiation. In macrophages, NF-κB activation promotes the differentiation of activated macrophages towards classically activated macrophages (M1), which are more pro-inflammatory than their alternatively-activated (M2) and regulatory (Mreg) counterparts (Mosser & Edwards, 2008; Wang *et al*, 2014). M1 macrophages depend on NF-κB signaling to produce a variety of inflammatory proteins, including TNF-α, IL-1β, IL-6, IL-12p40, and cyclooxygenase-2 (Liu *et al*, 2017). Following TCR activation and subsequent NF-κB signaling, naïve T cells differentiate into different subsets of effector T cells. It has been shown that in addition to the context provided by the cytokines and pathogens, NF-κB signaling influences T-cell differentiation by both cytokines secreted by other immune cells and T-cell intrinsic factors (Oh & Ghosh, 2013). Similarly to T lymphocytes, both canonical and non-canonical NF-κB signaling is also involved in B cell development, where it is critical for class-switching, affinity maturation, and differentiation (Pone *et al*, 2012).

1.3.3 Monogenic defects in receptors driving canonical NF-κB activation

The discovery of IEIs affecting genes that encode receptors that primarily signal through the NF-κB pathway has provided valuable insight into the specific roles of these receptors in host defense. The distinct patterns of pathogen susceptibility in these patients have helped define which microbial signals are sensed through each receptor, as well as highlighting their non-redundant contributions to human immunity (Zhang *et al*, 2017).

TLRs are a family of highly conserved receptors of the innate immune system that contribute to the first line of host defense against microbial pathogens by inducing the production of pro-inflammatory cytokines through the NF-κB and mitogen-activated protein kinase (MAPK) pathways, as well as Type I interferon (IFN) through interferon regulatory factor 3 (IRF3) and IRF7 (reviewed in Kawai *et al*, 2024). To date, 10 different TLRs have been identified in humans, each recognizing a wide array of PAMPs and DAMPs, classified into cell surface and endosomal subfamilies. Disease-causing monogenic mutations have been described in the cell surface TLR4 (Capitani *et al*, 2023) as well as in the endosomal receptors TLR3 (Zhang *et al*, 2007), TLR7 (van der Made *et al*, 2020) and TLR8 (Bleesing, 2022), highlighting their non-redundant roles in human antiviral and antibacterial immunity.

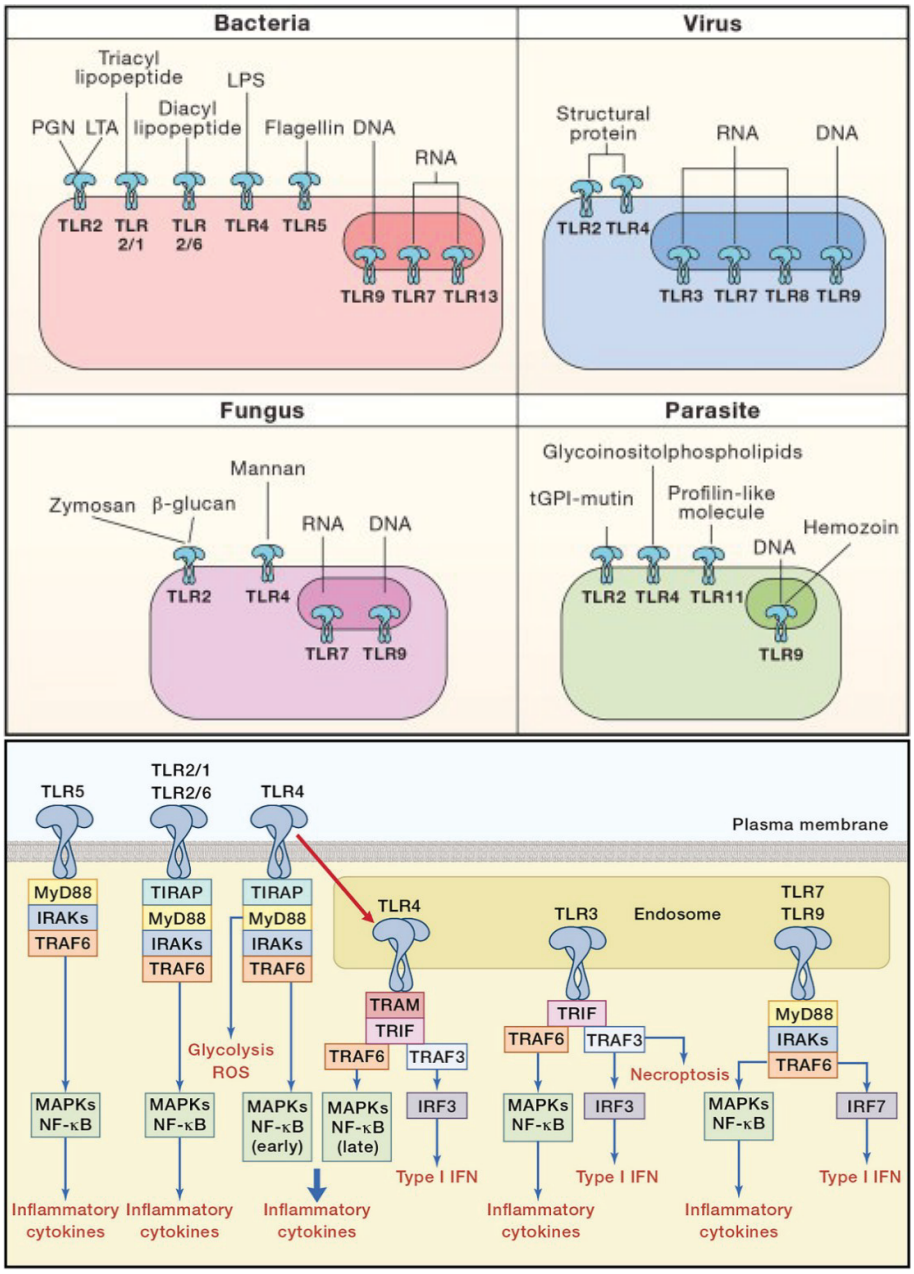

Figure 5. Activators and signaling pathways of Toll-like-receptors

(Top) Members of the TLR family recognize different PAMPs and DAMPs expressed or produced by a wide range of pathogens. Whereas receptors detecting extracellular microbial components are expressed on the cell surface, the TLRs detecting nucleic acids from viruses or bacteria are located intracellularly. (Bottom) With the exception of TLR3, all human TLRs primarily signal through the adaptor protein MyD88, resulting in the recruitment of IRAK kinases and TRAF6 and the subsequent activation of the NF-κB and

MAPK pathways. In contrast, TLR3 signals exclusively via the adaptor protein TRIF, while TLR4 can engage both MyD88 (at he plasma membrane) and RIF (following endocytosis). TRIF not only recruits TRAF6 but also TRAF3 in order to induce the Type I IFN pathway through IRF3 activation. Figure adapted from (Kawai et al*, 2024) and used with permission of Elsevier Science & Technology Austria conveyed through Copyright Clearance Center, Inc.*

TLR3 recognizes double-stranded RNA, which is produced during the viral replication of viruses such as herpes simplex virus 1 (HSV-1) (Lim *et al*, 2014). The importance of functional TLR3 signaling and subsequent interferon production is demonstrated by the susceptibility of children with TLR3 deficiency, who suffer from life-threatening herpes simplex encephalitis (HSE) as a complication of primary infection with HSV-1 (Zhang *et al*, 2007). A similar predisposition to HSE has been found in patients with mutations in TLR3-associated genes, such as UNC93B1, encoding for UNC-93B, an endoplasmic reticulum (ER) protein required for the trafficking of TLR3, TLR7, TLR8, and TLR9 from the ER to the endosomal compartment (Casrouge *et al*, 2006). Furthermore, defects in the gene encoding the adaptor protein TIR-domain-containing adapter-inducing interferon-β (TRIF), downstream of TLR3 and TLR4 activation, are also characterized by an inherent risk for developing HSE (Sancho-Shimizu *et al*, 2011). Interestingly, this clinical phenotype is also shared by patients carrying autosomal dominant mutations in TNF receptor-associated factor 3 (TRAF3), an E3 ubiquitin ligase and adaptor protein that is involved in multiple signaling pathways, including non-canonical NF-κB signaling and IRF3-induced type I IFN production (de Diego *et al*, 2010).

Surprisingly, biallelic mutations in TLR4 do not lead to increased susceptibility to viral infections but have instead been associated with a variable clinical presentation ranging from asymptomatic cases to inflammatory bowel disease (IBD) (Capitani *et al*, 2023). A potential explanation could be the wider spectrum of PAMPs detected by TLR4, including the bacterial cell wall component lipopolysaccharide (LPS), several viral structural proteins, and microbial carbohydrates commonly found on the surfaces of fungi and parasites. Myeloid differentiation factor 2 (MD-2) is a protein encoded by the *LY96* gene and an essential co-receptor for TLR4, facilitating the binding of LPS (Kawai *et al*, 2024). So far, only two siblings have been described, with one suffering from very early onset IBD, whereas the other from recurrent respiratory infections (Li *et al*, 2023). MD2-deficient cells showed decreased cytokine expression in response to LPS or gram-negative, but not gram-positive bacteria.

TLR7 and TLR8 recognize single-stranded RNA derived from viruses and bacteria and orchestrate host responses against RNA viruses, including influenza A virus, HIV, vesicular stomatitis virus, and severe acute respiratory syndrome coronavirus 2 (SARS-CoV-2) (Kawai *et al*, 2024). Loss-of-function mutations in TLR7 have been found in otherwise healthy young men with severe coronavirus disease 2019 (COVID-19) (van der Made *et al*, 2020). So far, no loss-of-function mutations in TLR8 have been identified, but one patient with a heterozygous gain-of-function mutation, causing spontaneous NF-κB activation and resulting in a clinical phenotype of autoinflammatory and autoimmune disease, highlighting that TLR8 signaling must be tightly regulated (Bleesing, 2022).

Several members of the TNF receptor superfamily primarily signal through the canonical NF-κB pathway (Guo *et al*, 2024). Heterozygous mutations in *TNFRSF13B* encoding TACI (transmembrane activator and calcium-modulator and cyclophilin ligand interactor) can result in CVID with variable clinical expression and penetrance, as some of the variants that have been identified as disease-causing are also present in 1-2% of the general population (Salzer & Grimbacher, 2021). Interestingly, *TNFRSF13B* is a highly polymorphic gene, which is an unusual finding for genes in IEI, as these are typically under selective pressure during evolution and therefore usually more conserved (Rapaport *et al*, 2021). TACI is expressed on B cells and mediates B-cell differentiation into plasma cells and isotype switching through MyD88-mediated NF-κB and mTOR-signaling following activation by its ligands BAFF and APRIL, fitting with the hypogammaglobulinemia commonly seen in TACI patients (Castigli *et al*, 2005).

CD137 is encoded by *TNFRSF9* and is expressed on activated lymphocytes, but its main role is to enhance proliferation, survival, and cytolytic activity of CD8 T-cells (Shen *et al*, 2023). Biallelic mutations in *TNFRSF9* lead to recurrent bacterial and viral infections, with a particular susceptibility to Epstein–Barr virus (EBV) infections resulting in chronic EBV viremia, EBV-driven lymphoproliferation, and EBV-related B-cell lymphoma in some of the patients, as well as signs of autoimmunity (Somekh *et al*, 2019; Alosaimi *et al*, 2019).

Kaposi sarcoma is an endothelial tumor that, though induced by a human herpes virus 8 (HHV-8), only appears in a small fraction of individuals infected with HHV-8 (Chang *et al*, 1994). To date, only one patient with disease-causing OX40 deficiency has been described in public literature

(Poli *et al*, 2025). OX40 expression was decreased in cells from these otherwise healthy adults, and they were also unable to bind OX40L, resulting in a specifically impaired response to HHV-8 and childhood-onset Kaposi sarcoma (Byun *et al*, 2013). Although $CD4^+$ T-cell recall responses to several antigens were markedly reduced, Epstein–Barr virus (EBV)-specific $CD8^+$ T cells were present at normal frequencies, indicating that OX40 is dispensable for at least some $CD8^+$ T-cell responses and potentially explaining the absence of notable susceptibility to common childhood infections in this patient (Buchan *et al*, 2018).

Furthermore, disease-causing mutations have been identified in *TNFRSF1A* (McDermott *et al*, 1999) and *TNFRSF6* (Rieux-Laucat *et al*, 1995). However, in these cases, the resulting autoinflammatory phenotype appears to arise less from dysregulated NF-κB activation and more from alternative pathogenic mechanisms. Autosomal dominant mutations in *TNFRSF1A*, which encodes TNFR-1, cause TNFR-associated periodic syndrome (TRAPS), a hereditary autoinflammatory disorder (McDermott *et al*, 1999). Though the precise mechanism of the disease is still unclear, it is believed that the autoinflammation is not caused by a typical gain-of-function mutation leading to increased TNFR1 and NF-κB activation, but is rather the result of intracellular accumulation of misfolded mutant protein, defective receptor shedding, TNF-induced cell death, production of reactive oxygen species, and autophagy impairment (Cudrici *et al*, 2020). The *TNFRSF6* gene encodes the FAS receptor, and pathogenic mutations in this gene are a known cause of autoimmune lymphoproliferative syndrome (ALPS) (Rieux-Laucat *et al*, 1995). The disease is driven by defective FAS-induced apoptosis due to impaired caspase signaling, resulting in an accumulation of autoreactive T cells that would otherwise be eliminated to prevent damage to the body (Paskiewicz *et al*, 2023).

Canonical NF-κB signaling can also be initiated through activation of BCR or TCR. Following antigen presentation via MHC to TCR, the binding is stabilized by either CD4 or CD8 on T cells. After forming the immunological synapse, multiple signaling molecules are recruited, including Zeta-chain-associated protein kinase 70 (ZAP-70), lymphocyte cell-specific protein tyrosine kinase (LCK), and activating linker for the activation of T cells (LAT), resulting in the activation of phospholipase C γ (PLCγ). In B cells, antigen binding to the BCR recruits spleen-associated tyrosine kinase (SYK) and members of the Src kinase family, followed by B cell linker (BLNK) and Bruton tyrosine kinase (BTK), which subsequently activate PLCγ. Both BCR and TCR signaling

use PLCγ to generate second messengers and activate protein kinase C (PKC). PKC recruits and establishes the “CBM complex”, a protein complex made of caspase recruitment domain family member 11 (CARMA1), B cell leukemia/lymphoma 10 (Bcl-10), and MALT1paracaspase (MALT1), that ultimately acts on TGF-beta-activated kinase 1 (TAK1) and the IKK complex (Guo *et al*, 2024).

Even though no pathogenic mutations have been identified to date in IL-1R and BCR, IEIs have been reported in individuals with mutations in *TRAC* encoding for the TCRα subunit. (Morgan *et al*, 2011). The mutation resulted in reduced expression of CD3 and TCRαβ on the surface of T lymphocytes, and the patients displayed a phenotype of combined immunodeficiency with susceptibility to viral and bacterial infections (Béziat *et al*, 2021). Additionally, the patients also showed signs of immune dysregulation with lymphoproliferation, eczema, eosinophilia, elevated IgE, and autoimmunity (Sagar & Ehl, 2025).

1.3.4 Non-canonical NF-κB signaling

In contrast to canonical signaling, the non-canonical pathway is triggered by a limited set of receptors, including B-cell activating factor receptor (BAFF-R), CD40, receptor activator of nuclear factor κB (RANK), and lymphotoxin beta receptor (LTβR) (Sun, 2011). While these receptors partially also activate the canonical pathway, they have a stronger preference for TRAF3 binding and activation of the non-canonical pathway (Sun, 2011).

Whereas regulation of canonical NF-κB signaling is dependent on inhibitory proteins of the IκB family controlling the processing of the precursor protein p105 to p50, non-canonical signaling is dependent on the inhibition of the protein NF-kappa-B-inducing kinase (NIK), and the binding of p100/NF-κB2 to RelB, preventing its nuclear translocation (Figure 4) (Régnier *et al*, 1997). Under resting conditions, NIK is continuously targeted for degradation by a complex consisting of TRAF2, TRAF3, and the E3 ubiquitin ligases cIAP1/2. TRAF2 acts as a scaffold protein, recruiting TRAF3, which binds to NIK, enabling its ubiquitination via cIAP1/ 2 (Zarnegar *et al*, 2008).

Upon receptor activation, the TRAF2-TRAF3-cIAP1/2 complex is recruited to the receptor, and TRAF2 facilitates a substrate switch of cIAP1/2-mediated ubiquitination to TRAF3 instead of NIK. Following TRAF3 degradation, NIK is no longer bound and targeted for degranulation, allowing it

to accumulate and initiate downstream signaling (Zarnegar *et al*, 2008). NIK then phosphorylates IKKa, which forms activated homodimers that then bind and phosphorylate p100, resulting in its subsequent ubiquitination and partial degradation to its active form p52. The p52 and Relb dimer then translocates into the nucleus, where it binds to κB sites in DNA and acts as a major transcription factor (Xiao *et al*, 2001).

1.3.5 Effects of non-canonical NF-κB signaling

As mentioned above, the non-canonical NF-κB is generally considered a slower-acting response compared to the canonical pathway, but it leads to more sustained and long-lasting effects. However, it is important to note that this is a simplified view, as there is extensive cross-talk between both pathways. Non-canonical NF-κB signaling has been shown to be critical for lymphocyte survival and homeostasis, especially in B cells, where activation through CD40 and BAFFR is essential for multiple aspects of their biology, including development, maturation, differentiation, activation, proliferation, and survival (Sun, 2017). Activation through RANK stimulates osteoclast generation and activation (Yang *et al*, 2010).

Non-canonical NF-κB signaling is critical for the development of SLOs during embryonic development (Rennert *et al*, 1996). A special subset of hematopoietic cells termed lymphoid tissue inducer (LTi) cells are formed in the fetal liver and are crucial for the initiation of lymph nodes by interacting with stromal cells (Figure 6) (White *et al*, 2007). Studies using genetic knockout or pharmacological inhibition have demonstrated that members of the TNF superfamily of ligands and receptors are essential for this process, particularly LTβR and its ligand lymphotoxin, a heterotrimer composed of lymphotoxin alpha and beta subunits. Knockout or blockade of either LTβR or the beta subunit of lymphotoxin results in diminished lymph node formation, whereas the spleen, tough expressed, shows significant aberrations in cellular organization, characterized by dysfunctional segregation of T-cell and B-cell zones (Rennert *et al*, 1996).

Whereas LTβR is expressed on a variety of cell types, most notably stromal cells, it is almost exclusively absent on lymphocytes, which instead express its ligands lymphotoxin and the less well-characterized LIGHT (homologous to **l**ymphotoxin, exhibits **i**nducible expression and

competes with HSV **g**lycoprotein D for binding to **h**erpesvirus entry mediator, a receptor expressed on **T**-lymphocytes) (Mauri *et al*, 1998). It can therefore be described as a communication tool between immune cells and non-immune cells. LTi cells respond to RANKL and IL-7, produced by stromal and endothelial cells at sites of prospective lymph nodes, by upregulating lymphotoxin (Yoshida *et al*, 2002). Lymphotoxin then binds to LTβR expressed on stromal cells, particularly a specific subset termed lymphoid tissue organizer (LTo) cells (Wang *et al*, 2018). This results in a positive feedback loop consisting of further differentiation of LTo cells, secretion of chemokines and cytokines, recruiting additional LTi cells and other lymphoid cells to these sites, ultimately forming the lymph nodes.

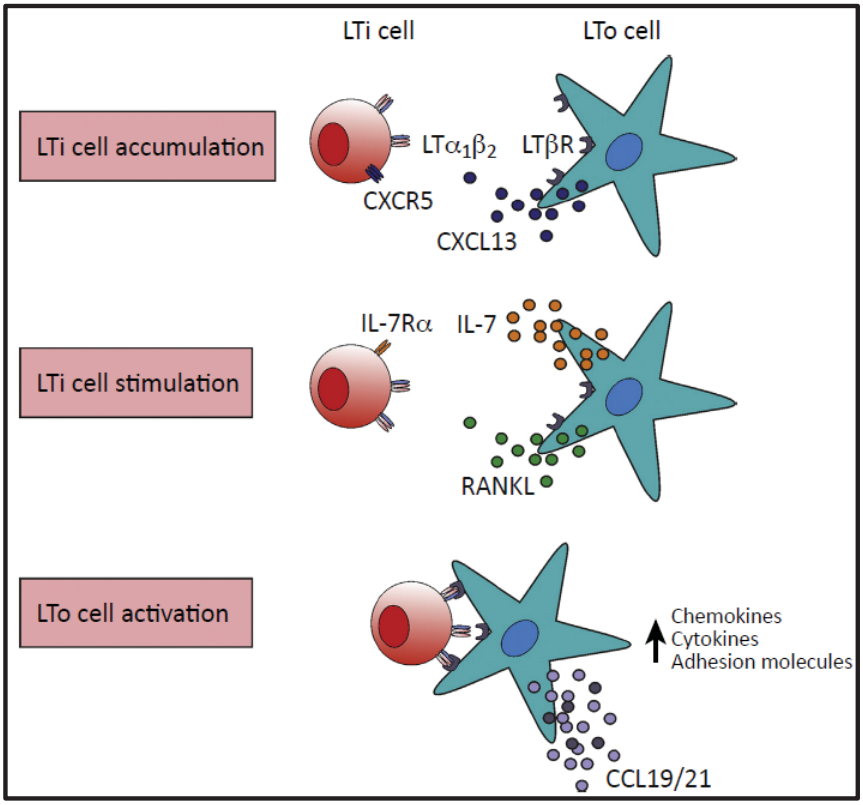

Figure 6. Early stage of lymph node development

Fetal liver derived lymphoid tissue inducer (LTi) cells interact with specialized stromal cells termed lymphoid tissue organizer (LTo) via lymphotoxin ($LT\alpha\beta_2$) and LTβR. This induces cytokine and chemokine production by the LTo cells, attracting additional LTi cells and other lymphocytes. Additionally, IL-7 and RANKL produced by the LTo cells further upregulates $LT\alpha\beta_2$ expression on LTi cells, causing a positive feedback loop.

Figure adapted from (Onder & Ludewig, 2018) *and used with permission of Elsevier Science & Technology Journals conveyed through Copyright Clearance Center, Inc.*

1.3.6 Monogenic defects in receptors driving canonical NF-κB activation

Unlike the canonical pathway, the non-canonical NF-κB pathway is almost exclusively activated by TNF receptor superfamily members, with the exception of the macrophage colony-stimulating factor receptor mediating the differentiation and proliferation of macrophages (Sun, 2017; Jin *et al*, 2014).

CD40 is expressed on a variety of cell types, including B cells, endothelial cells, monocytes/macrophages, epithelial cells, platelets, keratinocytes, and dendritic cells (Elgueta *et al*, 2009). It can be activated by both the membrane-bound and soluble forms of CD40L, which are primarily expressed on activated T-cells and platelets (Elgueta *et al*, 2009). Studies in murine models have established the essential role of CD40 signaling in germinal center formation, antibody class switching, somatic hypermutation, and the generation of memory B-cells (Foy *et al*, 1994). The discovery of individuals with complete CD40 deficiency has confirmed a similar role in human biology, as these patients are characterized by profoundly reduced memory B cells, despite normal B cell counts, along with decreased IgG and IgA serum levels, often coupled with elevated IgM levels (Ferrari *et al*, 2001). CD40 signaling also seems to affect dendritic cell function and cytokine production, resulting in a broader immunological defect that includes increased susceptibility to viral infections, hence making it a CID form of IEI (Banday *et al*, 2023).

BAFF binding to its receptor BAFF-R, which is differentially expressed at distinct stages of human B cell maturation, activates multiple downstream signaling pathways, including NF-κB2, PI3K, and ERK (Sevdali *et al*, 2021). Although various homozygous *TNFRSF13C* variants have been reported with incomplete penetrance and variable clinical phenotypes, only one homozygous deleterious variant leading to reduced BAFF-R expression has been identified in two siblings (Warnatz *et al*, 2009). These patients exhibited a developmental arrest at the transitional B cell stage, with a severe reduction in all subsequent B cell subsets, highlighting the essential role of BAFF-R signaling in B cell development and survival (Warnatz *et al*, 2009). Consequently, they had markedly decreased serum IgG and IgM levels and were unable to mount a T cell–

independent immune response against pneumococcal cell wall polysaccharides (Warnatz *et al*, 2009).

Like other members of the TNFRSF, RANK lacks intrinsic kinase activity and instead depends on the recruitment of adaptor proteins, particularly TRAFs, to initiate downstream signaling pathways, including both canonical and non-canonical NF-κB (Walsh & Choi, 2014). RANKL signaling through RANK is fundamental for osteoclast maturation, as demonstrated by osteopetrosis, the hardening of bones due to malfunctioning osteoclasts and their inability to resorb bone, in mice due to targeted deletion of either gene (Dougall *et al*, 1999). Additionally, the pathway is also critical for immune functions as highlighted by the deficiency of B cells in the spleen and complete absence of peripheral lymph nodes, whereas mucosal-associated lymphoid tissues, including Peyer's patches, were retained in $RANK^{-/-}$ mice (Dougall *et al*, 1999). A broad spectrum of diseases following mutations in *TNFRSF11A* encoding for RANKL have been described. Biallelic LOF mutations can result in severe osteopetrosis and hypogammaglobulinemia, or dysosteosclerosis, a milder sclerosing bone dysplasia typically without immune deficiency (Kırkgöz *et al*, 2022). In contrast, autosomal dominant *TNFRSF11A* mutations have been described that lead to enhanced bone resorption, presumably due to constitutive activation of RANK signaling (Guo *et al*, 2018). The gain-of-function variants result in increased osteoclastic activity and disrupted bone remodeling, causing disorganized bone architecture (Hughes *et al*, 2000; Alonso *et al*, 2021).

1.3.7 Monogenic mutations in NF-κB core members

Dysfunctional or dysregulated NF-κB signaling has been demonstrated in various diseases, including immune disorders, cancer, metabolic dysregulation, and skeletal disorders (Guo *et al*, 2024). Specifically, the multitude of identified IEIs caused by mutations in components of this pathway have clearly demonstrated the critical role of functional and regulated NF-κB signaling for immune homeostasis (Poli *et al*, 2025). The diverse functions of NF-κB in cellular processes such as proliferation, inflammation, survival, apoptosis, and tolerance give rise to a wide spectrum of phenotypes in IEIs, presenting as immunodeficiency, autoimmunity, autoinflammation, cancer susceptibility, and various combinations of these manifestations (Schnappauf & Aksentijevich, 2020). The increasing number of IEIs caused by members and regulators of this pathway not only improves our understanding of this complex master regulator

of gene transcription but also highlights the requirement of fine-tuning this important pathway. The inheritance patterns for these diseases include autosomal dominant, autosomal recessive, X-linked forms of genetic inheritance, and functional deviations following haploinsufficiency, loss-of-function (LoF), and GoF mutations (Dabbah-Krancher & Snow, 2023).

Disease-causing mutations have been described for all five members of the NF-κB family (Poli *et al*, 2025). Following their identification, heterozygous mutations in *NFKB1*(Fliegauf *et al*, 2015) and *NFKB2* (Chen *et al*, 2013) now represent the most common monogenic causes for common variable immunodeficiency with autosomal inheritance patterns (Tuijnenburg *et al*, 2018; Abolhassani *et al*, 2020). The associated clinical phenotype is highly variable and often exhibits incomplete penetrance, most likely caused by the diverse effects of individual mutations on DNA binding or nuclear translocation ability, or overall protein stability (Kaustio *et al*, 2017). Interestingly, the defect in NF-κB signaling not only causes the expected immunodeficiency, characterized primarily by recurrent infections, hypogammaglobulinemia, and impaired B-cell differentiation, but also increases the risk of autoimmunity and autoinflammation (Dabbah-Krancher & Snow, 2023). A large cohort study of *NFKB1* mutation carriers revealed that out of 156 individuals, 57.4% presented with autoimmunity, 29.6% with autoinflammation, and 16.8% with malignancy (Lorenzini *et al*, 2020). Mutations in *NFKB2* lead to an even more heterogeneous clinical phenotype, as different variants can result in either gain- or loss-of-function effects that impact the inhibitory role of p100 or the transcriptional activity of its processed form, p52, leading to a mixed clinical presentation of immune deficiency and autoimmunity (Fathi *et al*, 2024).

The identification and characterization of additional IEI patients with variants in known NF-κB pathway genes, as well as the discovery of patients with mutations in previously unlinked NF-κB–associated genes, will not only expand the clinical and genetic landscape of inborn errors of immunity but also provide critical insights into the intricate regulatory mechanisms governing NF-κB activation and its diverse roles in immune function and human disease.

1.4. Aims of this thesis

This thesis aimed to (1) identify the genetic defect underlying a novel immune disorder in three patients from two unrelated families, characterized primarily by a B cell defect, (2) provide clear evidence of a causal relationship between the genotype and phenotype, and (3) uncover novel functions of the identified gene in human immune biology.

To achieve these aims, we performed whole-exome sequencing on genomic DNA of patients 2 and 3, followed by a careful filtering strategy for the identification of potentially causative novel, rare, homo-/hemizygous-variants in immune-related genes. Following this process, the resulting list of variants in candidate genes was confirmed and segregated using Sanger sequencing on DNA isolated from blood samples of all three patients and their healthy relatives. This resulted in the identification of our main candidate gene, *LTBR,* encoding for the TNFRSF member LTβR.

Utilizing dermal fibroblasts obtained through skin biopsies from all three patients, we clearly showed the physical and functional absence of LTβR in patient cells, which we were able to correct using the CRISPR/Cas9 editing technology. We performed a variety of functional and biochemical assays to explore the consequences of absent LTβR signaling and to further our understanding of its function in human biology. Techniques applied included single-cell RNA sequencing and a newly developed ex vivo model to study the ability of different cell types to interact and induce B-cell differentiation to mimic the GC reaction. This approach allowed us to demonstrate that the lymphocytes of these patients are seemingly functional, but lack the necessary microenvironment typically provided by secondary lymphoid organs.

In summary, we define a novel human inborn error of immunity caused by biallelic loss-of-function mutations in *LTBR* encoding for the NF-κB activator LTβR, resulting primarily in a stromal defect affecting the development and function of SLOs. Our findings have a profound impact on the therapeutic strategy applied to these and potential future LTβR-deficient patients.

2. RESULTS

The following chapter contains content reprinted with permission from the American Association for the Advancement of Science, conveyed through Copyright Clearance Center, Inc. The article resulted from work done during the period of this doctoral thesis and was published in *Science Immunology* on November 22, 2024, at https://www.science.org/doi/10.1126/sciimmunol.adq8796.

The author of this thesis is the first author of this study, has acquired the majority of the published data, and was involved in the coordination of all experiments, as well as in the assembly of all figures and writing of the manuscript.

IMMUNODEFICIENCY

LTβR deficiency causes lymph node aplasia and impaired B cell differentiation

**Bernhard Ransmayr[1,2,3], Sevgi Köstel Bal[1,2,3], Marini Thian[1,2,3]†, Michael Svaton[1,2], Cheryl van de Wetering[1,2], Christoph Hafemeister[1], Anna Segarra-Roca[1], Jana Block[1,2,3], Alexandra Frohne[1], Ana Krolo[2,3]‡, Melek Yorgun Altunbas[4,5,6,7], Sevgi Bilgic-Eltan[4,5,6,7], Ayça Kıykım[8], Omer Aydiner[9], Selin Kesim[10], Sabahat Inanir[10], Elif Karakoc-Aydiner[4,5,6,7], Ahmet Ozen[4,5,6,7], Ümran Aba[11,12], Aylin Çomak[13], Gökçen Dilşa Tuğcu[14], Robert Pazdzior[2]§, Bettina Huber[15], Matthias Farlik[15], Stefan Kubicek[2], Horst von Bernuth[16,17,18,19], Ingrid Simonitsch-Klupp[20], Marta Rizzi[21,22,23], Florian Halbritter[1], Alexei V. Tumanov[24], Michael J. Kraakman[1,2,3], Ayşe Metin[25], Irinka Castanon[1,2], Baran Erman[11,12], Safa Baris[4,5,6,7], Kaan Boztug[1,2,3,26,27]*

Secondary lymphoid organs (SLOs) provide the confined microenvironment required for stromal cells to interact with immune cells to initiate adaptive immune responses resulting in B cell differentiation. Here, we studied three patients from two families with functional hyposplenism, absence of tonsils, and complete lymph node aplasia, leading to recurrent bacterial and viral infections. We identified biallelic loss-of-function mutations in *LTBR,* encoding the lymphotoxin beta receptor (LTβR), primarily expressed on stromal cells. Patients with LTβR deficiency had hypogammaglobulinemia, diminished memory B cells, regulatory and follicular T helper cells, and dysregulated expression of several tumor necrosis factor family members. B cell differentiation in an ex vivo coculture system was intact, implying that the observed B cell defects were not intrinsic in nature and instead resulted from LTβR-dependent stromal cell interaction signaling critical for SLO formation. Collectively, we define a human inborn error of immunity caused primarily by a stromal defect affecting the development and function of SLOs.

[1]St. Anna Children's Cancer Research Institute, Vienna, Austria. [2]CeMM Research Center for Molecular Medicine of the Austrian Academy of Sciences, Vienna, Austria. [3]Ludwig Boltzmann Institute for Rare and Undiagnosed Diseases, Vienna, Austria. [4]Department of Pediatrics, Division of Allergy and Immunology, Marmara University School of Medicine, Istanbul, Turkey. [5]Istanbul Jeffrey Modell Diagnostic Center for Primary Immunodeficiency Diseases, Istanbul, Turkey. [6]Işıl Berat Barlan Center for Translational Medicine, Marmara University, Istanbul, Turkey. [7]Marmara University, Immune Deficiency Application and Research Center, Istanbul, Turkey. [8]Istanbul University-Cerrahpasa, Faculty of Medicine, Department of Pediatric Allergy and Immunology, Istanbul, Turkey. [9]Kartal Dr. Lütfi Kırdar City Hospital, Department of Radiology, Istanbul, Turkey. [10]Marmara University, Faculty of Medicine, Department of Nuclear Medicine, Istanbul, Turkey. [11]Can Sucak Research Laboratory for Translational Immunology, Hacettepe University, Ankara, Turkey. [12]Institute of Child Health, Hacettepe University, Ankara, Turkey. [13]Ankara Bilkent City Hospital, Children's Hospital, Department of Nuclear Medicine, Ankara, Turkey. [14]Ankara Bilkent City Hospital, Children's Hospital, Department of Pediatric Pulmonology, Ankara, Turkey. [15]Medical University of Vienna, Department of Dermatology, Vienna, Austria. [16]Department of Pediatric Respiratory Medicine, Immunology and Critical Care Medicine, Charité University Medicine, Berlin, Corporate Member of Free University and Humboldt University and Berlin Institute of Health, Berlin, Germany. [17]Labor Berlin Charité-Vivantes, Department of Immunology, Berlin, Germany. [18]Berlin Institute of International Health Global Health Center Charité – Universitätsmedizin Berlin, Berlin, Germany. [19]Charité - Universitätsmedizin Berlin, corporate member of Freie Universität Berlin, Humboldt-Universität zu Berlin, and Berlin Institute of Health (BIH), Berlin-Brandenburg Center for Regenerative Therapies (BCRT), Berlin, Germany. [20]Medical University of Vienna, Department of Pathology, Vienna, Austria. [21]Department of Rheumatology and Clinical Immunology and Center for Chronic Immunodeficiency, Medical Center University of Freiburg, Faculty of Medicine, University of Freiburg, Freiburg, Germany. [22]CIBSS - Centre for Integrative Biological Signalling Studies, University of Freiburg, Freiburg, Germany. [23]Medical University of Vienna, Center for Pathophysiology, Infectiology and Immunology, Institute of Immunology, Vienna, Austria. [24]Department of Microbiology, Immunology, and Molecular Genetics, University of Texas Health Science Center at San Antonio, San Antonio, TX, USA. [25]Ankara Bilkent City Hospital, Children's Hospital, Department of Pediatric Immunology and Allergy, Ankara, Turkey. [26]Medical University of Vienna, Department of Pediatrics and Adolescent Medicine, Vienna, Austria. [27]St. Anna Children's Hospital, Vienna, Austria.
*Corresponding author. Email: kaan.boztug@ccri.at
†Present address: Drug Safety Research and Evaluation, Takeda Pharmaceuticals U.S.A. Inc. Cambridge, MA, USA.
‡Present address: Cancer Pharmacology and Disease Positioning at Boehringer Ingelheim, Vienna, Austria.
§Present address: Department of Chemistry, University of Konstanz, Konstanz, Germany.

INTRODUCTION

Secondary lymphoid organs (SLOs) are strategically localized throughout the body in the form of tonsils, lymph nodes, the spleen, and Peyer's patches (*1*). They act as surveillance centers and provide the specialized microenvironment necessary for the initiation of adaptive immune responses (*2*). Through a complex network of stromal cells, alongside tightly regulated chemical signals, they facilitate the interaction of various immune cell types, culminating in the formation of germinal centers (GCs) where high-affinity antibody-secreting plasma cells and memory B cells are formed (*3*).

Patients with inborn errors of immunity (IEIs), such as BTK (*4*), RAG1, and RAG2 (*5*) deficiencies, can present with nonpalpable lymph nodes. However, in these cases, the stromal compartment develops normally, and the lymph node structures are formed, although they are not populated by lymphocytes. After successful hematopoietic stem cell transplantation (HSCT), these lymph nodes can organize and function properly (*6*).

Still, there are rare cases of IEIs with aberrant SLO development beyond defects in lymphocytic compartments. Patients deficient in nuclear factor κB (NF-κB)–inducing kinase (NIK) exhibit lymph node aplasia (*7*), whereas 40*S* ribosomal protein SA (RPSA) deficiency is characterized by isolated congenital asplenia (*8*). NIK is ubiquitously expressed and hence directly influences lymphocyte function and development, whereas RPSA deficiency does not affect lymph node architecture or other lymphoid organs beyond the spleen (*7*, *8*). As far as we are aware, no isolated defect causing IEI by disrupting the stromal architecture of SLOs has been described (*9*).

NF-κB is a family of transcription factors with critical roles ranging from the coordination of immune and inflammatory responses in both innate and adaptive immune systems to the development and maintenance of lymphoid organs (*10*). Several receptors can activate NF-κB signaling in immune cells, including the T cell receptor (TCR),

B cell receptor (BCR), Toll-like receptors, and members of the tumor necrosis factor (TNF) superfamily (*10*). The lymphotoxin beta receptor (LTβR), a member of the TNF superfamily, is primarily expressed by stromal cells, such as endothelial, mesenchymal, and epithelial cells, as well as by myeloid cells, including dendritic cells (DCs) and macrophages (*11*, *12*). In contrast, its two ligands, lymphotoxin (LT) and TNF superfamily member 14 (TNFSF14/LIGHT), are predominantly expressed on activated lymphocytes and lymphoid tissue inducer cells (*11*, *13*). These inducer cells have been demonstrated to be required for lymph node formation during embryonic development in mice (*14*). Upon ligand binding, LTβR activates both the canonical NF-κB pathway and, to a greater extent, the noncanonical NF-κB pathway (*15*). The pivotal role of LTβR in the development and regulation of the immune system, through tight communication between stromal cells and lymphocytes, has been established in murine models where its absence (*16*) or inhibition (*17*) results in absent lymph nodes and Peyer's patches, as well as impaired splenic architecture. However, the role of LTβR signaling in humans has remained poorly defined. Here, we report an IEI caused by biallelic loss-of-function (LOF) mutations affecting LTβR and reveal the distinct role of LTβR signaling governing stromal cell function in shaping the microarchitecture and immunological functions of SLOs in humans previously unappreciated in murine studies.

RESULTS

An IEI with lymph node and tonsil aplasia and splenic defect

We studied three male patients (P1 to P3) from two unrelated consanguineous families (Fig. 1A) who had recurrent upper and lower respiratory tract infections starting 4 to 6 months after birth, predominantly of bacterial etiology and requiring intravenous antibiotic treatment. At the age of 3 years, P1 experienced meningitis caused by *Streptococcus pneumoniae* and recovered completely. P2 had an episode of acute hepatitis at the age of 9 years. No causative agent was identified, and a liver biopsy revealed biliary destruction (fig. S1A). We detected an accumulation of $CD4^+$ T cells and B cells as well as some $CD8^+$ T cells in the patient's biopsy, reminiscent of lymphoid infiltrates observed in studies of $Ltbr^{-/-}$ mice (*16*, *18*). After antibiotic treatment and cholecystectomy, the patient no longer exhibited symptoms of acute hepatitis. The older brother of P3 had similar disease manifestations and succumbed to disease complications, including pulmonary hypertension and cor pulmonale, at 18 years of age. Despite the recurrent infections, lymphadenopathy was not detected in any of the patients, and physical examination was remarkable for absent tonsils and nonpalpable lymph nodes. Clinical histories are summarized in Table 1 and supplemental patient clinical histories.

Lymphoscintigraphy in P1 to P3 showed complete lymph node aplasia despite normal lymphatic duct development (Fig. 1B and fig. S1B). The spleen had normal dimensions and morphology on ultrasonographic examination, but Howell-Jolly bodies in peripheral blood smears indicated severe functional hyposplenism (Fig. 1C and fig. S1C) (*19*). In addition, expression of CD47, a signal used by cells to protect themselves from splenic removal by macrophages and DCs (*20*), was decreased on lymphocytes from P1 to P3, further highlighting the impaired splenic function observed in patients with LTβR deficiency (Fig. 1D).

Laboratory studies revealed low levels of immunoglobulin A (IgA) and IgG in P1 to P3 (Table 1). IgM levels were below the age-adjusted normal range in P1 and P2, but normal in P3. After a clinical diagnosis of combined immunodeficiency, regular intravenous immunoglobulin (IVIG) substitution and antibiotic prophylaxis were initiated in P1 to P3, reducing exacerbations of respiratory tract infections. P1 tested DNA positive for genus β human papillomavirus type 24 (HPV-24) (Fig. 1E), which is associated with epidermodysplasia verruciformis and skin cancer (*21*). No other persistent viral infections were observed (Table 1 and supplemental patient clinical histories). Collectively, these results reveal an error of immunity with complete lymph node and tonsil aplasia and splenic defect.

Biallelic germline *LTBR* mutations resulting in loss of expression and impaired noncanonical NF-κB signaling

Given the enigmatic disease etiology, we performed whole-exome sequencing (WES) of P2 and P3 (fig. S2 and tables S1 to S4) and uncovered rare homozygous variants in the *lymphotoxin beta receptor* (*LTBR*) gene, segregating with the disease under the assumption of autosomal recessive inheritance (Fig. 1A and fig. S3A). The *LTBR* variant in P1 and P2 introduces a premature stop codon in exon 1 (c.91C>T, p.Gln31Ter), and P3 carries a missense variant in exon 4 (c.359G>C, p.Arg120Pro), located in a loop of the second cysteine-rich domain (fig. S3B) and predicted to destabilize the protein because of steric clashes of the substituting proline residue (fig. S3C). The identified variants were either absent or ultrarare in public databases (allele frequency < 0.00001), consistent with *LTBR* constraint metrics—a measure for negative selection based on the observed variation/expected variation ratio—hinting at intolerance to both missense and LOF variation. In silico predictions suggested a likely deleterious effect of these variants (table S5).

Serum analysis of P1 and P2 showed a decrease in B lymphocyte chemoattractant (CXCL13/BLC), a chemokine that is highly expressed in SLOs, where it controls the navigation of B cells (Fig. 1F and fig. S4, A to C) (*22*, *23*). CXCL13 is secreted after LTβR activation (*24*), and its reduction has been used as a serum biomarker of successful LTβR inhibition in clinical trials of LTβR antagonists (*25*, *26*). Dermal fibroblasts of P1 to P3 showed complete absence of LTβR protein expression (Fig. 1G). Upon binding its ligand LT, LTβR activates the noncanonical NF-κB pathway, during which the precursor p100 is processed into the active p52 form (*15*). Accordingly, treatment of patient-derived fibroblasts with LT failed to upregulate p52 (Fig. 1H and fig. S5A). In contrast, canonical NF-κB pathway activation induced by TNF-α remained intact (fig. S5B). Correction of the stop-gain variant in fibroblasts of P1 and P3 using CRISPR-Cas9 restored both LTβR expression and LT-induced p100 processing into p52 (Fig. 1, G and H, and fig. S5, A and C). Thus, these results demonstrate that the variants were LOF and causative of the observed, aberrant noncanonical NF-κB signaling.

Deficiency of memory B cells and regulatory and T_{FH} cells

Serial laboratory analyses for P1 to P3 revealed normal ranges of total leukocyte and lymphocyte counts (Table 1). Despite LTβR being absent in B and T lymphocytes (*11*, *12*, *27*) and given that terminal B cell maturation occurs mainly in SLOs, we hypothesized that B cell differentiation may be impaired (*3*). Correspondingly, despite normal total numbers of $CD19^+$ B cells, we detected a significant reduction in GC-like B cells (Fig. 2A), as well as a near absence of both class-switched and unswitched memory B cells (Fig. 2B and fig. S6) and IgA^+ or IgG^+ B cells (fig. S7A). Expansion of T-$bet^{high}CD21^{low}$ B cells is a hallmark of chronic activation of the

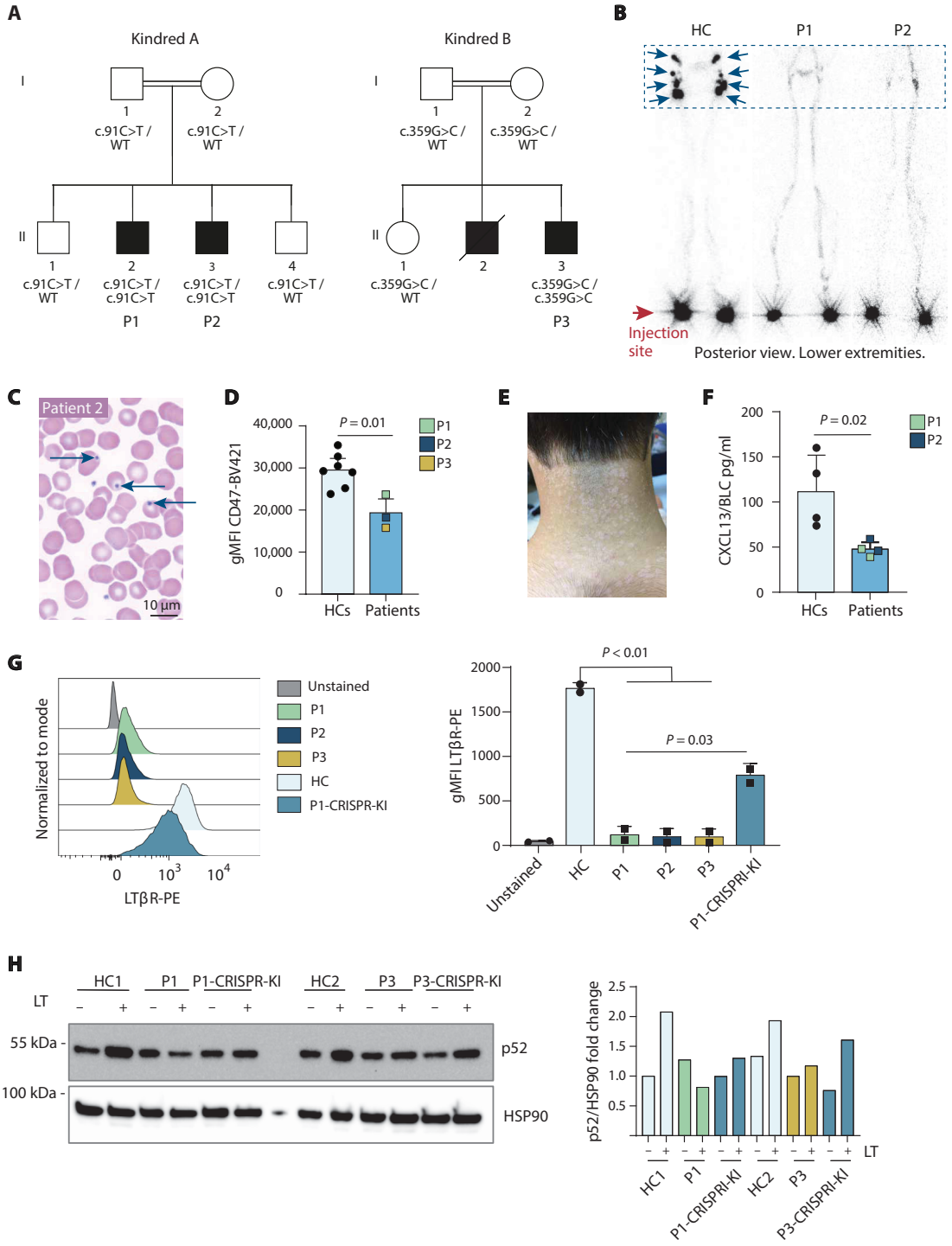

Fig. 1. Identification of patients with LTβR deficiency. (**A**) Pedigrees of the two unrelated families included in this study. Black solid symbols indicate affected individuals. Genotypes are indicated below the symbols. Squares indicate male family members, and circles female family members. Slashed symbols indicate that the individual has died. Roman numerals indicate generations, and Arabic numbers indicate individuals within a generation. (**B**) Lymphoscintigraphy images depicting the lower lymphatic system in an HC alongside P1 and P2 (posterior view). P1 and P2 display normal lymphatic duct development but lack inguinal and iliac lymph nodes (blue dashed rectangle). Blue arrows indicate the main lymphatic nodes. The red arrow indicates the injection sites. (**C**) Howell-Jolly bodies (blue arrows) in erythrocytes in a blood smear from P2. (**D**) Geometric mean fluorescence intensity (gMFI) of CD47 in lymphocytes. Data representative of $N = 2$; HCs ($n = 7$) and patients ($n = 3$). Statistical analysis performed on one of these experiments using unpaired *t* test with Welch's correction. (**E**) Innumerous verrucae planae (flat warts) on the neck of P1. (**F**) Serum values for CXCL13 for P1, P2, and controls ($n = 4$) from two separate Luminex multiplex assays (complete results displayed in fig. S4). (**G**) LTβR expression by flow cytometry analysis in fibroblasts from an HC, P1 to P3, as well as in P1-derived fibroblasts where the mutation was reverted to wild-type by CRISPR-Cas9 editing (CRISPR-KI). (**H**) Representative immunoblot displaying the expression of p52 before and after stimulation with the lymphotoxin (LT) ligand in HC-, P1-, and P1-derived CRISPR-KI fibroblasts. Quantification shown as fold change of p52/HSP90 relative to untreated HC1. HSP90 served as a loading control. Unpaired *t* test was used for statistical analysis in (D), (F), and (G).

Table 1. Clinical and immunological features of patients with LTβR deficiency. TREC and KREC reference values based on (*81*). n.d., not detected; n.a., not available; WBC, whole blood cell count; ALC, absolute lymphocyte count; ANC, absolute neutrophil count; ENA, extractable nuclear antigen; LSC, light signal count.

	Patient 1			Patient 2				Patient 3		
LTBR genomic change (HGVS, NC_000012.12)	g.6384449C>T			g.6384449C>T				g.6385266G>C		
LTBR CDS change (HGVS, ENST00000228918.9)	c.91C>T			c.91C>T				c.359G>C		
LTβR protein change (HGVS, ENSP00000228918.4)	p.Gln31Ter			p.Gln31Ter				p.Arg120Pro		
Age (years), sex	26, male			19, male				9, male		
Age (months) at onset	7			3				6		
Age at evaluation (years)	11	17	25	4	8	13	17	6 months	1.5	8
WBC (cells × 10^3/mm^3)	6.1	4.3	7.0	5.7	5.7	4.7	5.8	22.6	12.0	9.8
Normal range	4.5–13.5	4.5–13	4.5–11	5–15.5	4.5–13.5	4.5–13.5	4.5–13	6–17.5	6–17.5	4.5–13.5
ALC (cells × 10^3/mm^3)	2.1	2.1	2.0	4.0	4.0	2.8	2.6	15.0	11.0	2.5
Normal range	1.5–6.5	1.2–5.2	1–4.8	2–8	1.5–6.8	1.5–6.5	1.2–5.2	4–13.5	4–10.5	1.5–6.8
ANC (cells × 10^3/mm^3)	3.6	1.6	4.1	1.4	1.4	1.5	2.7	n.a.	n.a.	n.a.
Normal range	1.5–8.5	1.8–8	1.8–7.7	1.5–8.5	1.5–8	1.5–8.5	1.8–8			
Thrombocyte counts (cells ×10^3/mm^3)	229	218	195	295	315	490	297	n.a.	n.a.	n.a.
Normal range	150–350	150–350	150–350	150–350	150–350	150–350	150–350			
IgA (mg/dl)	<25	10	<27	24	60	4	27	<6.67	<6.67	<6.67
Normal range	(67–433)	(139–378)	(139–378)	(57–282)	(78–383)	(96–465)	(139–378)	(7–123)	(30–307)	(78–383)
IgG (mg/dl)	690	1700*	1060*	558	851	370*	1180*	150	630*	1000*
Normal range	(835–2694)	(913–1884)	(913–1884)	(745–1804)	(764–2134)	(987–1958)	(913–1884)	(304–1231)	(605–1430)	(764–2134)
IgM (mg/dl)	27	31	37	64	<17	n.a.	38	45	50	60
Normal range	(47–484)	(88–322)	(88–322)	(78–261)	(69–387)		(88–322)	(32–263)	(66–228)	(69–387)
IgE (IU/ml)	12	13.4	89	35	5	n.a.	9.72	<5	<5	<5
Normal range	<60	<60	<60	<60	<60		<60	<15	<60	<60
Anti-nuclear antibody	n.a.	n.a.	Negative	n.a.	n.a.	n.a.	Negative	n.a.	n.a.	AMA-M2, Anti-Ku
ENA profile	n.a.	n.a.	Negative	n.a.	n.a.	n.a.	Negative	n.a.	n.a.	n.a.
Anti-thyroid antibody	n.a.	n.a.	Negative	n.a.	n.a.	n.a.	Negative	n.a.	n.a.	Negative
Isohemagglutinin	1/64	1/64	1/8	1/2	n.a.	n.a.	1/2	n.a.	n.a.	n.a.
Normal range	>1/8	>1/8	>1/8	>1/8			>1/8			
TREC (copy number/10^6 cells)	912			572				n.a.		
Normal range (*81*)	Median (min–max): 6620 (1160–19,600)			Median (min–max): 12,600 (1120–36,200)						
KREC (copy number/10^6 cells)	725			520				n.a.		
Normal range (*81*)	Median (min–max): 1940 (1660–15,800)			Median (min–max): 11,335 (1720–61,000)						

(*Continued*)

(*Continued*)

	Patient 1	Patient 2	Patient 3
Anti–IFN-α antibody	n.a.	n.a.	121
Normal range < 1980 LSC			
Anti–IFN-ω antibody	n.a.	n.a.	110
Normal range < 1961 LSC			
Anti–IFN-γ antibody	n.a.	n.a.	78
Normal range < 1516 LSC			

*Patient was on IgRT at time of sampling.

adaptive immune system in certain infections or autoimmune disorders, and these numbers can be aberrant in patients with IEI (*28*). However, both P2 and P3 exhibited similar numbers of T-bet^{high}CD21^{low} B cells compared with healthy controls (HCs) (fig. S7B). After in vitro cytokine stimulation, patient B cells showed normal activation, proliferation, and, in principle, the ability to undergo class-switch into IgA- or IgG-positive cells (fig. S8). To assess the contribution of T cells to B cell dysfunction, we analyzed the T cell compartment and function in patients with LTβR deficiency. Mouse studies demonstrated the role of LTβR signaling in regulating thymic epithelial cells and stromal cells (*18*, *29*). Although P1 and P2 showed lower TCR excision circle (TREC) levels, their total number of T cells were in the normal range (Table 1), and P1 to P3 had proportions of recent thymic emigrants comparable with those of HCs (fig. S9A). Whereas the CD4$^+$ T cell subpopulations were unaffected, P1 and P2 displayed increased CD8$^+$ terminally differentiated effector memory T cells reexpressing CD45RA (TEMRA) (Fig. 2C), which may correlate with chronic antigenic exposure (*30*). T regulatory (T_{reg}) cells and T follicular helper (T_{FH}) cells were significantly reduced in P1 to P3 (Fig. 2, D and E). Murine studies have, thus far, displayed conflicting results regarding the impact of LT on T helper (T_H) cell differentiation (*13*). Whereas LT has been identified as a prototypical cytokine associated with T_H1 cell responses (*31*), observations in mice deficient in LTβR or its ligand have showed elevated levels of T_H1-type cytokines within their spleens and lungs (*32*). Conversely, exposure to *Leishmania major* infection resulted in a propensity toward T_H2 cell polarization in *Ltbr*$^{-/-}$ mice, resulting in an increase in the severity of the systemic infection (*33*). Stimulation of lymphocytes and assessment of cytokine production revealed a significant reduction in interleukin-4 (IL-4)–producing T_H2 cells in P1 to P3, as well as a trend toward lower interferon-γ (IFN-γ)–producing T_H1 and IL-17A–producing T_H17 cells (Fig. 2F). P1 and P2 T lymphocytes exhibited functionality similar to those from HCs across various in vitro functional assays, including assessments of proliferation and activation, and naïve T cell differentiation into T_{reg} cells (fig. S9B and fig. S10).

Single-cell RNA sequencing (scRNA-seq) of lymphocytes of P1 and P2 confirmed the shift in the CD8$^+$ compartment toward effector memory cells and a lower proportion of T_{reg} cells (Fig. 3, A and B, and fig. S11). Among the most differentially down-regulated genes in CD8$^+$ T lymphocytes were *LTB*, encoding for lymphotoxin-β (LT-β), which binds to LT-α to form the main ligand for LTβR, the lymphotoxin heterotrimer LTα1β2 or lymphotoxin alpha2/beta1 (LTα2β1), and *FOS*, which plays a major role in response to antigenic activation (Fig. 3C) (*17*, *34*). Despite a history of recurrent infections in both patients, differential gene expression analysis revealed no overt differences in the expression of genes associated with chronic inflammation and exhaustion pathways (table S6). Clonality analysis via bulk TCR sequencing (Fig. 3D) and scRNA-seq analysis (fig. S12) showed a reduction in the diversity of T cells from P1 and P2; however, this was driven by the expansion of a few clones on a polyclonal background. Together, these findings confirm a phenotypic shift in T cells toward an effector memory population with a constrained clonotype arrangement, suggesting their relatively quiescent state despite repetitive antigenic challenge. The conserved in vitro functions of patient lymphocytes in contrast with altered in vivo differentiation imply that the observed alterations in subpopulation distributions may not stem from an intrinsic defect within lymphocytes themselves but from alterations in the stromal compartments and the SLOs of the patients.

Alterations in the LTβR and TNF network

Having noticed the significant down-regulation of *LTB* expression across multiple CD8$^+$ cell subtypes from P1 and P2 in the scRNA-seq (Fig. 3C), we measured LTB serum levels in P2 and P3, which were significantly lower compared with HCs (Fig. 4B). We then assessed other members of the TNF family as well. Serum analysis showed a modest increase in TNF-α in P1 and P2 (Fig. 4A and fig. S13A), as well as TNF-β (the soluble homotrimer of LT-α) in P1 (Fig. 4A). TNF superfamily member 14 (TNFSF14/LIGHT), the other known ligand of LTβR, was also elevated in a multiplex analysis of serum from P1 and P2 (Fig. 4A), which was further confirmed via enzyme-linked immunosorbent assay (ELISA) in all three patients (Fig. 4C) (*12*). In addition, Fas ligand (FasL) was also increased in the patients (Fig. 4D). Similar to TNF-α and TNF-β/LTα3 (*35*), both LIGHT (*36*) and FasL (*37*) can also induce apoptosis. Furthermore, overexpression of LIGHT in mice results in autoimmunity (*38*), and increased levels of LIGHT or FasL are associated with autoimmunity in humans (*39*, *40*). In previous studies, *Ltbr*$^{-/-}$ mice exhibited a phenotype of immune dysregulation characterized by splenomegaly, autoantibody production, and

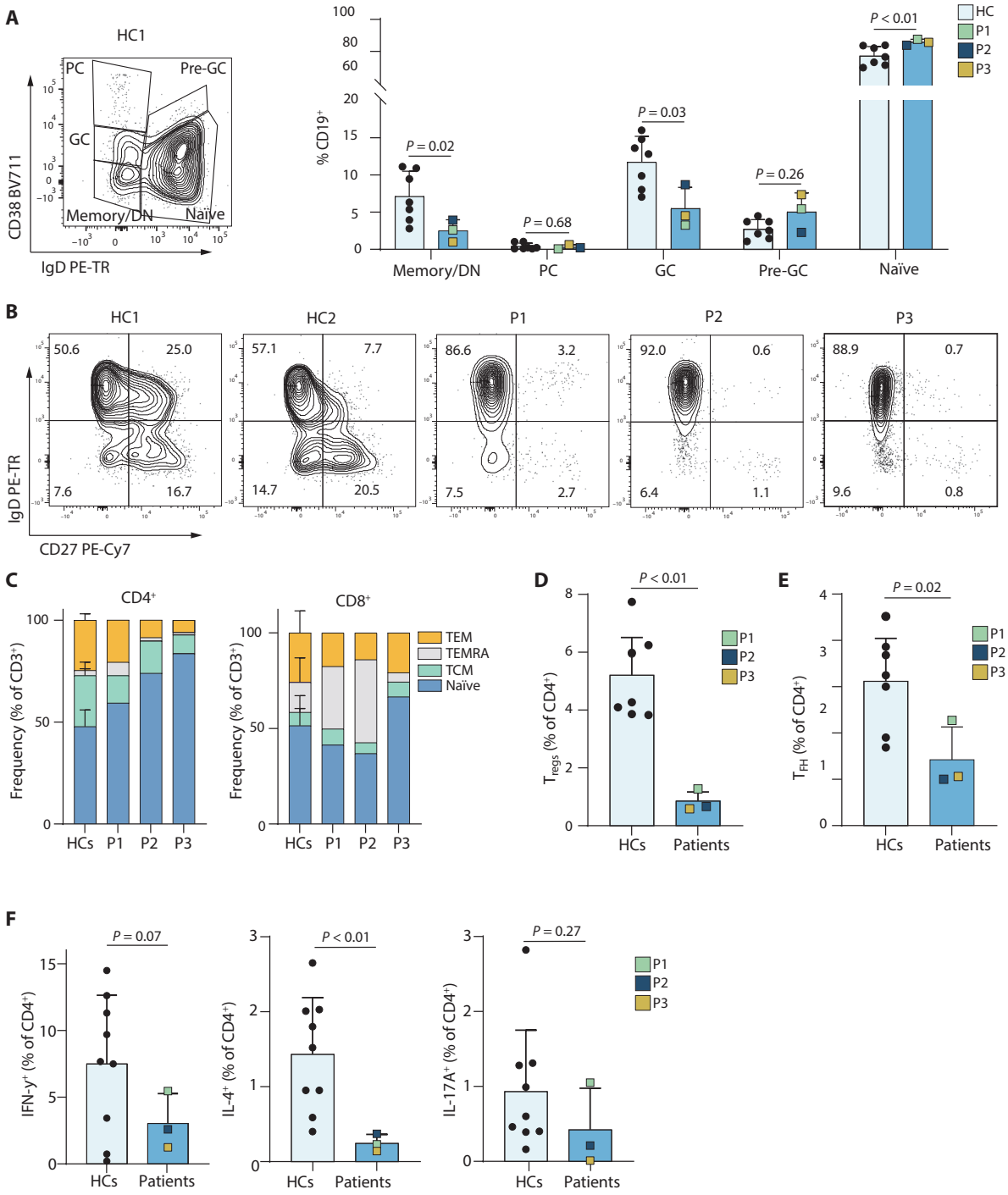

Fig. 2. In-depth characterization of the immune cell compartment from patients with LTβR deficiency. (**A**) Gating strategy to identify subpopulations of $CD19^+$ B cells using flow cytometry and results from patients and HCs ($n = 9$). Subpopulations were classified as plasmablasts, pre-GC, and GC naïve or memory/DN (double-negative). Data shown here are from one experiment, representative of $N = 5$; HCs ($n = 7$) and patients ($n = 3$). (**B**) Representative plots from two HCs and P1 to P3, highlighting the reduction of both class-switched (IgD^-CD27^+) and unswitched (IgD^+CD27^+) $CD19^+$ B cells in the patients. (**C**) Distribution of naïve ($CD45RA^+CCR7^+$), central memory (TCM $CD45RA^-CCR7^+$), terminally differentiated effector memory T cells reexpressing CD45RA (TEMRA $CD45RA^+CCR7^-$), and effector memory (TEM $CD45RA^-CCR7^-$) subpopulations within $CD4^+$ and $CD8^+$ T cell fractions. The data shown here are from one experiment, representative of $N = 4$; HCs ($n = 7$) and patients ($n = 3$). (**D**) Frequency of $CD25^+FOXP3^+$ T_{reg} cells. The data shown here are from one experiment, representative of $N = 2$; HCs ($n = 7$) and patients ($n = 3$). Statistical analysis was performed on one of these experiments. (**E**) Frequency of $CD45RA^-CCR7^-CXCR5^+$ T_{FH} cells. The data shown here are from one experiment, representative of $N = 5$; HCs ($n = 7$) and patients ($n = 3$). Statistical analysis was performed on one of these experiments. (**F**) Distribution of T_H subsets, characterized by cytokine expression on $CD3^+CD4^+CD25^-CD45RA^-$ T cells after 5-hour stimulation with PMA and ionomycin. Results show a shift in the patients from IL-4–producing T_H2 and IL-17–producing T_H17 subsets toward the IFN-γ–producing T_H1 cells (HCs, $n = 10$). The experiment was performed twice with cells from P1 and P2. Statistical analysis was done using ANOVA followed by Bonferroni correction in (A) and unpaired *t* test with Welch's correction in (D) to (F).

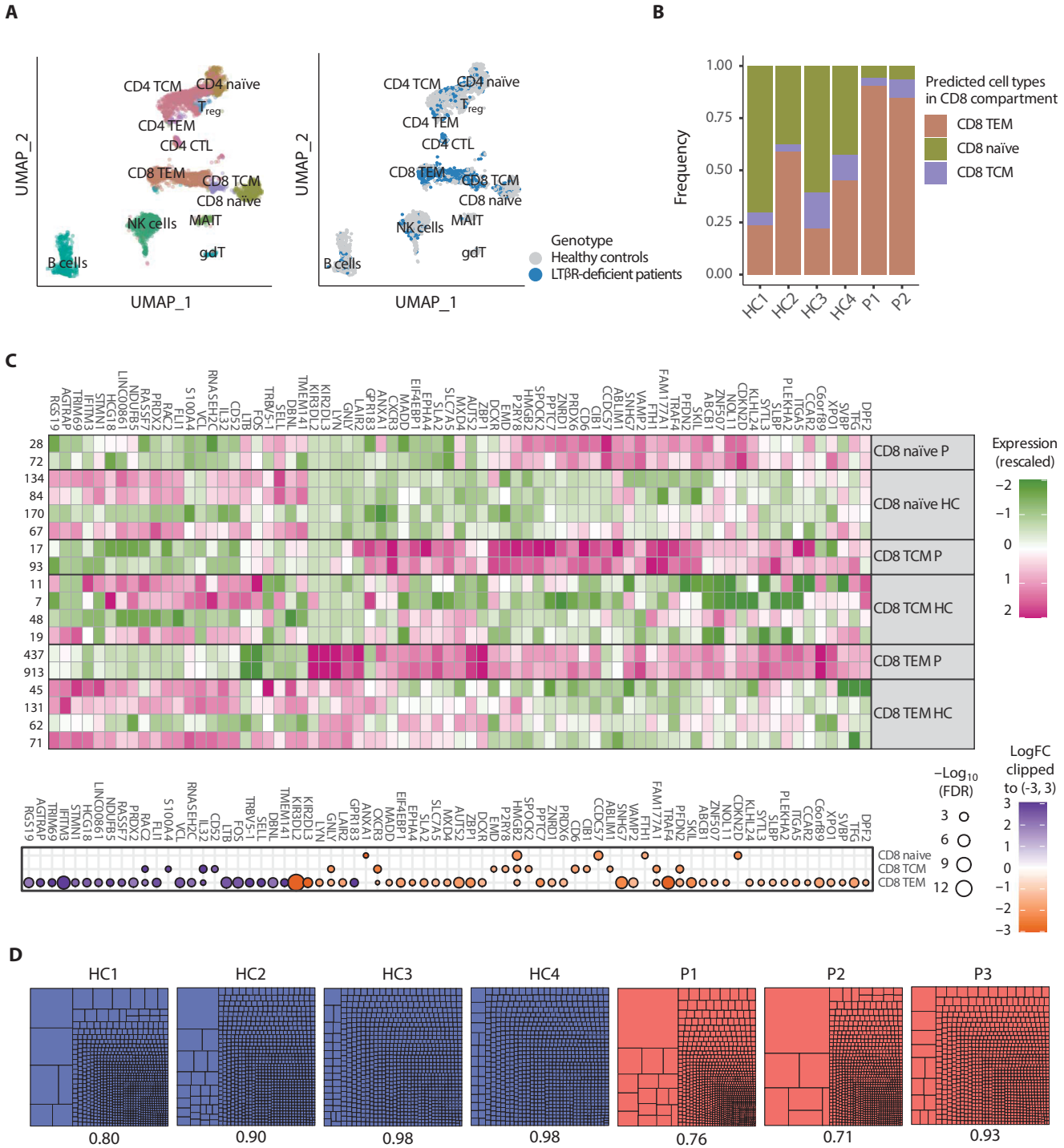

Fig. 3. Sequencing analysis reveals LTB down-regulation and reduced TCR clonality. (**A**) Low-dimensional projection (UMAP plot) of the combined scRNA-seq dataset from P1 and P2 and four HCs. In the left panel, colors correspond to the cell type identified by label transfer from a reference dataset of healthy PBMCs. The right panel displays the same projection, with colors indicating the distribution of patient cells (blue) with the clusters compared with controls (gray). (**B**) Distribution of CD8 T cell compartments in the scRNA-seq data. (**C**) Heatmap showing pseudobulk expression data for genes (shown as columns) that are differentially expressed among P1, P2, and HCs within the $CD8^+$ T cell population (samples and cell types shown as rows). Numbers on the left indicate cell count per group. Dot plots indicate the degree of significance and in which subtypes they were observed. (**D**) TCR clonality results obtained from bulk DNA TCRB sequencing in the 1000 most abundant clones with a productive TCRB VDJ rearrangement and Shannon's evenness indices below each plot.

lymphocytic infiltrates (*16*, *18*, *41*). None of the patients in our cohort had clinically overt autoimmunity or autoinflammation. We screened the patients with extensive autoantibody detection panels, which were negative in P1 and P2. However, P3 tested positive for anti-Ku and anti-mitochondrial antibodies (AMA-M2) despite normal serum liver and renal parameters (Table 1), implying that the presence of these

autoantibodies has not resulted in any clinical manifestations or organ-related disease in this patient to date. Although autoantibodies against type I IFNs have recently been reported in several monogenic IEIs affecting the noncanonical NF-κB pathway (*42*), we could not detect these antibodies in serum from P3 (Table 1).

In addition, increased levels of decoy receptor 3 (DcR3/TNFRSF6B) were observed in the patient's serum compared with those in HCs (Fig. 4E and fig. S13B). DcR3 is a soluble protein with anti-inflammatory properties, acting through the inhibition of both LIGHT and FASL (*43*, *44*). Unexpectedly, we were also able to detect DcR3 in various samples of commercially available IVIG products (Fig. 4D and fig. S13, B and C). Furthermore, we observed that IVIG treatment of a patient with an IEI resulted in increased DcR3 serum levels (fig. S13C). Previous studies have linked DcR3 production to

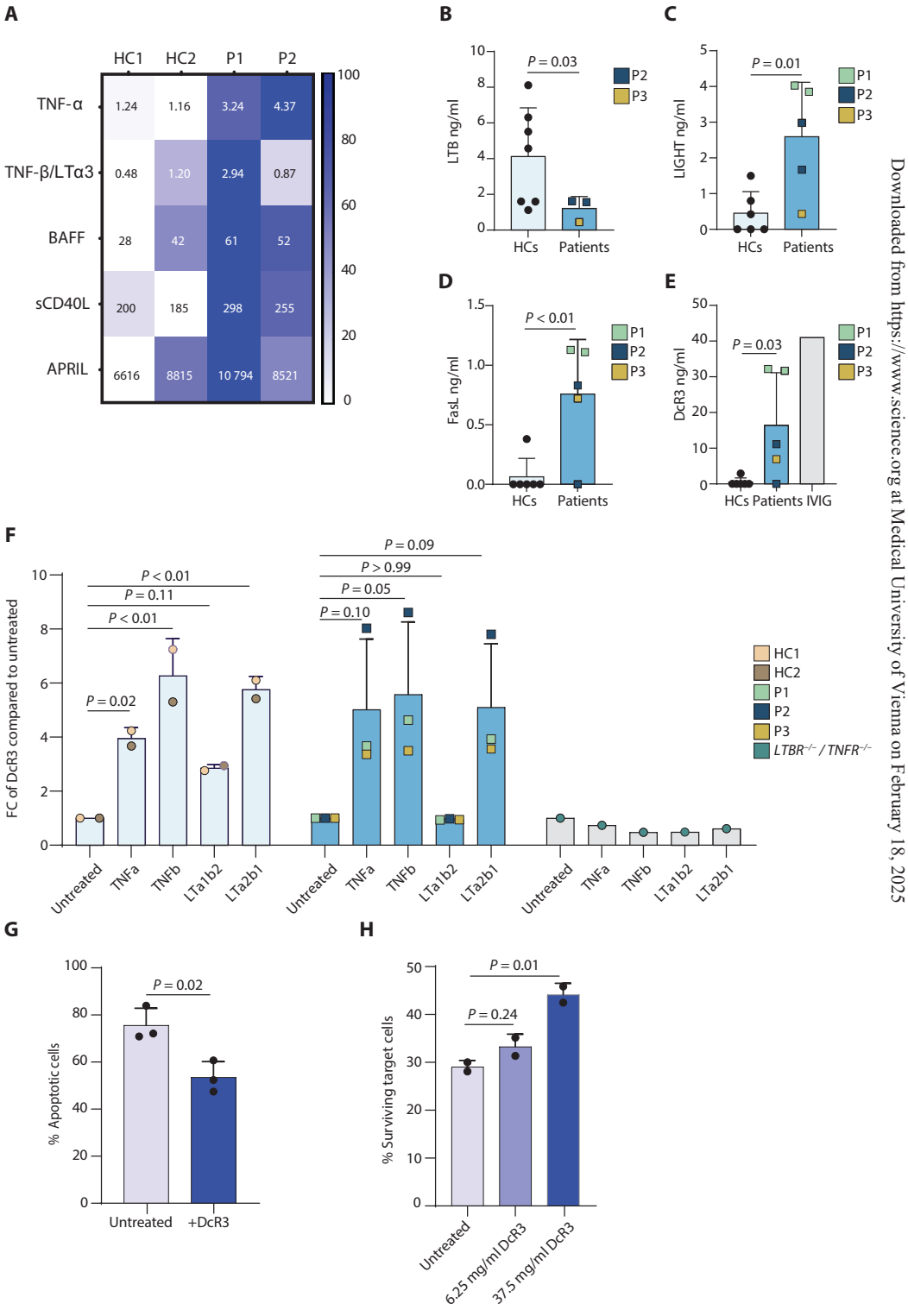

Fig. 4. Alterations in the LTβR/TNF network and the immunomodulatory effect of DcR3. (**A**) Heatmap depicting LEGENDplex multiplex assay for serum samples from P1 and P2 compared with HCs ($n = 2$). Results were individually normalized, with the lowest value set to 0 and the highest value set to 100. All other values were scaled proportionally between these two extremes. Numbers shown are absolute values in picogram per milliliter. (**B**) ELISA serum analysis for LTB. Data are from one experiment with HCs ($n = 7$) and from P2 ($n = 2$) and P3 ($n = 1$). (**C** to **E**) ELISA results for LIGHT/TNFSF14 (C), FasL (D), and DcR3 (E) for serum samples from HCs ($n = 6$) and samples pooled from P1 and P2, from two blood draws, and one from P3. In (E), commercially available IVIG was also tested. Samples from P1 and P2 were taken from two time points. (**F**) ELISA results of DcR3 fold change in treated fibroblasts normalized to untreated cells for HCs ($n = 2$), patients ($n = 3$), and cells from P2 where TNFR1 was knocked out. Each data point represents the average of $N = 2$. (**G**) AICD after restimulation of feeder-expanded T cells with soluble anti-CD3 (sCD3). Graph representing the percentage of apoptotic cells with or without DcR3 treatment. Dots represent average of individual healthy donors ($n = 3$) over two independent experiments. (**H**) Effect of DcR3 treatment on the killing capacity of expanded T cells based on percentage of surviving cocultured p815 target cells treated with sCD3 (0.1 μg/ml) compared with the results in the same condition without the addition of sCD3. Data are representative of two independent experiments, including two of the HCs repeated as a biological replicate. Statistical analysis performed on one of these experiments. Analysis in (B) was performed using unpaired *t* test with Welch's correction. Analysis in (C) to (E) and (G) was performed using unpaired *t* test. Analysis in (F) and (H) was performed using ANOVA followed by Dunnett's post hoc test for multiple comparisons.

PI3K/NF-κB activation (*45*). Treatment of dermal fibroblasts with either TNF-α or TNF-β/LTα3 resulted in the secretion of DcR3 (Fig. 4F), as did treatment with the two known isoforms of lymphotoxin, LTα1β2 and LTα2β1. This effect was dependent on TNFR1 and LTβR stimulation, respectively, because fibroblasts from P2 with an additional TNFR1 knockout showed no response to any of the ligands. Whereas LTα2β1 is capable of binding both receptors, LTα1β2 binds exclusively to LTβR (*46*). Subsequently, LTα1β2 had no effect on patient-derived fibroblasts, whereas LTα2β1 was also able to induce DcR3 production comparably to that of HCs. To assess the immune modulatory function of DcR3, we treated feeder-expanded T cells with DcR3, which protected the T cells from activation-induced cell death (AICD) (Fig. 4G) and reduced the potency of their effector functions such as cytotoxic killing (Fig. 4H). Although the encoding gene is present in the human genome, there is no ortholog in mice (*43*). Collectively, these data demonstrate dysregulation of several members of the TNF superfamily in patients with LTβR deficiency.

Ex vivo coculture reveals functional B cell activation and differentiation

To further characterize the B cell compartment in patients with LTβR deficiency, we performed BCR sequencing and analyzed the somatic hypermutation (SHM) rate in the Ig heavy-chain variable regions (*IGHV*). Whereas the B cell repertoire diversity was comparable between the patients and HCs, indicating that the process of V-D-J recombination and the ability to generate mature naïve B cells is intact in the patients, we observed a significant reduction in the number of mutations in the *IGHV* regions and the percentage of individual B cell clones in which SHM occurred (Fig. 5A and fig. S14, A and B), further corroborating the lack of an efficient GC reaction. Although LTβR signaling is critical for SLO development (*17*, *27*), its direct role in GC formation is less clear (*12*). Established assays to measure B cell differentiation use cytokine stimulation instead of direct cell-cell interactions. We devised an ex vivo model to study the ability of different cell types to interact and induce B cell differentiation to mimic the GC reaction (fig. S15, A to C). We cocultured different combinations of peripheral blood mononuclear cells (PBMCs), DCs, and dermal fibroblasts with or without additional stimulation of a vaccine for measles, mumps, and rubella (MMR) in a transwell system. The DCs were differentiated ex vivo from monocytes and then activated with polyinosinic:polycytidylic acid (poly I:C) (fig. S15B). The dermal fibroblasts were either donor derived or modified by generating *BM2*$^{-/-}$ fibroblasts to inhibit human leukocyte antigen I (HLA-I) expression and prevent T cell–mediated apoptosis (fig. S15C). After the coculture, B cells from HCs, despite some level of variability, showed an up-regulation of the activation marker CD25 as well as activation-induced cytidine deaminase (AID), the enzyme initiating SHM (Fig. 5B) (*47*).

Despite the absence of LTβR signaling, patient B cells were able to differentiate into CD27^{+} memory B cells when coculturing lymphocytes with activated monocyte-derived DCs and stromal cells (Fig. 5C and fig. S16). The additional stimulation with the MMR vaccine induced the differentiation into GC-like (IgD^{-}CD38^{+}) B cells (Fig. 5C and fig. S16). Hence, LTβR deficiency does not result in an intrinsic B cell defect.

Together, these data suggest that LTβR signaling, although critical for SLO development, becomes redundant for B cell differentiation in a GC-like setting if immune cells and stromal cells are brought into close proximity artificially. Therefore, the observed humoral defects in patients with LTβR deficiency may stem from the absence of a conducive environment typically provided by the stromal compartment in SLOs.

DISCUSSION

SLOs play a crucial role in initiating the adaptive immune response and establishing immune memory. Although the formation and organization of SLOs remain active areas of research, LTβR signaling has been identified as a key factor in lymph node development in mice. However, its relevance to humans has been less clear. In this study, we identify LTβR deficiency as the underlying cause of a previously unknown combined immunodeficiency, characterized by a distinct absence of functional SLOs, resulting in hypogammaglobulinemia and low memory B cell levels. The T cell compartment alterations are likely contributing to the observed susceptibility to viral infections, including β-HPV (*21*, *48*).

Although the observed defects in the SLOs are consistent with previously published *Ltbr*$^{-/-}$ mouse models (*12*, *16*, *49*), other key signs of immune dysregulation observed in mice (*18*, *41*, *50*) were not as prominent in patients with LTβR deficiency. We speculate that the defect in the SLOs and subsequently aberrated B cell differentiation and activation may, paradoxically, protect patients from developing and sustaining autoantibody-producing plasma cells. All three patients have been receiving IgG substitution, which is a well-established immune replacement therapy for various autoimmune disorders (*51*), despite its heterogeneity and unclear composition (*52*). We detected increased levels of the DcR3 protein in serum samples at different time points throughout disease progression in all three patients. DcR3 is a protein that has previously been reported to be anti-inflammatory and antiapoptotic via blockade of FasL and LIGHT (*53*), in line with the increased survival and decreased killing activity shown in our study. Intriguingly, DcR3 is not encoded in mice (*43*, *44*). In addition to confirming the immunoregulatory function of DcR3 on human T lymphocytes, we detected high concentrations of DcR3 in various commercially available IVIG solutions. Therefore, it is possible that the increase of DcR3 in patients with LTβR deficiency is in part due to the imbalance of several TNF members or the IVIG replacement therapy. Further delineation of a potential role of DcR3 in modulating immune dysregulation will require additional studies in the future.

The TNF superfamily receptors, particularly RANK, CD40, and LTβR, play crucial roles in the formation of the thymic microenvironment and the induction of central tolerance (*54*). The RANK and CD40 signaling pathways are essential for the development of medullary thymic epithelial cells (mTECs) and the expression of the autoimmune regulator (AIRE), a master regulator of ectopic peripheral antigen expression (*55*). AIRE is vital for negative selection by promoting the expression of peripheral tissue-restricted antigens (TRAs) in mTECs, thereby preventing autoimmunity by ensuring self-tolerance. Mutations in *AIRE* lead to autoimmune polyendocrinopathy candidiasis ectodermal dystrophy, a monogenic disorder characterized by multiorgan autoimmune destruction with a distinct IFN-γ–mediated inflammatory signature (*56*). In contrast, although the LTβR signaling pathway is also necessary for normal thymic architecture and mTEC differentiation, it does not influence AIRE expression or AIRE-dependent TRA expression. Instead, LTβR signaling induces the transcriptional regulator FEZF2, which governs the expression of a distinct set of TRAs (*54*). In LTβR-deficient mice, FEZF2-dependent TRA

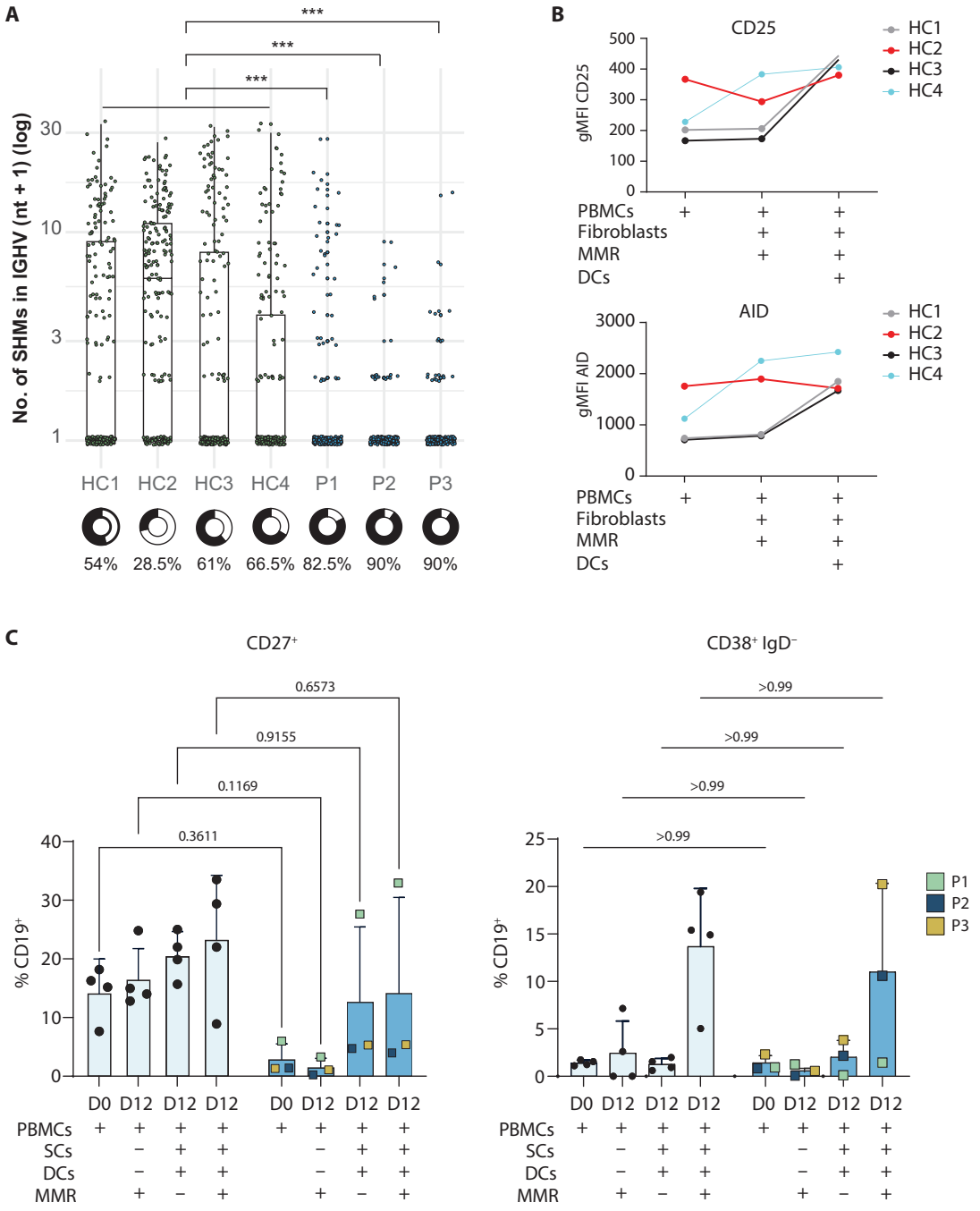

Fig. 5. Functional ex vivo B cell activation in LTβR-deficient cells. (**A**) The rate of SHM in the *IGHV* of the top 200 B cell clones with productive IGH rearrangements. Each dot represents a unique B cell clone with the number of mutated nucleotides (nt) plus one on the *y* axis (logarithmic scale). The percentage of clones with no SHM is shown below each sample in a circular plot. Asterisks represent *P* values <0.001 of Dunnett's test comparison between individual patient samples and the aggregate of HC samples. (**B**) Up-regulation of the activation marker CD25 and AID in $CD19^+$ B cells from HCs ($n = 4$) after 7 days of coculture in various combinations of PBMCs, SCs, DCs, and MMR vaccine as indicated in the panel. (**C**) Differentiation of $CD19^{+S}$ B cells from controls ($n = 4$) and patients into $CD27^+$ memory or $CD38^+IgD^-$ GC-like B cells after 12 days of coculture. Measurements were compared with day 0. Indicated conditions include the addition of stromal cells (SCs), monocyte-derived DCs, or additional treatment with an MMR vaccine. All conditions were stimulated with BAFF every other day. Readout was performed using flow cytometry.

expression is reduced in mTECs, highlighting an alternative pathway for TRA expression independent of AIRE, which implies that LTβR signaling supports the maintenance of thymic stromal cell subsets and chemokine production, playing a broader role in the regulation of the thymic microenvironment. Consistent with this distinct downstream transcriptional impact, the clinical phenotype of patients with LTβR deficiency is quite different from that of AIRE deficiency (*56*), presenting predominantly as B cell dysfunction without the IFN-γ–mediated chronic inflammation and autoimmunity.

Not only $Ltbr^{-/-}$ mice but also mice overexpressing the LTβR ligands LT or LIGHT can exhibit signs of autoimmunity (*39*, *57*), likely to be caused by the unregulated formation of tertiary lymphoid

organs (TLOs) (*58*). These are ectopic lymphoid structures that arise temporarily in proximity to sites of chronic inflammation and resemble SLOs in their organization, function, and dependence on LTβR signaling (*58*). Despite their role as gatekeepers and as a favorable prognostic factor in cancer, TLOs are associated with increased tissue damage in autoimmune diseases (*58*). Thus, LTβR signaling has been a therapeutic target in autoimmune diseases, including rheumatoid arthritis or Sjögren's syndrome, but clinical trials using inhibitors for LTβR (*25*) or its ligand (*26*) have been unsuccessful. The results from our ex vivo GC model suggest that once the process of GC formation has been initiated in either SLOs or TLOs, blockade of LTβR may not suffice to stop the ongoing GC reaction and production of autoantibody-secreting plasma cells.

Our study shows that biallelic LOF mutations in *LTBR* cause an IEI with a predominantly humoral immune deficiency and milder T cell defects, in contrast with murine models where the role for LTβR signaling in autoimmunity was demonstrated by controlling thymic stroma and intestinal microbiota (*59*). Further corroborated by murine data, the nonlymphocyte lineage–specific expression of LTβR suggests that allogeneic HSCT may not provide a curative treatment for human LTβR deficiency (*12*), whereas anti-infective prophylaxis using IVIG and prophylactic antibiotics is imperative. Our study advances our understanding of LTβR as a critical factor of human immune homeostasis, with implications for potential targeted therapies in the context of severe infections and autoimmunity. Whether the observed increase in DcR3 modulates the clinical phenotype warrants further research, and to refine therapeutic strategies, a more profound comprehension of human-specific molecular regulation and tissue specificity in lymphotoxin signaling is paramount. Another limitation of our study—similar to other studies identifying genetic etiologies of rare diseases—is the relatively low numbers of patients identified with this genetic defect, implying that future studies with additional affected individuals will enable the delineation of the full phenotypic spectrum of disease and potential genotype-phenotype correlations.

MATERIALS AND METHODS

Study design

The objective of this study was to investigate the role of LTβR in human immune homeostasis. For this purpose, we performed an array of functional and multiomic experiments on primary material from the patients carrying a germline-encoded homozygous mutation in *LTBR*, after genetic analysis. Furthermore, we made use of cellular models to investigate the effects of the *LTBR* mutation on the function of lymphocytes and stromal cells using biochemical and proteomic approaches. This included a self-developed coculture system of different immune and stromal cells to assess their interaction and capacity to stimulate B cell differentiation. Control samples were used either from healthy shipment controls or taken from healthy local donors.

Study oversight

The study was approved by the relevant institutional review boards and performed in accordance with the guidelines of good clinical practice and the current version of the Declaration of Helsinki. Written informed consent was obtained from the patients or the patients' legal representatives.

Patient and human cell lines

PBMCs from the patients and HCs were isolated via Ficoll gradient. Patient- and HC-derived T cells were expanded by stimulation of PBMCs with irradiated feeder cells, phytohemagglutinin (PHA; 1 μg/ml, Sigma-Aldrich), and IL-2 (100 IU/ml, Novartis) in RPMI 1640 medium containing 5% human serum (IBJB – Inst. Biotechnologies J.BOY, 201021334) and supplemented with 1 mM sodium pyruvate (Thermo Fisher Scientific, 11360039), minimum essential medium nonessential amino acid solution (Sigma-Aldrich, M7145), penicillin (50 U/ml), streptomycin (50 mg/ml), and 10 mM Hepes. Fibroblasts were isolated from skin biopsies from patients and HCs and cultured in Dulbecco's modified Eagle's medium (DMEM) containing 10% fetal calf serum (FCS), penicillin (50 U/ml), streptomycin (50 mg/ml), and 10 mM Hepes. All cells were cultured at 37°C in a humidified atmosphere with 5% CO_2.

Whole-exome sequencing

Genomic DNA (gDNA) was isolated from peripheral blood samples using commercial extraction kits [P2: DNeasy Blood and Tissue Kit (Qiagen); P3: GenEx Blood (GeneAll)]. WES of P2 involved library preparation and exome enrichment using Nextera Rapid Capture Exome kit (Illumina), followed by 150–base pair (bp) paired-end sequencing on the Illumina HiSeq3000 system. Sequenced DNA reads were mapped to the human reference genome (GRCh38/hg38 assembly) by means of the Burrows-Wheeler Aligner (*60*). After variant calling with the Genome Analysis Toolkit HaplotypeCaller (*61*), variant effect predictor was used for annotating single-nucleotide variants and small insertions/deletions (*62*). From the obtained variant calls, nonsynonymous (nonsense, missense, small insertions, and deletions) and splice-region variants (±8 bp from the intron/exon boundaries) were then filtered to exclude those with a minor allele frequency > 0.01 in gnomAD v2.1.1 (*63*).

An in-house database including sequencing data from >1200 individuals was used to further exclude recurrent variants with an allele frequency > 0.02. The remaining variants were prioritized on the basis of literature research and their combined annotation dependent depletion pathogenicity prediction score (*64*).

For P3, the WES library was prepared using the Nextera DNA Prep with Enrichment Kit (Illumina), and sequencing was performed with 150-bp paired-end reads on the Illumina NextSeq 550 platform. Data processing, including mapping, variant calling, and annotation, was conducted with the SEQ Platform v8 (Genomize).

Sanger sequencing

Isolation and purification of gDNA from the probands and family members of both kindreds was performed from peripheral blood using the DNeasy Blood and Tissue Kit (Qiagen). Sanger sequencing was used for the validation and segregation of the *LTBR* variants identified via WES in the patients and their family members. Specific primers were designed to amplify the genomic regions encompassing each of the two identified variants. Sanger sequencing primers used for validation and segregation

of *LTBR* variants in the patient and family members are shown in table S7.

Protein structure visualization

The three-dimensional (3D) structural model of wild-type LTβR was obtained from AlphaFold and visualized with PyMOL (Molecular Graphics System, version 2.0 Schrödinger LLC) (*65*, *66*). MISSENSE3D was used to predict possible effects of p.Arg120Pro on the protein (*67*, *68*).

CRISPR-Cas9 editing of human cells

For the reconstitution experiments, dermal fibroblasts derived from P1 and P3 were edited using CRISPR-Cas9 to reexpress LTβR. Cells were collected and resuspended in Opti-MEM (Thermo Fisher Scientific, 31985062). For electroporation, 10^6 cells were used per condition. Before electroporation, 125 pmol of Cas9 protein (IDT, Alt-R S.p. Cas9 Nuclease V3) and 150 pmol of single gRNA were mixed and incubated for 15 min at room temperature. Subsequently, 100 pmol of single-stranded oligodeoxynucleotide (ssODN) template was added to the cells (table S8). A NEPA21 electroporator (NepaGene) was used for electroporation with the following settings: poring pulse: 250 V, 2.5-ms pulse length, total of two pulses with 50-ms interval between the pulses, 10% decay rate with + polarity; transfer pulse: 20 V, 50-ms pulse length, total of five pulses with 50-ms intervals between the pulses, 40% decay rate with ± polarity. Next, the cells were seeded in DMEM supplemented with 10% FCS. Ten days later, the cells were stained with LTβR antibody and sorted using a fluorescence-activated cell sorting (FACS) Aria Fusion cell sorter. Positive cells were used for further analysis.

For the coculture experiments, dermal fibroblasts from an HC were edited using CRISPR-Cas9 to knock out B2M to prevent expression of HLA-I. Except for the addition of an ssODN template, the electroporation was performed the same way as described above. Afterward, the cells were seeded in DMEM supplemented with 10% FCS. Ten days later, the cells were stained with HLA-I antibody and sorted using an FACS Aria Fusion cell sorter. Negative cells were used for further analysis. Dermal fibroblasts from P2 were used and processed for TNFR1 knockout the same way.

Flow cytometry

PBMCs, either fresh or cryopreserved in liquid nitrogen, were used for immunophenotyping. To reduce unspecific antibody binding, the cells were blocked in RPMI 1640 containing 10% FCS for at least 1 hour before surface staining with antibodies (listed in table S9) for 30 min in the dark at 4°C. Stained cells were acquired with an LSR-Fortessa (BD Biosciences) or FACSymphony (BD Biosciences). FlowJo v10 was used to analyze the data, and Prism v.8 (GraphPad) was used to produce graphs. For intracellular staining, the cells were permeabilized after surface staining with BD 1× Perm/Wash buffer before additional staining with intracellular antibodies for 30 min in the dark at 4°C. The complete list of antibodies used in this study is shown in table S9.

T cell activation and proliferation assay

Feeder-expanded T cells from patients and HCs were stained with violet proliferation dye (VPD450, BD Biosciences) and seeded on 96-well U-shaped plates at 400,000 cells per well in 100 μl of RPMI 1640 supplemented with 10% FCS. The cells were stimulated with either soluble anti-CD3 (sCD3, clone: OKT3; 1 μg/ml), a combination of sCD3 (1 μg/ml) with soluble anti-CD28 (sCD3/CD28, 1 μg/ml, eBioscience), PHA (5 μg/ml, Peprotech), CD3/CD28 DynaBeads (Beads, Invitrogen), or left untreated. Activation was assessed after 24 hours using flow cytometry. Proliferation was measured after 4 days of stimulation by diluting the VPD450.

T_{reg} cell differentiation assay

The T_{reg} cell differentiation assay was used according to the to the manufacturer's protocol (CellXVivo Human T_{reg} Cell Differentiation Kit #CDK006) with small adaptations. In brief, cryopreserved PBMCs from HCs and patients were thawed, and naïve T cells were isolated via magnetic bead separation (Miltenyi, 130-097-095). From each donor, 50,000 cells were either resuspended with RPMI 1640 complete supplemented with 10% FCS or treated using human T_{reg} differentiation medium as prepared using the manufacturer's instructions. Treated cells were then seeded into a 96-well ELISA plate that had been coated with anti-CD3 (clone: OKT3) for 24 hours, whereas the untreated cells were added to uncoated wells. Differentiation of T_{reg} cells was measured after 5 days of cultivation using flow cytometry.

T_H cell cytokine production assay

Cryopreserved PBMCs from patients and HCs were thawed and seeded on 96-well U-shaped plates at 300,000 to 500,000 cells per well in RPMI 1640 supplemented with 10% FCS. Cells were stimulated with 200 nM phorbol 12-myristat 13-acetat (PMA, Sigma-Aldrich) and ionomycin (1 μg/ml, Sigma-Aldrich) or left untreated for a total of 6 hours. After 1 hour of stimulation, brefeldin-A (BioLegend) was added to the cells. Cells were stained with surface antibodies before fixation and stained with intracellular cytokine antibodies. Cells were analyzed using flow cytometry.

B cell activation and proliferation and class switch assay

Cryopreserved PBMCs from P1, P2, and HCs were thawed and stained with violet proliferation dye (VPD450, BD Biosciences) before being seeded on 96-well U-shaped plates at 400,000 cells per well in 100 μl of RPMI 1640 supplemented with 10% FCS. The cells were stimulated with either IL-4 (100 ng/ml, Peprotech) + CD40L (200 ng/ml, Peprotech), IL-21 (20 ng/ml, Peprotech) + CD40L (200 ng/ml), CpG (50 nM, InvivoGen), or left untreated. Activation was assessed after 24 hours using flow cytometry. Proliferation was measured after 6 days of stimulation by diluting the VPD450. Class switch was measured after 5 days of stimulation by $CD19^+$ B cells expressing IgA or IgG.

B cell differentiation assay

Cryopreserved PBMCs from patients and HCs were thawed, and B cells were isolated via magnetic bead separation (Miltenyi 130-101-638). Cells were seeded in 96-well U-shaped plates at 50,000 cells per well in 100 μl of RPMI 1640 supplemented with 10% FCS. The cells were stimulated with a combination of 5 μg of unconjugated goat anti-human F(ab)2 fragments (the Jackson Laboratory), IL-21 (50 ng/ml, Peprotech), CD40L (1 μg/ml, Peprotech), and CpG (1 μg/ml, Peprotech), or left untreated. Differentiation was measured after 6 days of stimulation using flow cytometry.

Stimulation of dermal fibroblasts for DcR3 production

Dermal fibroblasts from HCs, patients, and P2 where TNFR1 was knocked out using the CIRSPR-Cas9 system were seeded at 15,000 cells per well in 200 μl in 48-well plates. After 24 hours, the cells were stimulated with human TNF-α (100 ng/ml, Miltenyi), human TNF-β/LTα3 (200 ng/ml, Peprotech), human LTα1β2 (200 ng/ml, R&D Research), or human LTα2β (200 ng/ml, R&D Research), or left untreated. After 24 hours, the supernatant was collected and used for DcR3 analysis using ELISA (R&D Systems). Results from two independent experiments were averaged before each sample was normalized to its untreated result, followed by pooling of the data of HCs and patients.

Effect of DcR3 on AICD in T cells

Before being washed with phosphate-buffered saline (PBS), 96-well U-shaped plates were coated with CD3 (clone OKT3, 2 μg/ml) overnight at 4°C. After 10 days of feeder stimulation with IL-2 (Novartis) and PHA, expanded T cells from HCs and from P2 were seeded at 100,000 cells per well and treated with DcR3 (3.75 μg/ml, MedChemExpress) or left untreated. After 24 hours of stimulation, the cells were harvested, apoptosis was assessed via staining with annexin V–allophycocyanin (APC) (BD Biosciences), and propidium iodide (BioLegend), and readout was performed using flow cytometry.

Effect of DcR3 on T cell killing function

GFP^+ P815 target cells were treated with anti-CD3 (1 μg/ml, clone: OKT3) antibody for 1 hour or left untreated. Expanded T cells from two HCs previously stimulated for 10 days with feeder cells, IL-2 (Novartis), and PHA were assessed for $CD4^+$ and $CD8^+$ ratio before treatment for 1 hour with DcR3 (6.25 μg/ml, MedChemExpress) or DcR3 (37.5 μg/ml) or left untreated. P815 cells were washed before being cocultured with the expanded T cells at a 1:1 ratio in 96-well U-shaped plates. Aphidicolin (0.2 μg/ml, Sigma-Aldrich) was added to inhibit proliferation of the cells. After 6 hours of coculture, the cells were harvested, and the killing function of T cells was estimated by measuring the number of 7-AAD–negative (BD Biosciences) P815 cells by flow cytometry.

Coculture for B cell differentiation

For the coculture, different combinations of PBMCs, DCs, and fibroblasts were combined with or without additional stimulation of a vaccine for MMR (Merck Sharp und Dohme). PBMCs from patients and HCs were thawed and $CD14^+$ monocytes isolated using CD14 MicroBeads (Miltenyi). Monocytes were then differentiated to DCs over 6 days by adding IL-4 (1000 IU/ml, Peprotech) and granulocyte-macrophage colony-stimulating factor (1000 IU/ml, Peprotech). DCs were stimulated by adding poly I:C (10 μg/ml, InvivoGen) for 24 hours. CRISPR-Cas9–edited *B2M* knockout fibroblasts or patient-derived fibroblasts were seeded at 5000 cells per well into a 24-well transwell. The next day, the donor-specific PBMCs were added at 300,000 cells per well together with donor-specific DCs at 30,000 cells per well with or without addition of 5 μl of MMR per well. RPMI 1640 (1 ml) supplemented with 10% FCS was added in the transwell below. Cells were stimulated with B cell–activating factor (BAFF; 50 ng/ml, Peprotech) every other day. Cells were harvested on day 7 for activation readout or on day 12 for differentiation readout using flow cytometry.

NF-κB stimulation in fibroblasts

For canonical NF-κB activation, dermal fibroblasts were stimulated with human TNF-α (20 ng/ml, Miltenyi) for 10 to 60 min followed by immunoblot analysis. For noncanonical NF-κB activation, dermal fibroblasts were stimulated with human LTα1β2 (200 ng/ml, R&D Research) for 6 hours followed by immunoblot analysis.

Immunoblot

Cell lysates of HC and patient fibroblasts were prepared in radioimmunoprecipitation assay buffer containing protease and phosphatase inhibitor cocktail (Thermo Fisher Scientific). Protein concentrations were determined using the DC Protein Assay Kit II (Bio-Rad), and 20 μg of protein was used and resolved by reducing SDS–polyacrylamide gel electrophoresis with 4 to 15% mini-protean TGX precast protein gels, followed by transfer to polyvinylidene difluoride (PVDF) membranes using the Trans-Blot Turbo RTA Mini 0.45-μm LF PVDF Transfer Kit and the Trans-Blot Turbo transfer system (Bio-Rad). Then, membranes were blocked in 5% bovine serum albumin (BSA) solution for 1 hour at room temperature and subsequent incubation with primary antibodies NF-κB2 p100/p52 (Cell Signaling Technology) and heat shock protein 90 (HSP90) α/β (Santa Cruz Biotechnology) or with phospho–NF-κB p65 (Cell Signaling), IκBα (Cell Signaling Technology), and HSP90α/β (Santa Cruz Biotechnology) overnight at 4°C. Subsequently, membranes were washed three times in tris-buffered saline with Tween 20 detergent (TBST) and incubated with peroxidase-conjugated secondary antibodies for 1 hour at room temperature followed by washing three times in TBST and visualized using chemiluminescence with the ECL Prime Western blot detection reagent (Cytiva) and the ChemiDoc MP imaging system (Bio-Rad).

Enzyme-linked immunosorbent assay

LTB, TNF-α, CXCL13/BLC, DcR3/TNFRSF6B, FasL/TNFSF6, and LIGHT/TNFSF14 levels were detected using ELISA (LTB: catalog no. A312081, Antibodies.com; TNF-α: catalog no. 10737663, Thermo Fisher Scientific; CXCL13/BLC: catalog no. 15444963, Thermo Fisher Scientific; DcR3: catalog no. 15405163, Thermo Fisher Scientific; FasL: catalog no. DY126, DuoSet kit R&D Systems; LIGHT: catalog no. DY664, DuoSet kit, R&D Systems), Luminex Multiplex Assay (Thermo Fisher Scientific) and LEGENDplex (catalog no. 741182, Biolegend) in HC and patient serum samples according to the manufacturer's instructions. Fifty microliters of each serum sample in duplicates was used in all assays.

scRNA sequencing

Samples from P1 and P2 were analyzed along with those from four HCs as previously described (*69*). In brief, cryopreserved PBMCs from the two patients and four HCs were thawed, washed in RPMI 1640 medium, and resuspended in sterile PBS with 0.04% BSA. A single-cell suspension was obtained by passing 1 million cells into a 5-ml FACS tube through a cell strainer and sorting for the live lymphocytes and monocytes on the basis of the forward and side scatter using the FACSAria Fusion (BD). scRNA-seq was then performed on the live samples using the Chromium Single Cell Controller and Chromium Next GEM Single Cell 5' Kit v2 (10x Genomics, Pleasanton, CA) according to the manufacturer's protocol. TCR sequences were enriched at the cDNA stage using the respective reagents, in accordance with the instructions of the VDJ Kit workflow by 10x

Genomics. Sequencing was performed using the Illumina NovaSeq platform in the 75-bp paired-end configuration.

CellRanger v5.0.1 software (10x Genomics) was used for demultiplexing and alignment to the GRCh38-2020-A human reference transcriptome. The R statistics software was used to analyze the processed data. Briefly, CellRanger outputs (filtered count matrices) were further filtered to exclude cells with more than 15% mitochondrial counts or with numbers of detected genes either fewer than 300 or unusually high (per-sample z-score > 2.5). Cell types were annotated using Seurat (v 4.1.0) with sctransform (*70*) normalization (v.0.3.3) and Azimuth (v 0.4.3) (*71*). The reference used was human PBMC annotation level 2. Cells with an annotation score or mapping score less than 0.5 were excluded from further analysis. For visualization, the Azimuth reference space [Uniform Manifold Approximation and Projection (UMAP)] was used, and cell types with fewer than 20 cells annotated (cDC2, pDC, CD16 mono, platelet, HSPC, ILC, and dnT) were excluded. Clonality analysis of the TCR repertoires was based on cells that were assigned exactly one alpha chain CDR3 and one beta chain CDR3. A clonotype was defined as a unique combination of these CDR3 motifs, and clonality for patients and cell types was calculated as 1 minus normalized entropy as done in other studies (*72*). scRNA-seq differential expression (DE) testing of patients versus HCs was done using edgeR (*73*) (v 3.36, default parameters, exact test) and pseudobulk profiles (aggregated counts per patient) to minimize false discoveries (*74*). Each test was filtered to exclude genes with false discovery rate (FDR)–adjusted P value >0.05; the remaining genes were ordered by P value. Several tests were performed, each focusing on different cell populations. Tests were performed within $CD8^+$ T cells (aggregating CD8 naïve, CD8 TCM, and CD8 TEM) and within the individual $CD8^+$ cell types. Expression heatmaps show normalized expression (DESeq2 vst function after aggregating counts of all cells per group) z-scored per gene and cropped to the range of −2 to 2. Genes selected for display in the heatmaps had to have P value rank ≤ 45 and logFC rank ≤ 45 (grouped by fold-change direction) in one of the CD8 cell type DE tests. After differential gene expression analysis, we performed gene set enrichment analysis using hypergeometric tests. For the tests, we considered all the genes retained by edgeR as background, whereas the DE genes (FDR ≤ 0.05) were considered the genes of interest. The following genes defined the "exhaustion" gene set: *PDCD1*, *CTLA4*, *NFATC1*, *SPRY2*, *BATF*, *VHL*, *FOXO1*, *FOXP1*, *LAG3*, *CD244*, *CD160*, *HAVCR2*, *TRAF1*, *TNFRSF9*, *IL10RA*, *IL10*, *PRDM1*, *STAT3*, *IFNA1*, *IFNB1*, *IL21*, *CXCR5*, *SOCS3*, *GATA3*, *IKZF2*, *BCL6*, *BCL2*, *TBX21*, and *EOMES*. A significant enrichment for exhaustion was not observed in any of the DE test results (P values >0.1).

BCR and TCR sequencing

For BCR and TCR sequencing, DNA was isolated from PBMCs or whole blood of patients and HCs. The DNA used for BCR sequencing of P1 and P2 was isolated from B cell–enriched samples using magnetic cell sorting separation as described previously in the B cell differentiation protocol. Sequencing was performed using protocols and primers standardized by the EuroClonality-NGS Working Group and sequenced with the Illumina MiSeq v3 600-sequencing kit (MS-102-3003) with 20% PhiX v3 Control library (FC-110-3001; both Illumina, San Diego, CA, USA) following the manufacturer's instructions (*75*, *76*). Demultiplexed sequencing data were analyzed using the ARResT/Interrogate platform to annotate individual clones for further processing with R (*77*, *78*). For the analysis of clonality, only productively rearranged IGH and TCRB clones were included in the analysis, and only the top 1000 clones by frequency were included for the figure plots and diversity calculations. For the analysis of the SHM rate, all productively rearranged IGH clones with a unique amino acid sequence in the CDR3 and with a coverage of at least five reads in the sample were used, and its representative sequence with the highest number of reads was used for alignment. The alignment to the *IGHV* gene reference sequences was performed using the IMGT/HighV-QUEST platform, and the resulting files were processed using custom R code to generate statistics and plots (*79*, *80*). The number of nucleotide mutations was calculated for each clone with a productive IGH rearrangement in the CDR1, CDR2, FR2, and FR3 regions of the rearrangement. For the figure plots and underlying statistics, the top 200 clones by their frequency were analyzed for each sample. A detailed analysis of the *IGHV3-23* gene was performed for all clones with a productive rearrangement of this *IGHV* gene, and a mutational rate was calculated for each amino acid position on the basis of the alignment to the IMGT reference. A mutational rate is shown as a median per position for all four HCs with an error bar corresponding to the 75th percentile and individual values per position for all patients.

Statistical analysis

For individual comparisons of independent groups, the Student's t test was performed. Welch's correction was used if the two groups had unequal variances or sample sizes. For multiple comparisons, a one- or two-way analysis of variance (ANOVA) was applied, followed by Bonferroni post hoc test to correct for multiple comparisons. In the case of multiple comparisons toward one dataset (e.g., untreated), Dunnet's post hoc test was used instead. Data graphs and analyses were made using PRISM software (GraphPad Software Inc.), and error bars display the SDs.

Supplementary Materials

The PDF file includes:
Materials
Figs. S1 to S16
Tables S1 to S9
References (*82*–*85*)

Other Supplementary Material for this manuscript includes the following:
Data file S1
MDAR Reproducibility Checklist

REFERENCES AND NOTES

1. H. L. Horsnell, R. J. Tetley, H. De Belly, S. Makris, L. J. Millward, A. C. Benjamin, L. A. Heeringa, C. M. de Winde, E. K. Paluch, Y. Mao, S. E. Acton, Lymph node homeostasis and adaptation to immune challenge resolved by fibroblast network mechanics. *Nat. Immunol.* **23**, 1169–1182 (2022).
2. P. C. de Casas, K. Knopper, R. D. Sarkar, W. Kastenmuller, Same yet different - How lymph node heterogeneity affects immune responses. *Nat. Rev. Immunol.* **24**, 358–374 (2024).
3. G. D. Victora, M. C. Nussenzweig, Germinal Centers. *Annu. Rev. Immunol.* **40**, 413–442 (2022).
4. D. Vetrie, I. Vorechovsky, P. Sideras, J. Holland, A. Davies, F. Flinter, L. Hammarstrom, C. Kinnon, R. Levinsky, M. Bobrow, C. I. E. Smith, D. R. Bentley, The gene involved in X-linked agammaglobulinaemia is a member of the src family of protein-tyrosine kinases. *Nature* **361**, 226–233 (1993).
5. A. Villa, L. D. Notarangelo, *RAG* gene defects at the verge of immunodeficiency and immune dysregulation. *Immunol. Rev.* **287**, 73–90 (2019).
6. R. J. O'Reilly, B. Dupont, S. Pahwa, E. Grimes, E. M. Smithwick, R. Pahwa, S. Schwartz, J. A. Hansen, F. P. Siegal, M. Sorell, A. Svejgaard, C. Jersild, M. Thomsen, P. Platz,

P. L'Esperance, R. A. Good, Reconstitution in severe combined immunodeficiency by transplantation of marrow from an unrelated donor. *N. Engl. J. Med.* **297**, 1311–1318 (1977).
7. K. L. Willmann, S. Klaver, F. Dogu, E. Santos-Valente, W. Garncarz, I. Bilic, E. Mace, E. Salzer, C. D. Conde, H. Sic, P. Majek, P. P. Banerjee, G. I. Vladimer, S. Haskologlu, M. G. Bolkent, A. Kupesiz, A. Condino-Neto, J. Colinge, G. Superti-Furga, W. F. Pickl, M. C. van Zelm, H. Eibel, J. S. Orange, A. Ikincioğullari, K. Boztug, Biallelic loss-of-function mutation in *NIK* causes a primary immunodeficiency with multifaceted aberrant lymphoid immunity. *Nat. Commun.* **5**, 5360 (2014).
8. A. Bolze, N. Mahlaoui, M. Byun, B. Turner, N. Trede, S. R. Ellis, A. Abhyankar, Y. Itan, E. Patin, S. Brebner, P. Sackstein, A. Puel, C. Picard, L. Abel, L. Quintana-Murci, S. N. Faust, A. P. Williams, R. Baretto, M. Duddridge, U. Kini, A. J. Pollard, C. Gaud, P. Frange, D. Orbach, J. F. Emile, J.-L. Stephan, R. Sorensen, A. Plebani, L. Hammarstrom, M. E. Conley, L. Selleri, J.-L. Casanova, Ribosomal protein SA haploinsufficiency in humans with isolated congenital asplenia. *Science* **340**, 976–978 (2013).
9. S. G. Tangye, W. Al-Herz, A. Bousfiha, C. Cunningham-Rundles, J. L. Franco, S. M. Holland, C. Klein, T. Morio, E. Oksenhendler, C. Picard, A. Puel, J. Puck, M. R. J. Seppanen, R. Somech, H. C. Su, K. E. Sullivan, T. R. Torgerson, I. Meyts, Human inborn errors of immunity: 2022 update on the classification from the international union of immunological societies expert committee. *J. Clin. Immunol.* **42**, 1473–1507 (2022).
10. S.-C. Sun, The non-canonical NF-κB pathway in immunity and inflammation. *Nat. Rev. Immunol.* **17**, 545–558 (2017).
11. C. F. Ware, T. L. VanArsdale, P. D. Crowe, J. L. Browning, The ligands and receptors of the lymphotoxin system. *Curr. Top. Microbiol. Immunol.* **198**, 175–218 (1995).
12. C. F. Ware, Network communications: Lymphotoxins, LIGHT, and TNF. *Annu. Rev. Immunol.* **23**, 787–819 (2005).
13. V. Upadhyay, Y.-X. Fu, Lymphotoxin signalling in immune homeostasis and the control of microorganisms. *Nat. Rev. Immunol.* **13**, 270–279 (2013).
14. G. Eberl, S. Marmon, M.-J. Sunshine, P. D. Rennert, Y. Choi, D. R. Littman, An essential function for the nuclear receptor RORγ(t) in the generation of fetal lymphoid tissue inducer cells. *Nat. Immunol.* **5**, 64–73 (2004).
15. E. Dejardin, N. M. Droin, M. Delhase, E. Haas, Y. Cao, C. Makris, Z.-W. Li, M. Karin, C. F. Ware, D. R. Green, The lymphotoxin-β receptor induces different patterns of gene expression via two NF-κB pathways. *Immunity* **17**, 525–535 (2002).
16. A. Futterer, K. Mink, A. Luz, M. H. Kosco-Vilbois, K. Pfeffer, The lymphotoxin β receptor controls organogenesis and affinity maturation in peripheral lymphoid tissues. *Immunity* **9**, 59–70 (1998).
17. P. D. Rennert, J. L. Browning, R. Mebius, F. Mackay, P. S. Hochman, Surface lymphotoxin alpha/beta complex is required for the development of peripheral lymphoid organs. *J. Exp. Med.* **184**, 1999–2006 (1996).
18. T. Nitta, M. Tsutsumi, S. Nitta, R. Muro, E. C. Suzuki, K. Nakano, Y. Tomofuji, S. Sawa, T. Okamura, J. M. Penninger, H. Takayanagi, Fibroblasts as a source of self-antigens for central immune tolerance. *Nat. Immunol.* **21**, 1172–1180 (2020).
19. M. V. Lenti, S. Luu, R. Carsetti, F. Osier, R. Ogwang, O. E. Nnodu, U. Wiedermann, J. Spencer, F. Locatelli, G. R. Corazza, A. Di Sabatino, Asplenia and spleen hypofunction. *Nat. Rev. Dis. Primers.* **8**, 71 (2022).
20. B. R. Blazar, F. P. Lindberg, E. Ingulli, A. Panoskaltsis-Mortari, P. A. Oldenborg, K. Iizuka, W. M. Yokoyama, P.-A. Taylor, CD47 (integrin-associated protein) engagement of dendritic cell and macrophage counterreceptors is required to prevent the clearance of donor lymphohematopoietic cells. *J. Exp. Med.* **194**, 541–550 (2001).
21. P. M. Howley, H. J. Pfister, Beta genus papillomaviruses and skin cancer. *Virology* **479–480**, 290–296 (2015).
22. S. A. van de Pavert, B. J. Olivier, G. Goverse, M. F. Vondenhoff, M. Greuter, P. Beke, K. Kusser, U. E. Hopken, M. Lipp, K. Niederreither, R. Blomhoff, K. Sitnik, W. W. Agace, T. D. Randall, W. J. de Jonge, R. E. Mebius, Chemokine CXCL13 is essential for lymph node initiation and is induced by retinoic acid and neuronal stimulation. *Nat. Immunol.* **10**, 1193–1199 (2009).
23. K. M. Ansel, V. N. Ngo, P. L. Hyman, S. A. Luther, R. Forster, J. D. Sedgwick, J. L. Browning, M. Lipp, J. G. Cyster, A chemokine-driven positive feedback loop organizes lymphoid follicles. *Nature* **406**, 309–314 (2000).
24. V. N. Ngo, H. Korner, M. D. Gunn, K. N. Schmidt, D. S. Riminton, M. D. Cooper, J. L. Browning, J. D. Sedgwick, J. G. Cyster, Lymphotoxin α/β and tumor necrosis factor are required for stromal cell expression of homing chemokines in B and T cell areas of the spleen. *J. Exp. Med.* **189**, 403–412 (1999).
25. E. W. S. Clair, A. N. Baer, C. Wei, G. Noaiseh, A. Parke, A. Coca, T. O. Utset, M. C. Genovese, D. J. Wallace, J. McNamara, K. Boyle, L. Keyes-Elstein, J. L. Browning, N. Franchimont, K. Smith, J. M. Guthridge, I. Sanz, J. A. James, E. Autoimmunity, Centers of clinical efficacy and safety of baminercept, a lymphotoxin β receptor fusion protein, in primary sjogren's syndrome: Results from a phase II randomized, double-blind, placebo-controlled trial. *Arthritis Rheumatol.* **70**, 1470–1480 (2018).
26. W. P. Kennedy, J. A. Simon, C. Offutt, P. Horn, A. Herman, M. J. Townsend, M. T. Tang, J. L. Grogan, F. Hsieh, J. C. Davis, Efficacy and safety of pateclizumab (anti-lymphotoxin-α) compared to adalimumab in rheumatoid arthritis: A head-to-head phase 2 randomized controlled study (The ALTARA Study). *Arthritis Res. Ther.* **16**, 467 (2014).
27. S. A. van de Pavert, R. E. Mebius, New insights into the development of lymphoid tissues. *Nat. Rev. Immunol.* **10**, 664–674 (2010).
28. B. Keller, V. Strohmeier, I. Harder, S. Unger, K. J. Payne, G. Andrieux, M. Boerries, P. T. Felixberger, J. J. M. Landry, A. Nieters, A. Rensing-Ehl, U. Salzer, N. Frede, S. Usadel, R. Elling, C. Speckmann, I. Hainmann, E. Ralph, K. Gilmour, M. W. J. Wentink, M. van der Burg, H. S. Kuehn, S. D. Rosenzweig, U. Kolsch, H. von Bernuth, P. Kaiser-Labusch, F. Gothe, S. Hambleton, A. D. Vlagea, A. G. Garcia, L. Alsina, G. Markelj, T. Avcin, J. Vasconcelos, M. Guedes, J. Y. Ding, C. L. Ku, B. Shadur, D. T. Avery, N. Venhoff, J. Thiel, H. Becker, L. Erazo-Borras, C. M. Trujillo-Vargas, J. L. Franco, C. Fieschi, S. Okada, P. E. Gray, G. Uzel, J.-L. Casanova, M. Fliegauf, B. Grimbacher, H. Eibel, S. Ehl, R. E. Voll, M. Rizzi, P. Stepensky, V. Benes, C. S. Ma, C. Bossen, S. G. Tangye, K. Warnatz, The expansion of human T-bet^{high}CD21^{low} B cells is T cell dependent. *Sci. Immunol.* **6**, eabh0891 (2021).
29. A. Borelli, M. Irla, Lymphotoxin: From the physiology to the regeneration of the thymic function. *Cell Death Differ.* **28**, 2305–2314 (2021).
30. A. Salumets, L. Tserel, A. P. Rumm, L. Turk, K. Kingo, K. Saks, A. Oras, R. Uibo, R. Tamm, H. Peterson, K. Kisand, P. Peterson, Epigenetic quantification of immunosenescent CD8$^+$ TEMRA cells in human blood. *Aging Cell* **21**, e13607 (2022).
31. I. Gramaglia, D. N. Mauri, K. T. Miner, C. F. Ware, M. Croft, Lymphotoxin αβ is expressed on recently activated naive and Th1-like CD4 cells but is down-regulated by IL-4 during Th2 differentiation. *J. Immunol.* **162**, 1333–1338 (1999).
32. H.-S. Kang, S. E. Blink, R. K. Chin, Y. Lee, O. Kim, J. Weinstock, T. Waldschmidt, D. Conrad, B. Chen, J. Solway, A. I. Sperling, Y.-X. Fu, Lymphotoxin is required for maintaining physiological levels of serum IgE that minimizes Th1-mediated airway inflammation. *J. Exp. Med.* **198**, 1643–1652 (2003).
33. J. M. Ehrchen, J. Roth, K. Roebrock, G. Varga, W. Domschke, R. Newberry, C. Sorg, C. Muller-Tidow, C. Sunderkotter, T. Kucharzik, T. W. Spahn, The absence of cutaneous lymph nodes results in a Th2 response and increased susceptibility to *Leishmania major* infection in mice. *Infect. Immun.* **76**, 4241–4250 (2008).
34. G. Xiao, A. Deng, H. Liu, G. Ge, X. Liu, Activator protein 1 suppresses antitumor T cell function via the induction of programmed death 1. *Proc. Natl. Acad. Sci. U.S.A.* **109**, 15419–15424 (2012).
35. O. Micheau, J. Tschopp, Induction of TNF receptor I-mediated apoptosis via two sequential signaling complexes. *Cell* **114**, 181–190 (2003).
36. Y. Zhai, R. Guo, T. L. Hsu, G. L. Yu, J. Ni, B. S. Kwon, G. W. Jiang, J. Lu, J. Tan, M. Ugustus, K. Carter, L. Rojas, F. Zhu, C. Lincoln, G. Endress, L. Xing, S. Wang, K. O. Oh, R. Gentz, S. Ruben, M. E. Lippman, S. L. Hsieh, D. Yang, LIGHT, a novel ligand for lymphotoxin beta receptor and TR2/HVEM induces apoptosis and suppresses in vivo tumor formation via gene transfer. *J. Clin. Invest.* **102**, 1142–1151 (1998).
37. D. C. Huang, M. Hahne, M. Schroeter, K. Frei, A. Fontana, A. Villunger, K. Newton, J. Tschopp, A. Strasser, Activation of Fas by FasL induces apoptosis by a mechanism that cannot be blocked by Bcl-2 or Bcl-x(L). *Proc. Natl. Acad. Sci. U.S.A.* **96**, 14871–14876 (1999).
38. J. Wang, J. C. Lo, A. Foster, P. Yu, H. M. Chen, Y. Wang, K. Tamada, L. Chen, Y. X. Fu, The regulation of T cell homeostasis and autoimmunity by T cell-derived LIGHT. *J. Clin. Invest.* **108**, 1771–1780 (2001).
39. C. F. Ware, M. Croft, G. A. Neil, Realigning the LIGHT signaling network to control dysregulated inflammation. *J. Exp. Med.* **219**, e20220236 (2022).
40. C. Giordano, G. Stassi, R. De Maria, M. Todaro, P. Richiusa, G. Papoff, G. Ruberti, M. Bagnasco, R. Testi, A. Galluzzo, Potential involvement of Fas and its ligand in the pathogenesis of Hashimoto's thyroiditis. *Science* **275**, 960–963 (1997).
41. T. Boehm, S. Scheu, K. Pfeffer, C. C. Bleul, Thymic medullary epithelial cell differentiation, thymocyte emigration, and the control of autoimmunity require lympho-epithelial cross talk via LTβR. *J. Exp. Med.* **198**, 757–769 (2003).
42. T. Le Voyer, A. V. Parent, X. Liu, A. Cederholm, A. Gervais, J. Rosain, T. Nguyen, M. P. Lorenzo, E. Rackaityte, D. Rinchai, P. Zhang, L. Bizien, G. Hancioglu, P. Ghillani-Dalbin, J.-L. Charuel, Q. Philippot, M. S. Gueye, M. R. L. M. Renkilaraj, M. Ogishi, C. Soudee, M. Migaud, F. Rozenberg, M. Momenilandi, Q. Riller, L. Imberti, O. M. Delmonte, G. Muller, B. Keller, J. Orrego, W. A. F. Gallego, T. Rubin, M. Emiroglu, N. Parvaneh, D. Eriksson, M. Aranda-Guillen, D. I. Berrios, L. Vong, C. H. Katelaris, P. Mustillo, J. Raedler, J. Bohlen, J. B. Celik, C. Astudillo, S. Winter, NF-κB Consortium, COVID Human Genetic Effort, C. McLean, A. Guffroy, J. L. DeRisi, D. Yu, C. Miller, Y. Feng, A. Guichard, V. Beziat, J. Bustamante, Q. Pan-Hammarstrom, Y. Zhang, L. B. Rosen, S. M. Holland, M. Bosticardo, H. Kenney, R. Castagnoli, C. A. Slade, K. Boztug, N. Mahlaoui, S. Latour, R. S. Abraham, V. Lougaris, F. Hauck, A. Sediva, F. Atschekzei, G. Sogkas, M. C. Poli, M. A. Slatter, B. Palterer, M. D. Keller, A. Pinzon-Charry, A. Sullivan, L. Droney, D. Suan, M. Wong, A. Kane, H. Hu, C. Ma, H. Grombirikova, P. Ciznar, I. Dalal, N. Aladjidi, M. Hie, E. Lazaro, J. Franco, S. Keles, M. Malphettes, M. Pasquet, M. E. Maccari, A. Meinhardt, A. Ikincioğullari, M. Shahrooei, F. Celmeli, P. Frosk, C. C. Goodnow, P. E. Gray, A. Belot, H. S. Kuehn, S. D. Rosenzweig, M. Miyara, F. Licciardi, A. Servettaz, V. Barlogis, G. Le Guenno, V. M. Herrmann, T. Kuijpers, G. Ducoux, F. Sarrot-Reynauld, C. Schuetz, C. Cunningham-Rundles, F. Rieux-Laucat, S. G. Tangye, C. Sobacchi, R. Doffinger, K. Warnatz, B. Grimbacher, C. Fieschi, L. Berteloot,

V. L. Bryant, S. T. Assant, H. Su, B. Neven, L. Abel, Q. Zhang, B. Boisson, A. Cobat, E. Jouanguy, O. Kampe, P. Bastard, C. M. Roifman, N. Landegren, L. D. Notarangelo, M. S. Anderson, J.-L. Casanova, A. Puel, Autoantibodies against type I IFNs in humans with alternative NF-κB pathway deficiency. *Nature* **623**, 803–813 (2023).
43. D. Liang, Y. Hou, X. Lou, H. Chen, Decoy receptor 3 improves survival in experimental sepsis by suppressing the inflammatory response and lymphocyte apoptosis. *PLOS ONE* **10**, e0131680 (2015).
44. S.-C. Weng, M.-C. Wen, S.-L. Hsieh, N.-J. Chen, D.-C. Tarng, Decoy receptor 3 suppresses T-cell priming and promotes apoptosis of effector T-cells in acute cell-mediated rejection: The role of reverse signaling. *Front. Immunol.* **13**, 879648 (2022).
45. D.-Y. Liang, S. Sha, Q. Yi, J. Shi, Y. Chen, Y. Hou, Q. Chang, Hepatitis B X protein upregulates decoy receptor 3 expression via the PI3K/NF-κB pathway. *Cell. Signal.* **62**, 109346 (2019).
46. L. Williams-Abbott, B. N. Walter, T. C. Cheung, C. R. Goh, A. G. Porter, C. F. Ware, The lymphotoxin-α (LTα) subunit is essential for the assembly, but not for the receptor specificity, of the membrane-anchored LTα1β2 heterotrimeric ligand. *J. Biol. Chem.* **272**, 19451–19456 (1997).
47. P. Revy, T. Muto, Y. Levy, F. Geissmann, A. Plebani, O. Sanal, N. Catalan, M. Forveille, R. Dufourcq-Labelouse, A. Gennery, I. Tezcan, F. Ersoy, H. Kayserili, A. G. Ugazio, N. Brousse, M. Muramatsu, L. D. Notarangelo, K. Kinoshita, T. Honjo, A. Fischer, A. Durandy, Activation-induced cytidine deaminase (AID) deficiency causes the autosomal recessive form of the hyper-IgM syndrome (HIGM2). *Cell* **102**, 565–575 (2000).
48. A. El Kettani, F. Ailal, J. El Bakkouri, K. Zerouali, V. Beziat, E. Jouanguy, J.-L. Casanova, A. A. Bousfiha, HPV-related skin phenotypes in patients with inborn errors of immunity. *Pathogens* **11**, 857 (2022).
49. Y. Shou, E. Koroleva, C. M. Spencer, S. A. Shein, A. A. Korchagina, K. A. Yusoof, R. Parthasarathy, E. A. Leadbetter, A. N. Akopian, A. R. Munoz, A. V. Tumanov, Redefining the role of lymphotoxin beta receptor in the maintenance of lymphoid organs and immune cell homeostasis in adulthood. *Front. Immunol.* **12**, 712632 (2021).
50. R. K. Chin, J. C. Lo, O. Kim, S. E. Blink, P. A. Christiansen, P. Peterson, Y. Wang, C. Ware, Y.-X. Fu, Lymphotoxin pathway directs thymic *Aire* expression. *Nat. Immunol.* **4**, 1121–1127 (2003).
51. Z. Yu, V. A. Lennon, Mechanism of intravenous immune globulin therapy in antibody-mediated autoimmune diseases. *N. Engl. J. Med.* **340**, 227–228 (1999).
52. N. Washburn, R. Meccariello, S. Hu, M. Hains, N. Bhatnagar, H. Sarvaiya, B. Kapoor, J. Schaeck, I. Pino, A. Manning, J. C. Lansing, C. J. Bosques, High-resolution physicochemical characterization of different intravenous immunoglobulin products. *PLOS ONE* **12**, e0181251 (2017).
53. K.-Y. Yu, B. Kwon, J. Ni, Y. Zhai, R. Ebner, B. S. Kwon, A newly identified member of tumor necrosis factor receptor superfamily (TR6) suppresses LIGHT-mediated apoptosis. *J. Biol. Chem.* **274**, 13733–13736 (1999).
54. H. Takaba, Y. Morishita, Y. Tomofuji, L. Danks, T. Nitta, N. Komatsu, T. Kodama, H. Takayanagi, Fezf2 orchestrates a thymic program of self-antigen expression for immune tolerance. *Cell* **163**, 975–987 (2015).
55. J. L. Bautista, N. T. Cramer, C. N. Miller, J. Chavez, D. I. Berrios, L. E. Byrnes, J. Germino, V. Ntranos, J. B. Sneddon, T. D. Burt, J. M. Gardner, C. J. Ye, M. S. Anderson, A. V. Parent, Single-cell transcriptional profiling of human thymic stroma uncovers novel cellular heterogeneity in the thymic medulla. *Nat. Commun.* **12**, 1096 (2021).
56. V. Oikonomou, G. Smith, G. M. Constantine, M. M. Schmitt, E. M. N. Ferre, J. C. Alejo, D. Riley, D. Kumar, L. Dos Santos Dias, J. Pechacek, Y. Hadjiyannis, T. Webb, B. A. Seifert, R. Ghosh, M. Walkiewicz, D. Martin, M. Besnard, B. D. Snarr, S. Deljookorani, C. R. Lee, T. DiMaggio, P. Barber, L. B. Rosen, A. Cheng, A. Rastegar, A. A. de Jesus, J. Stoddard, H. S. Kuehn, T. J. Break, H. H. Kong, L. Castelo-Soccio, B. Colton, B. M. Warner, D. E. Kleiner, M. M. Quezado, J. L. Davis, K. P. Fennelly, K. N. Olivier, S. D. Rosenzweig, A. F. Suffredini, M. S. Anderson, M. Swidergall, C. Guillonneau, L. D. Notarangelo, R. Goldbach-Mansky, O. Neth, M. T. Monserrat-Garcia, J. Valverde-Fernandez, J. M. Lucena, A. L. Gomez-Gila, A. Garcia Rojas, M. R. J. Seppanen, J. Lohi, M. Hero, S. Laakso, P. Klemetti, V. Lundberg, O. Ekwall, P. Olbrich, K. K. Winer, B. Afzali, N. M. Moutsopoulos, S. M. Holland, T. Heller, S. Pittaluga, M. S. Lionakis, The role of interferon-γ in autoimmune polyendocrine syndrome type 1. *N. Engl. J. Med.* **390**, 1873–1884 (2024).
57. G. M. Seleznik, J. Zoller, T. O'Connor, R. Graf, M. Heikenwalder, The role of lymphotoxin signaling in the development of autoimmune pancreatitis and associated secondary extra-pancreatic pathologies. *Cytokine Growth Factor Rev.* **25**, 125–137 (2014).
58. Y. Sato, K. Silina, M. van den Broek, K. Hirahara, M. Yanagita, The roles of tertiary lymphoid structures in chronic diseases. *Nat. Rev. Nephrol.* **19**, 525–537 (2023).
59. Y. Zhang, T.-J. Kim, J. A. Wroblewska, V. Tesic, V. Upadhyay, R. R. Weichselbaum, A. V. Tumanov, H. Tang, X. Guo, H. Tang, Y.-X. Fu, Type 3 innate lymphoid cell-derived lymphotoxin prevents microbiota-dependent inflammation. *Cell. Mol. Immunol.* **15**, 697–709 (2018).
60. H. Li, R. Durbin, Fast and accurate long-read alignment with Burrows-Wheeler transform. *Bioinformatics* **26**, 589–595 (2010).
61. R. Poplin, V. Ruano-Rubio, M. A. De Pristo, T. J. Fennell, M. O. Carneiro, G. A. Van der Auwera, D. E. Kling, L. D. Gauthier, A. Levy-Moonshine, D. Roazen, K. Shakir, J. Thibault, S. Chandran, C. Whelan, M. Lek, S. Gabriel, M. J. Daly, B. Neale, D. G. MacArthur, E. Banks, Scaling accurate genetic variant discovery to tens of thousands of samples. bioRxiv 201178 [Preprint] (2017); https://doi.org/10.1101/201178.
62. W. McLaren, L. Gil, S. E. Hunt, H. S. Riat, G. R. S. Ritchie, A. Thormann, P. Flicek, F. Cunningham, The ensembl variant effect predictor. *Genome Biol.* **17**, 122 (2016).
63. K. J. Karczewski, L. C. Francioli, G. Tiao, B. B. Cummings, J. Alfoldi, Q. Wang, R. L. Collins, K. M. Laricchia, A. Ganna, D. P. Birnbaum, L. D. Gauthier, H. Brand, M. Solomonson, N. A. Watts, D. Rhodes, M. Singer-Berk, E. M. England, E. G. Seaby, J. A. Kosmicki, R. K. Walters, K. Tashman, Y. Farjoun, E. Banks, T. Poterba, A. Wang, C. Seed, N. Whiffin, J. X. Chong, K. E. Samocha, E. Pierce-Hoffman, Z. Zappala, A. H. O'Donnell-Luria, E. V. Minikel, B. Weisburd, M. Lek, J. S. Ware, C. Vittal, I. M. Armean, L. Bergelson, K. Cibulskis, K. M. Connolly, M. Covarrubias, S. Donnelly, S. Ferriera, S. Gabriel, J. Gentry, N. Gupta, T. Jeandet, D. Kaplan, C. Llanwarne, R. Munshi, S. Novod, N. Petrillo, D. Roazen, V. Ruano-Rubio, A. Saltzman, M. Schleicher, J. Soto, K. Tibbetts, C. Tolonen, G. Wade, M. E. Talkowski, Genome Aggregation Database Consortium, B. M. Neale, M. J. Daly, D. G. MacArthur, The mutational constraint spectrum quantified from variation in 141,456 humans. *Nature* **581**, 434–443 (2020).
64. M. Kircher, D. M. Witten, P. Jain, B. J. O'Roak, G. M. Cooper, J. Shendure, A general framework for estimating the relative pathogenicity of human genetic variants. *Nat. Genet.* **46**, 310–315 (2014).
65. J. Jumper, R. Evans, A. Pritzel, T. Green, M. Figurnov, O. Ronneberger, K. Tunyasuvunakool, R. Bates, A. Zidek, A. Potapenko, A. Bridgland, C. Meyer, S. A. A. Kohl, A. J. Ballard, A. Cowie, B. Romera-Paredes, S. Nikolov, R. Jain, J. Adler, T. Back, S. Petersen, D. Reiman, E. Clancy, M. Zielinski, M. Steinegger, M. Pacholska, T. Berghammer, S. Bodenstein, D. Silver, O. Vinyals, A. W. Senior, K. Kavukcuoglu, P. Kohli, D. Hassabis, Highly accurate protein structure prediction with AlphaFold. *Nature* **596**, 583–589 (2021).
66. M. Varadi, S. Anyango, M. Deshpande, S. Nair, C. Natassia, G. Yordanova, D. Yuan, O. Stroe, G. Wood, A. Laydon, A. Zidek, T. Green, K. Tunyasuvunakool, S. Petersen, J. Jumper, E. Clancy, R. Green, A. Vora, M. Lutfi, M. Figurnov, A. Cowie, N. Hobbs, P. Kohli, G. Kleywegt, E. Birney, D. Hassabis, S. Velankar, AlphaFold protein structure database: Massively expanding the structural coverage of protein-sequence space with high-accuracy models. *Nucleic Acids Res.* **50**, D439–D444 (2022).
67. T. Khanna, G. Hanna, M. J. E. Sternberg, A. David, Missense3D-DB web catalogue: An atom-based analysis and repository of 4M human protein-coding genetic variants. *Hum. Genet.* **140**, 805–812 (2021).
68. S. Ittisoponpisan, S. A. Islam, T. Khanna, E. Alhuzimi, A. David, M. J. E. Sternberg, Can predicted protein 3D structures provide reliable insights into whether missense variants are disease associated? *J. Mol. Biol.* **431**, 2197–2212 (2019).
69. S. Kostel Bal, S. Giuliani, J. Block, P. Repiscak, C. Hafemeister, T. Shahin, N. Kasap, B. Ransmayr, Y. Miao, C. van de Wetering, A. Frohne, R. Jimenez Heredia, M. Schuster, S. Zoghi, V. Hertlein, M. Thian, A. Bykov, R. Babayeva, S. Bilgic Eltan, E. Karakoc-Aydiner, L. E. Shaw, I. Chowdhury, M. Varjosalo, R. J. Arguello, M. Farlik, A. Ozen, E. Serfling, L. Dupre, C. Bock, F. Halbritter, J. T. Hannich, I. Castanon, M. J. Kraakman, S. Baris, K. Boztug, Biallelic *NFATC1* mutations cause an inborn error of immunity with impaired $CD8^+$ T cell function and perturbed glycolysis. *Blood* **142**, 827–845 (2023).
70. C. Hafemeister, R. Satija, Normalization and variance stabilization of single-cell RNA-seq data using regularized negative binomial regression. *Genome Biol.* **20**, 296 (2019).
71. Y. Hao, S. Hao, E. Andersen-Nissen, W. M. Mauck III, S. Zheng, A. Butler, M. J. Lee, A. J. Wilk, C. Darby, M. Zager, P. Hoffman, M. Stoeckius, E. Papalexi, E. P. Mimitou, J. Jain, A. Srivastava, T. Stuart, L. M. Fleming, B. Yeung, A. J. Rogers, J. M. McElrath, C. A. Blish, R. Gottardo, P. Smibert, R. Satija, Integrated analysis of multimodal single-cell data. *Cell* **184**, 3573–3587.e29 (2021).
72. A. Reuben, J. Zhang, S. H. Chiou, R. M. Gittelman, J. Li, W. C. Lee, J. Fujimoto, C. Behrens, X. Liu, F. Wang, K. Quek, C. Wang, F. Kheradmand, R. Chen, C.-W. Chow, H. Lin, C. Bernatchez, A. Jalali, X. Hu, C.-J. Wu, A. K. Eterovic, E. R. Parra, E. Yusko, R. Emerson, S. Benzeno, M. Vignali, X. Wu, Y. Ye, L. D. Little, C. Gumbs, X. Mao, X. Song, S. Tippen, R. L. Thornton, T. Cascone, A. Snyder, J. A. Wargo, R. Herbst, S. Swisher, H. Kadara, C. Moran, N. Kalhor, J. Zhang, P. Scheet, A. A. Vaporciyan, B. Sepesi, D. L. Gibbons, H. Robins, P. Hwu, J. V. Heymach, P. Sharma, J. P. Allison, V. Baladandayuthapani, J. J. Lee, M. M. Davis, I. I. Wistuba, P. A. Futreal, J. Zhang, Comprehensive T cell repertoire characterization of non-small cell lung cancer. *Nat. Commun.* **11**, 603 (2020).
73. D. J. McCarthy, Y. Chen, G. K. Smyth, Differential expression analysis of multifactor RNA-seq experiments with respect to biological variation. *Nucleic Acids Res.* **40**, 4288–4297 (2012).
74. J. W. Squair, M. Gautier, C. Kathe, M. A. Anderson, N. D. James, T. H. Hutson, R. Hudelle, T. Qaiser, K. J. E. Matson, Q. Barraud, A. J. Levine, G. La Manno, M. A. Skinnider, G. Courtine, Confronting false discoveries in single-cell differential expression. *Nat. Commun.* **12**, 5692 (2021).
75. M. Bruggemann, M. Kotrova, H. Knecht, J. Bartram, M. Boudjogrha, V. Bystry, G. Fazio, E. Fronkova, M. Giraud, A. Grioni, J. Hancock, D. Herrmann, C. Jimenez, A. Krejci,

J. Moppett, T. Reigl, M. Salson, B. Scheijen, M. Schwarz, S. Songia, M. Svaton, J. J. M. van Dongen, P. Villarese, S. Wakeman, G. Wright, G. Cazzaniga, F. Davi, R. Garcia-Sanz, D. Gonzalez, P. J. T. A. Groenen, M. Hummel, E. A. Macintyre, K. Stamatopoulos, C. Pott, J. Trka, N. Darzentas, A. W. Langerak, EuroClonality-NGS working group, EuroClonality, Standardized next-generation sequencing of immunoglobulin and T cell receptor gene recombinations for MRD marker identification in acute lymphoblastic leukaemia; a EuroClonality-NGS validation study. *Leukemia* **33**, 2241–2253 (2019).

76. H. Knecht, T. Reigl, M. Kotrova, F. Appelt, P. Stewart, V. Bystry, A. Krejci, A. Grioni, K. Pal, K. Stranska, K. Plevova, J. Rijntjes, S. Songia, M. Svaton, E. Fronkova, J. Bartram, B. Scheijen, D. Herrmann, R. Garcia-Sanz, J. Hancock, J. Moppett, J. J. M. van Dongen, G. Cazzaniga, F. Davi, P. J. T. A. Groenen, M. Hummel, E. A. Macintyre, K. Stamatopoulos, J. Trka, A. W. Langerak, D. Gonzalez, C. Pott, M. Bruggemann, N. Darzentas, EuroClonality-NGS working group, Quality control and quantification in IG/TR next-generation sequencing marker identification: Protocols and bioinformatic functionalities by EuroClonality-NGS. *Leukemia* **33**, 2254–2265 (2019).
77. V. Bystry, T. Reigl, A. Krejci, M. Demko, B. Hanakova, A. Grioni, H. Knecht, M. Schlitt, P. Dreger, L. Sellner, D. Herrmann, M. Pingeon, M. Boudjoghra, J. Rijntjes, C. Pott, A. W. Langerak, P. Groenen, F. Davi, M. Bruggemann, N. Darzentas, EuroClonality-NGS, ARResT/Interrogate: An interactive immunoprofiler for IG/TR NGS data. *Bioinformatics* **33**, 435–437 (2017).
78. R Core Team, R: A language and environment for statistical computing (2021).
79. X. Brochet, M.-P. Lefranc, V. Giudicelli, IMGT/V-QUEST: The highly customized and integrated system for IG and TR standardized V-J and V-D-J sequence analysis. *Nucleic Acids Res.* **36**, W503–W508 (2008).
80. M.-P. Lefranc, V. Giudicelli, C. Ginestoux, J. Jabado-Michaloud, G. Folch, F. Bellahcene, Y. Wu, E. Gemrot, X. Brochet, J. Lane, L. Regnier, F. Ehrenmann, G. Lefranc, P. Duroux, IMGT, the international ImMunoGeneTics information system. *Nucleic Acids Res.* **37**, D1006–D1012 (2009).
81. G. Senturk, Y. Y. Ng, S. B. Eltan, D. Baser, I. Ogulur, D. Altindirek, S. Firtina, H. Yilmaz, B. Kocamis, A. Kiykim, Y. Camcioglu, M. C. Ar, T. Sudutan, S. Beken, S. G. Temel, Y. Alanay, E. Karakoc-Aydiner, S. Baris, A. Ozen, U. Ozbek, M. Sayitoglu, O. H. Ng, Determining T and B Cell development by TREC/KREC analysis in primary immunodeficiency patients and healthy controls. *Scand. J. Immunol.* **95**, e13130 (2022).
82. L. L. Andersen, N. Mork, L. S. Reinert, E. Kofod-Olsen, R. Narita, S. E. Jorgensen, K. A. Skipper, K. Honing, H. H. Gad, L. Ostergaard, T. F. Orntoft, V. Hornung, S. R. Paludan, J. G. Mikkelsen, T. Fujita, M. Christiansen, R. Hartmann, T. H. Mogensen, Functional IRF3 deficiency in a patient with herpes simplex encephalitis. *J. Exp. Med.* **212**, 1371–1379 (2015).
83. S. Petrovski, Q. Wang, E. L. Heinzen, A. S. Allen, D. B. Goldstein, Genic intolerance to functional variation and the interpretation of personal genomes. *PLOS Genet.* **9**, e1003709 (2013).
84. N. M. Ioannidis, J. H. Rothstein, V. Pejaver, S. Middha, S. K. McDonnell, S. Baheti, A. Musolf, Q. Li, E. Holzinger, D. Karyadi, L. A. Cannon-Albright, C. C. Teerlink, J. L. Stanford, W. B. Isaacs, J. Xu, K. A. Cooney, E. M. Lange, J. Schleutker, J. D. Carpten, I. J. Powell, O. Cussenot, G. Cancel-Tassin, G. G. Giles, R. J. MacInnis, C. Maier, C. L. Hsieh, F. Wiklund, W. J. Catalona, W. D. Foulkes, D. Mandal, R. A. Eeles, Z. Kote-Jarai, C. D. Bustamante, D. J. Schaid, T. Hastie, E. A. Ostrander, J. E. Bailey-Wilson, P. Radivojac, S. N. Thibodeau, A. S. Whittemore, W. Sieh, REVEL: An ensemble method for predicting the pathogenicity of rare missense variants. *Am. J. Hum. Genet.* **99**, 877–885 (2016).
85. University of Michigan; National Heart, Lung, and Blood Institute (NHLBI), NHLBI Trans-Omics for Precision Medicine (TOPMed) Whole Genome Sequencing Program. BRAVO variant browser. (2024) [accessed 27 February 2024].

Acknowledgments: We thank the clinical cooperation partners and the patients and their families for participation in our study; H. Schachner from the Medical University of Vienna (MUW) for providing histologic stains of the biopsy; L. Shaw from the MUW for preparing the library for scRNA-seq; A. Skotnicova and E. Fronkova from the Second Faculty of Medicine, Charles University and University Hospital Motol in Prague, and K. Liszt from the St. Anna Children's Cancer Research Institute Vienna for providing valuable reagents and assistance with BCR and TCR sequencing; and R. Kirnbauer from the MUW for assistance in analyzing the skin biopsy. We would like to thank "Can Sucak Candan Biseyler" Foundation (CSCBF) for support. CSCBF was founded in 2018 to honor C. Sucak, who lost his life because of complications of primary immunodeficiency. CSCBF supports research in the field of primary immunodeficiency and promotes awareness. We would like to express our gratitude to T. Meyer, C. Meisel, and N. Unterwalder from the Department of Immunology at Labor Berlin for assistance in testing material from P3 for IFN autoantibodies. We thank A. Bykov from the St. Anna Children's Cancer Research Institute Vienna for helping to archive the raw sequencing data on the European Genome-Phenome Archive. We thank U. Pötschger, Statistics Team Leader at the St. Anna Children's Cancer Research Institute, for valuable support in the statistical analysis of our data. **Funding:** This work was supported by an European Research Council Consolidator Grant ("iDysChart", grant no. 820074, to K.B.); Austrian Research Promotion Agency (FFG), Research Partnerships programme (B.R.); P.T. Engelhorn Foundation, Postdoctoral Fellowship (C.v.d.W.); Austrian Academy of Sciences, DOC Fellowship (no. 25590) (J.B.); FWF, Lise Meitner Postdoctoral Fellowship (M.J.K.); the Scientific and Technological Research Council of Turkey (318S202) (S.B.); and Alex's Lemonade Stand Foundation for Childhood Cancer (ALSF) 20-17258 (M.F. and F.H.). **Author contributions:** B.R. performed most of the experiments, including flow cytometry, generation of CRISPR-Cas9–edited cells, and the set-up and optimization of coculture experiments; B.R. and S.K.B. interpreted clinical and immunological data; S.K.B. supervised B.R. while performing functional in vitro experiments together; M.T. initiated the project and provided critical initial input; B.R. and M.T. performed the initial immunophenotyping and B cell activation and class-switch assay; M.S. performed the BCR and TCR sequencing and analyzed the data; C.H. analyzed scRNA-seq data under the supervision of F.H. of samples prepared by B.R. and S.K.B., who also helped in the interpretation of the scRNA-seq data; A.K., M.T., A.S.-R., B.E., and Ü.A. analyzed WES data and identified the *LTBR* variants; A.S.-R. and A.K. performed Sanger sequencing validation and segregation analyses; B.R., M.T., and C.v.d.W. performed immunoblotting; B.R. and C.v.d.W. performed ELISA experiments; J.B., M.S., and B.R. performed the T_H subset analysis; A.F. performed the LTβR protein structure visualization; S.B., M.Y.A., A.O., E.K.-A., A.K., S.B.E., O.A., S.K., and S.I. took care of P1 and P2; S.B., M.Y.A., and A.M. collected patient samples and organized their shipment; A.M., G.D.T., and A.C. took care of P3; B.H. analyzed the skin biopsy from P1; M.F. supervised the scRNA-seq; I.S.-K. provided histopathologic evaluation of the biopsy sample from P2 and the blood smears from P1 and P2; H.v.B. assessed interferon autoantibodies in P3; R.P. and S.K. provided technical input; M.J.K., M.R., and A.V.T. provided critical intellectual input; B.R., S.K.B., M.J.K., M.S., C.v.d.W., I.C., and K.B. wrote the manuscript with input from all co-authors; K.B. conceptualized and coordinated the study, provided laboratory resources, and took overall responsibility of the study. All authors vouch for the data and the analysis. All authors approved the final version of the manuscript and agreed to publish the paper. **Competing interests:** The authors declare that they have no competing interests. **Data and materials availability:** Raw sequencing reads are deposited in the European Genome-Phenome Archive [accession numbers EGAS00001007271 (BCR/TCRseq) and EGAS00001007271 (scRNA-seq)]. These data are available via controlled access to safeguard patient privacy. The R code used for the analysis of single-cell RNA-sequencing data is available on GitHub at https://github.com/cancerbits/ransmayr2024_ltbr and for the analysis of the BCR and TCR sequencing results at https://github.com/msvtnCCRI/ransmayr2024_ltbr_igtr. All data needed to evaluate the conclusions in the paper are present in the paper or the Supplementary Materials. Tabulated underlying data for all figures can be found in data file S1.

Submitted 4 June 2024
Accepted 22 October 2024
Published 22 November 2024
10.1126/sciimmunol.adq8796

Science Immunology
AAAS

Supplementary Materials for

LTβR deficiency causes lymph node aplasia and impaired B cell differentiation

Bernhard Ransmayr *et al.*

Corresponding author: Kaan Boztug, kaan.boztug@ccri.at

Sci. Immunol. **9**, eadq8796 (2024)
DOI: 10.1126/sciimmunol.adq8796

The PDF file includes:

Other Supplementary Material for this manuscript includes the following:

SUPPLEMENTARY MATERIALS

SUPPLEMENTAL PATIENT CLINICAL HISTORIES

The patient cohort consists of three individuals from two unrelated consanguineous families from Turkey. Patient 1 (P1, born 1997, 27 years, male) has experienced, from 7 months of age, recurrent pneumonia along with frequent episodes of otitis and sinusitis, which required 2 times hospitalization for administration of intravenous antibiotics. At the age of 3 years, he had *S. pneumoniae* meningitis, with complete recovery. During another hospitalization episode due to pneumonia, bronchiectasis was detected in the thorax computed tomography scan. The physical examination revealed the absence of tonsils and no lymph nodes were palpable. The patient further exhibited signs of failure to thrive, with his weight falling below the 3rd percentile and his height ranging between the 3rd and 10th percentiles. Laboratory assessment revealed panhypogammaglobulinemia. Inverted $CD4^+/CD8^+$ T cell ratio as well as high naïve and decreased class-switched memory B cells were observed upon immunological evaluation. Lymphocyte proliferation responses were comparable to age-matched controls. At 10 years of age, he started to receive intravenous immunoglobulin replacement treatment along with azithromycin prophylaxis, leading to a notable reduction in infections. Since then, he has been experiencing episodes of otitis media 1-2 times per year and has had facial verruca vulgaris for the last 10 years, extended to his neck and shoulders, which was DNA-positive for human papillomavirus type 24 (Fig. 1F). It is associated with *epidermodysplasia verruciformis* and an increased risk of developing squamous cell carcinomas particularly in sun-exposed areas early in life (*21*). No additional infections were observed during the follow-up period.

Patient 2 (P2, born 2005, 19 years, male) is the younger brother of P1. He consistently had recurrent sinopulmonary infections since 3 months of age. At the age of 9 years, he experienced acute hepatitis and cholecystitis. No causative infectious agent could be isolated, and autoantibodies were negative. A liver biopsy showed biliary destruction and T cell infiltration without evidence of cirrhosis. The patient benefitted from cholecystectomy and antibiotics, as well as systemic methylprednisolone, at a dose of 1 mg/kg/day for 2 weeks. Based on the panhypogammaglobulinemia, low isohemagglutinin levels, and decreased total pneumococcal vaccine response, he was commenced on intravenous immunoglobulin replacement treatment and antibiotic prophylaxis at the age of 12 years, which provided good infection control. Similar to P1, absence of tonsils was noted during physical examination, and immunological evaluation of PBMCs showed an inverted $CD4^+/CD8^+$ T cell ratio with high naïve and decreased class-switched memory B cells.

Patient 3 (P3, born 2015, 9 years, male), the second-born male child of another unrelated Turkish family was evaluated in an immunology clinic at 6 months of age due to the previous history of his deceased brother. At this time, he was completely asymptomatic. However, although his IgM levels were normal, his IgA and IgG levels were lower than age references. Immunological evaluation showed comparable numbers of $CD4^+$, $CD8^+$ and $CD19^+$ cells to the age-matched controls. He was commenced on intravenous immunoglobulin substitution and trimethoprim-sulfamethoxazole prophylaxis. *CD40* and *CD40LG* gene defects were excluded via Sanger sequencing. Immunological evaluation was performed again at the age of 1 year, revealing the lack of class-switched B cells. Currently, the patient has an asymptomatic clinical course under intravenous immunoglobulin substitution and antibiotic prophylaxis.

The patient's brother had hypogammaglobulinemia and recurrent pulmonary infections leading to severe bronchiectasis and pulmonary hypertension. He succumbed to cor pulmonale at the age of 18 years. No genetic material from this patient was available.

SUPPLEMENTARY FIGURES

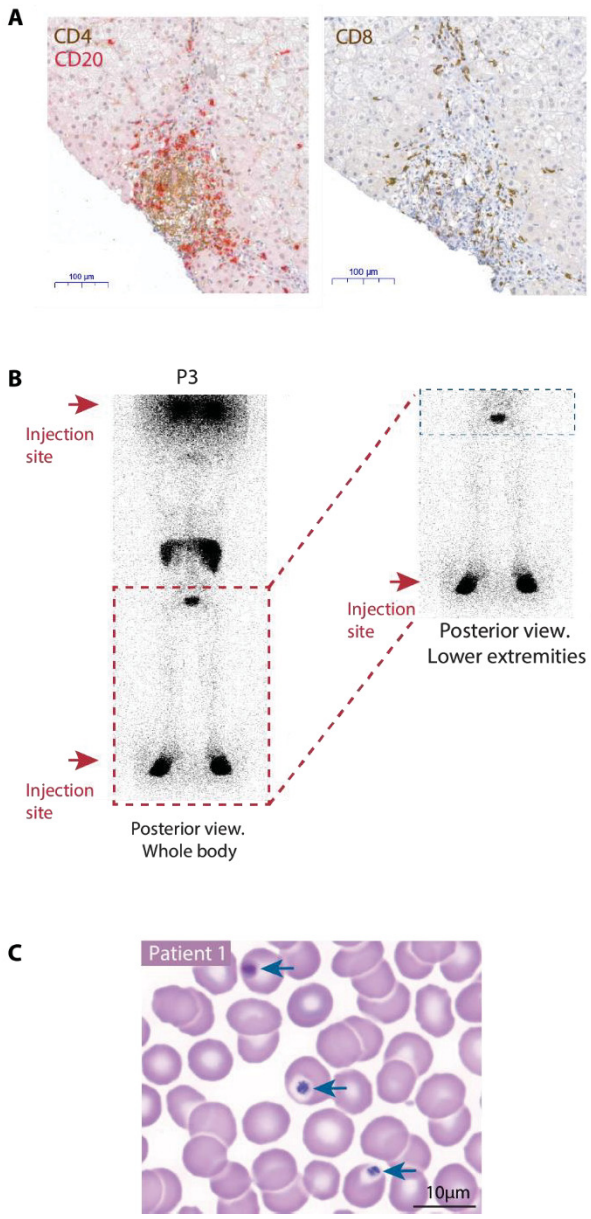

Figure S1. Liver biopsy showing accumulation of lymphocytes in P2 and SLO defects in P3 and P1

(**A**) Liver biopsy from P2 during an episode of acute hepatitis showing accumulation of $CD4^+$ T cells (brown) and $CD20^+$ B cells (red) (left panel), and a low number of $CD8^+$ T cells (brown) distinct from the typical organization of an ectopic lymphoid structure (right panel). (**B**) Whole-body lymphoscintigraphy showing the absence of lymph nodes in P3. The red arrows indicate the injection sites. (**C**) Presence of Howell-Jolly bodies (blue arrows) in blood smear from P1.

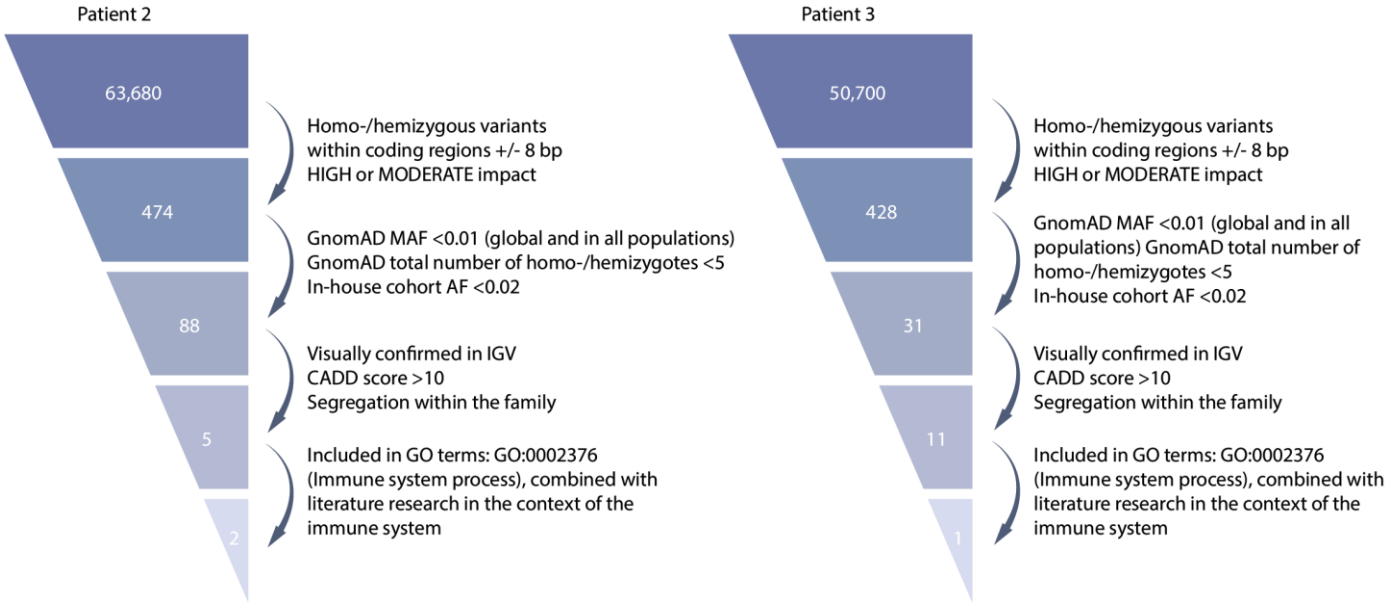

Figure S2. WES filtering strategy for the identification of potentially causative rare homo-/hemizygous variants

WES variant filtering strategy in P2 and P3 for the identification of potentially causative novel, rare, homo-/hemizygous-variants in immune-related genes (see Table S1-S4). The number of variants remaining after each filtering step are indicated on the left. MAF, minor allele frequency; CADD, Combined Annotation Dependent Depletion; GO, Gene Ontology.

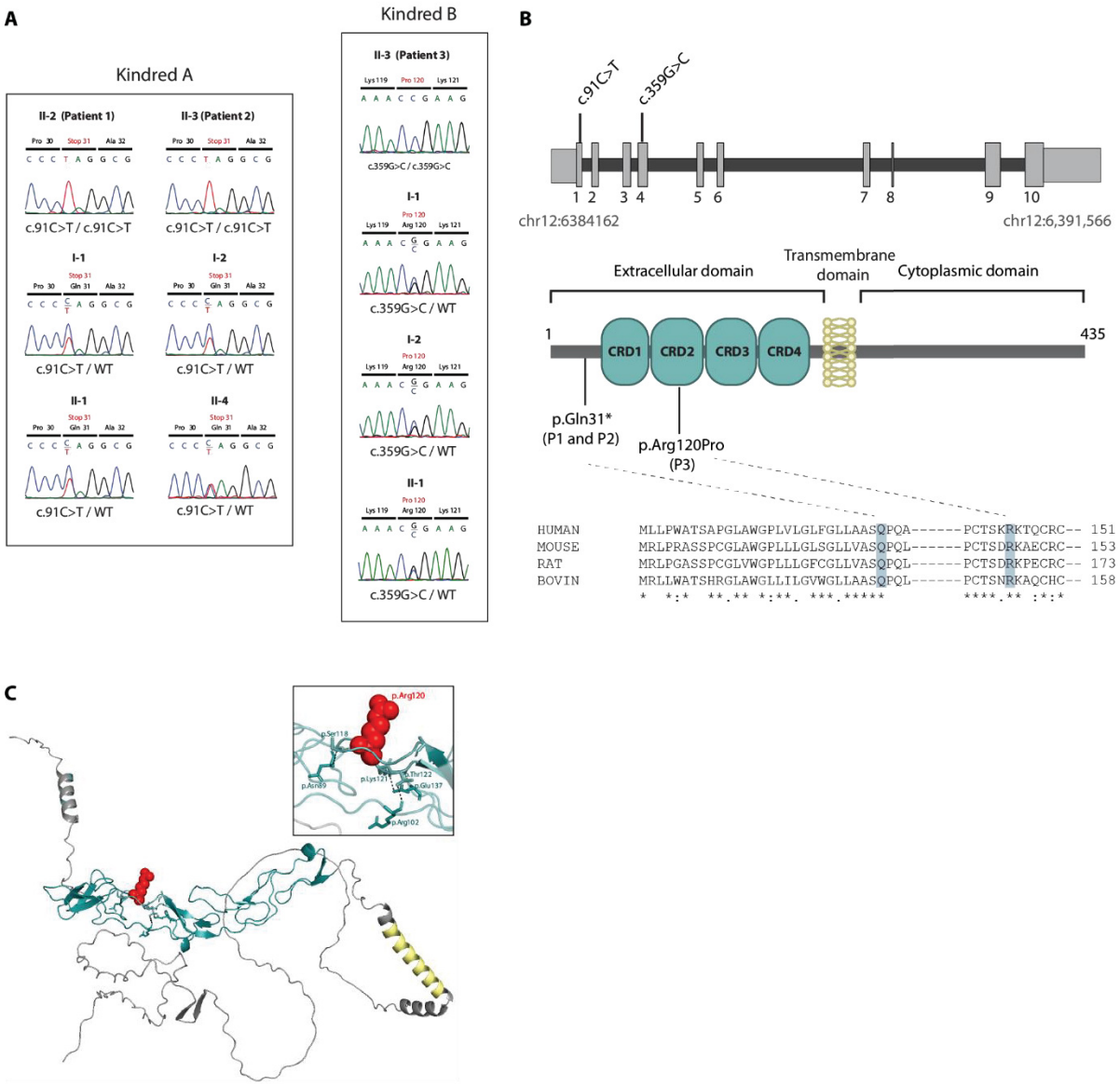

Figure S3. Analysis of the identified *LTBR* germline mutations

(**A**) Sanger sequencing chromatograms of *LTBR* encompassing the identified variants in the respective families. Mutant residues are highlighted in red. Roman numbers indicate generations while Arabic numbers indicate individuals within a generation (see Fig. 1A). (**B**) Diagram displaying the position of the mutations within the *LTBR* exons in the cDNA (upper panel) and the different protein domains of LTβR, with the position of the identified variants also indicated (lower panel). CRD: Cysteine Residue Domain. Multiple protein sequence alignment shows conserved p.Gln31 and p.Arg120 residues across several mammal species. Highly conserved residues within the selected species are marked by asterisks (*). (**C**) 3D structural model of LTβR predicted by Alphafold (*66, 67*), with a close-up view showing the mutated arginine residue at position 120 (shown as red spheres) found in P3. This residue is located in a loop of the CRD2 domain that contains multiple residues predicted to form interactions with residues within the CRD1 domain. The software MISSENSE3D predicts that the proline resulting from the mutation introduces steric clashes (disallowed phi/psi), consistent with a destabilizing effect on the protein. The transmembrane domain is depicted in yellow and the CRD domains in green.

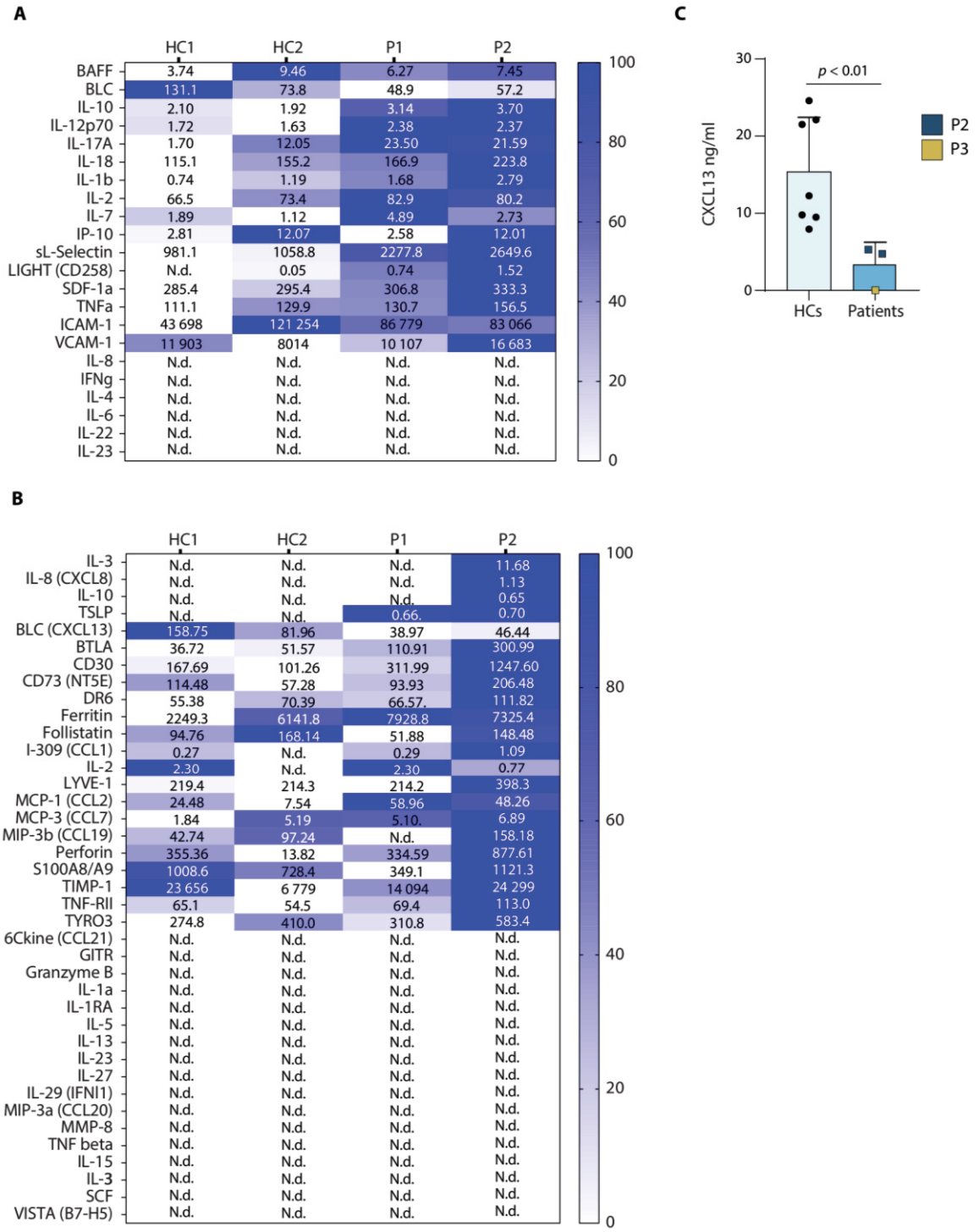

Figure S4. Serum analysis using Luminex multiplex assay and ELISA

(**A**) Heatmap summarizing the Luminex multiplex results of various cytokines in the serum from P1 and P2 compared to HC (n=2). (**B**) Heatmap summarizing the Luminex multiplex results of various cytokines in serum from P1 and P2 taken at a different timepoint than the serum analyzed in (A), compared to HC (n=2). Results for each parameter were individually normalized, with the lowest value set to 0 and the highest value set to 100. All other values were scaled proportionally between these two

extremes. Numbers inside the figure show the absolute concentration measured in pg/mL. (**C**) Serum CXCL13 determination by ELISA. Data from one experiment with P2 (n=2) and P3 (n=1) compared to HC (n=7). Statistical analysis was performed using Unpaired *t* test with Welch's correction.

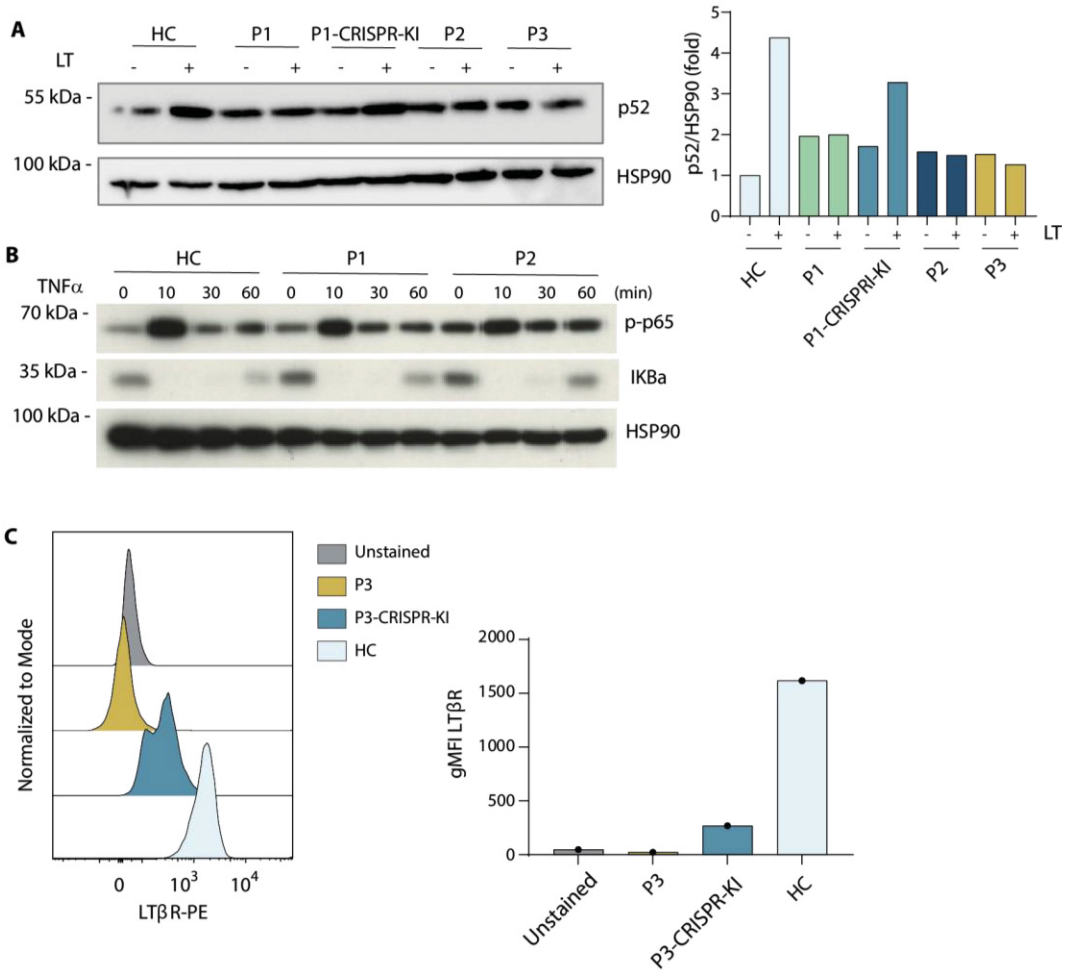

Figure S5. Non-canonical and canonical NF-κB signaling in response to TNFα- or LT-stimulation

(**A**) Immunoblot displaying p52 expression before and after stimulation with LTαβ_2 in a HC, P1 to P3 and P1-derived CRISPR-KI fibroblasts reverting the mutation to wild type. Quantification shown as fold change of p52/HSP90 compared to untreated HC. Heat shock protein 90 (HSP90) as a housekeeping protein serves as loading control. (**B**) Immunoblot displaying the activation of canonical NF-κB signaling via upregulated expression levels of p-p65 (phosphorylated p65 protein) and diminished IKBα (nuclear factor of kappa light polypeptide gene enhancer in B cells inhibitor alpha) following stimulation with Tumor Necrosis Factor Alpha (TNFα) for the indicated time points (in minutes). Heat shock Protein 90 (HSP90) as a housekeeping protein serves as loading control. (**C**) gMFI of LTβR-PE in flow cytometry in dermal fibroblasts from HC and P3 before and after CRISPR/Cas9 editing to correct the *LTBR* mutation.

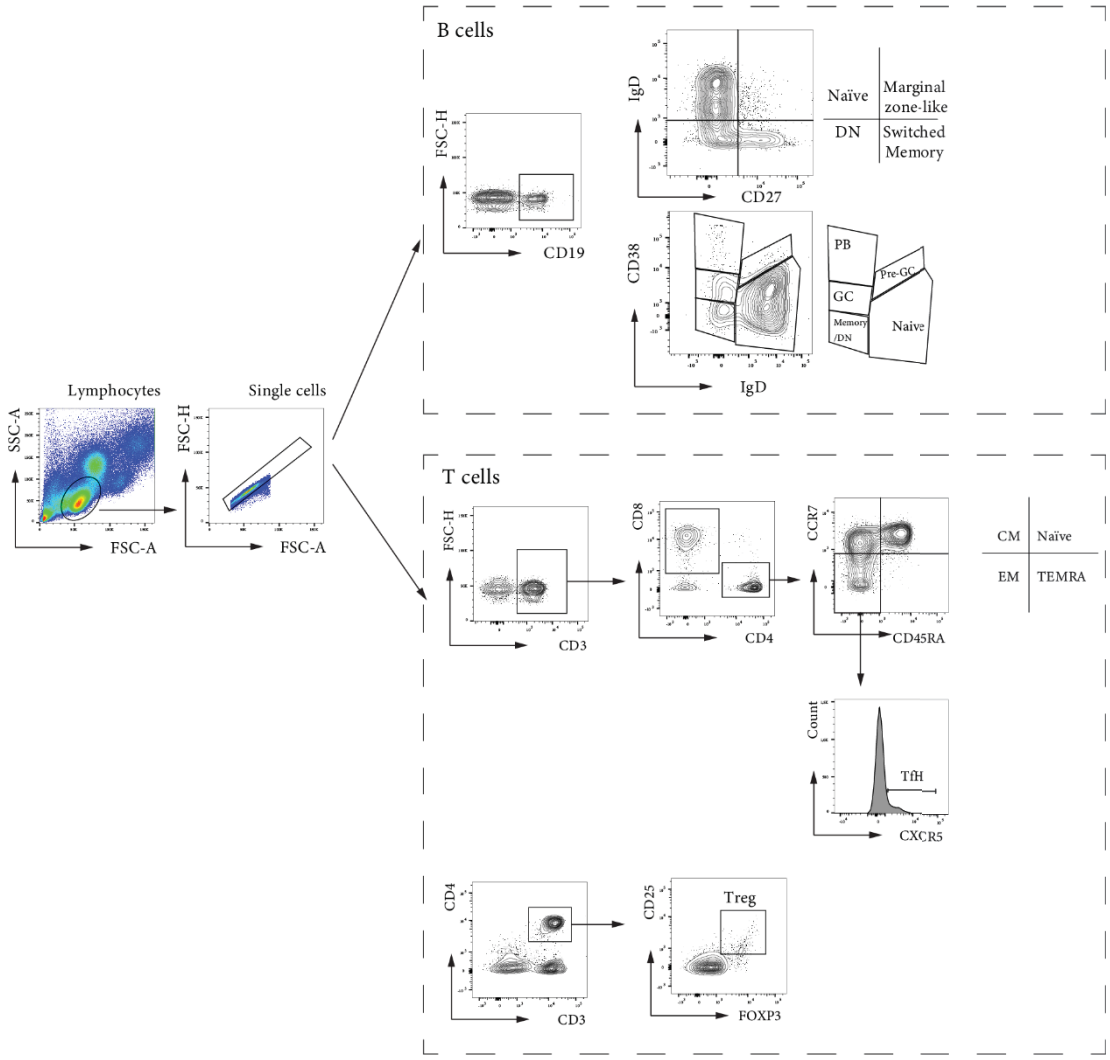

Figure S6. Gating scheme for flow cytometry analysis of B and T cell subsets.

Gating scheme for immune cell subset flow cytometry analysis of PBMCs obtained from patients and healthy controls. SSC - side scatter, FSC - forward scatter; Ig –immunoglobulin; DN - double negative; GC - germinal center; PB – plasmablast; TEMRA - terminally differentiated effector memory re-expressing CD45RA T cells; CM - central memory; EM - effector memory; TfH – T follicular helper cells; Treg – T regulatory cells.

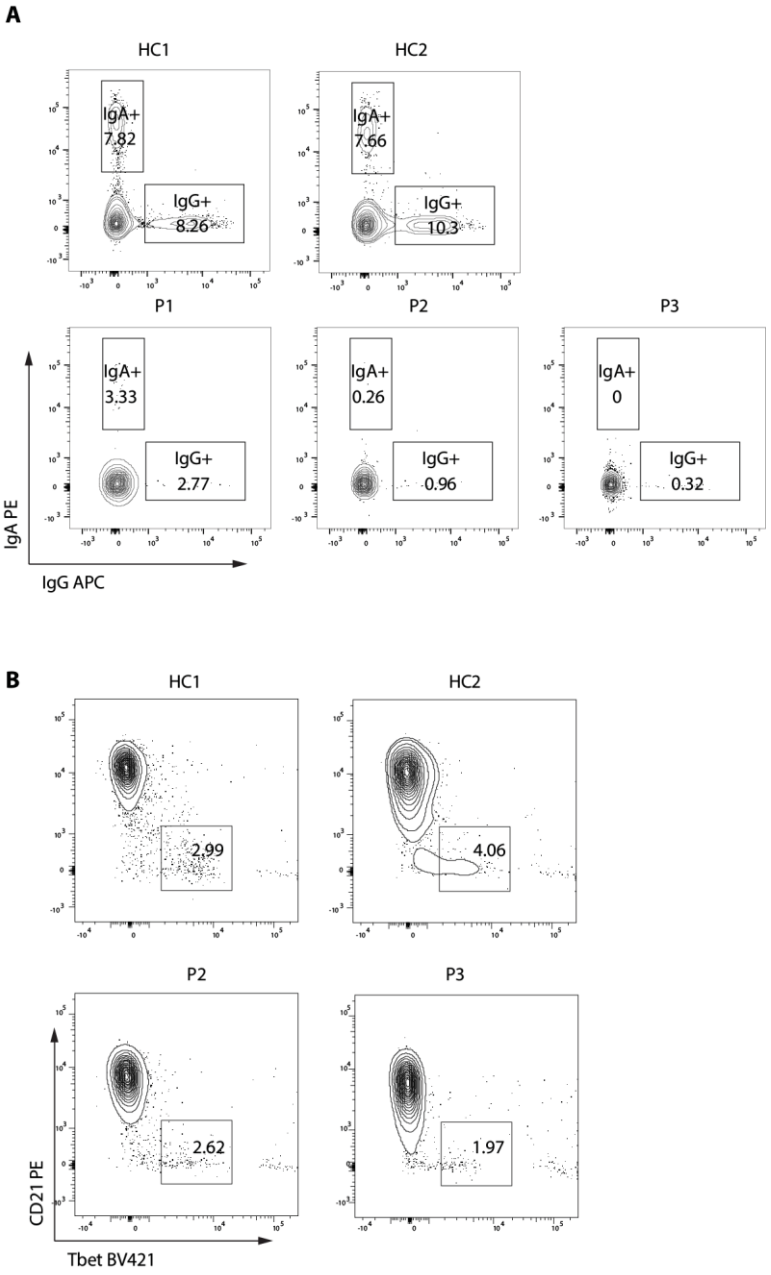

Figure S7. Reduction of class switched B cells whilst CD21^{low}Tbet^{+} B cells were not increased

(**A**) Representative FACS blots showing the fraction of CD19^{+} B cells expressing IgA or IgG, exhibiting a clear reduction of class-switched B cells in P1 to P3 compared to two representative healthy controls. (**B**) FACS blot depicting a comparable frequency of CD21^{low}Tbet^{+} CD19^{+} B cells in P2 and P3.

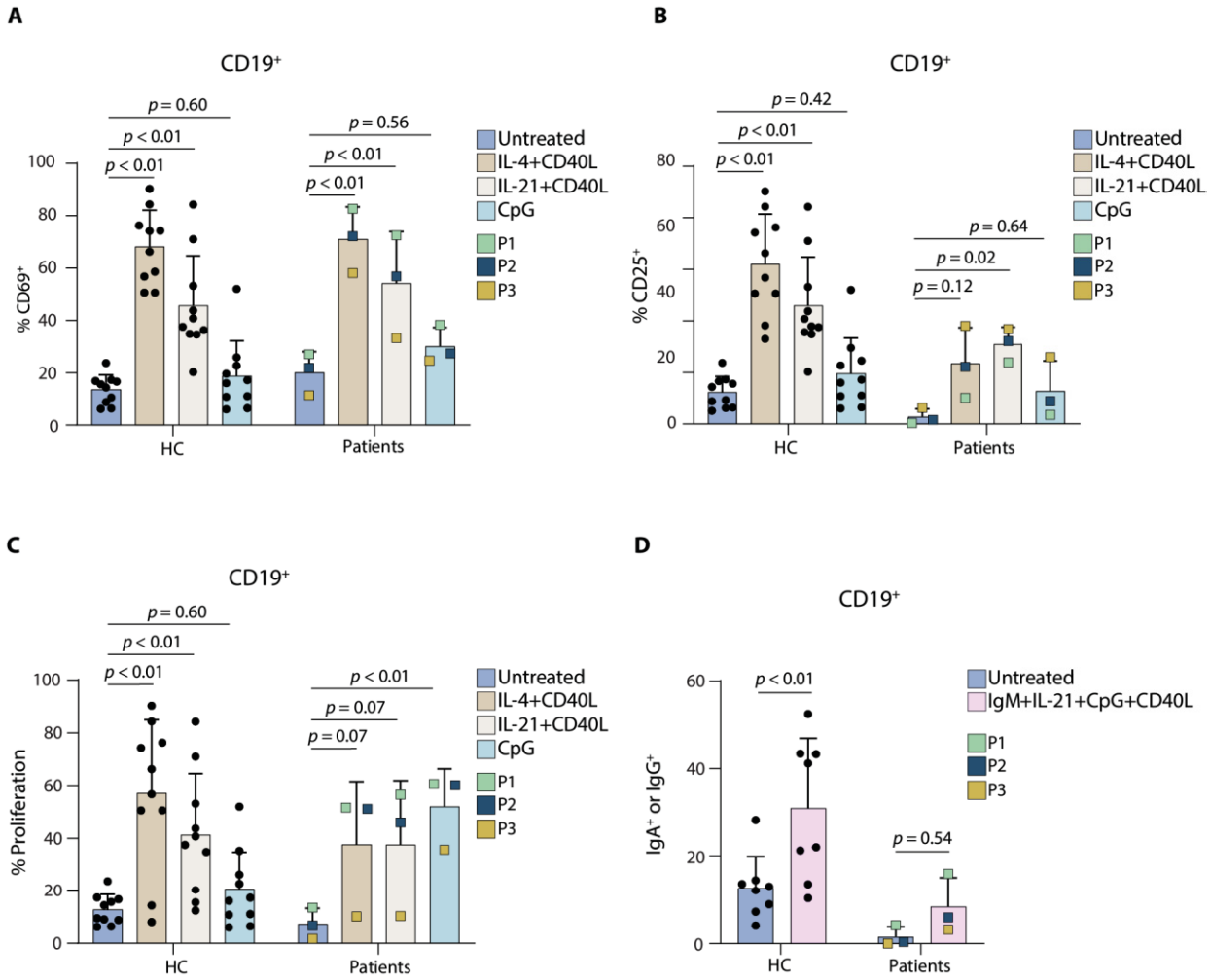

Figure S8. Normal B cell functional responses to stimulation

(**A**) Upregulation of activation markers CD69 and (**B**) CD25 in CD19$^+$ cells from P1 to P3 along HCs (n=12) following stimulation with either IL-4+CD40L, IL-21+CD40L or CpG for 24 hours. (**C**) Corresponding proliferating cells as measured by the dilution of the violet proliferation dye (VPD450) following 5 days of stimulation. Data pooled from three independent experiments with a total of 10 different HCs and data averaged from P1 (n=2), P2 (n=3) and P3 (n=2). Analysis was performed using two-way analysis of variance (ANOVA) with Bonferroni post hoc test to correct for multiple comparisons. (**D**) Immunoglobulin class switch assessment using flow cytometric readout for IgA or IgG positive CD19$^+$ cells. PBMCs from HCs and patients were stimulated for 5 days with IgM+IL-21+CpG+CD40L. Data pooled from two different independent experiments with a total of 8 different HCs and data averaged from P1 (n=1), P2 (n=2) and P3 (n=1). Analysis was performed using two-way analysis of variance (ANOVA) with Bonferroni post hoc test to correct for multiple comparisons.

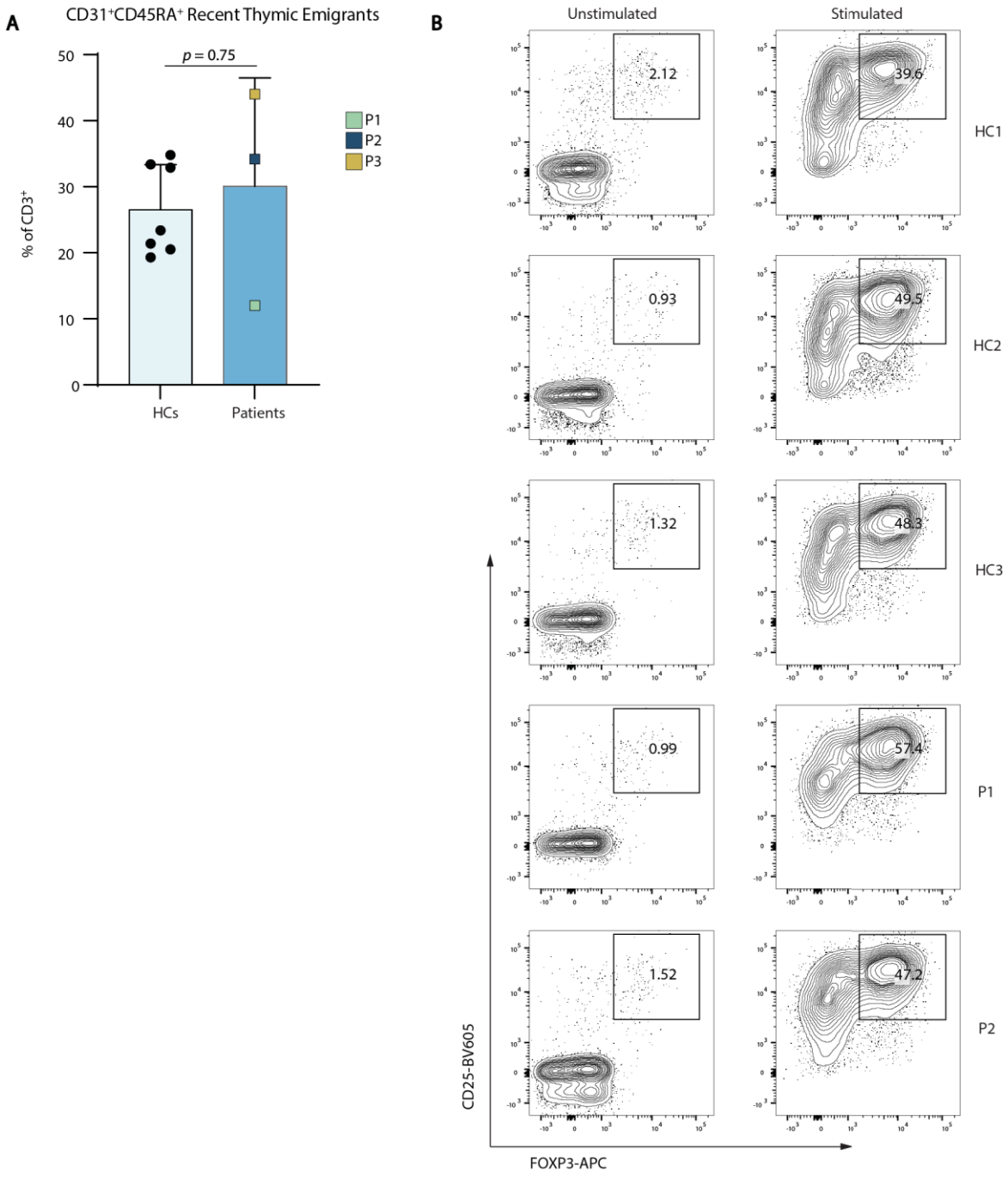

Figure S9. Normal number of recent thymic emigrants and functional ex vivo Treg differentiation

(**A**) Flow cytometry results showing the frequency of $CD31^{+}CD45RA^{+}$ recent thymic emigrants (RTE) in peripheral PBMCs. The data shown here is from one experiment, representative of *N*=3; HC (n=7) and patients (n=3). Statistical analysis was performed on one of these experiments using Unpaired *t* test with Welch's correction. (**B**) Sorted naïve T cells were either treated with Human Treg Differentiation Media and seeded into anti-CD3-coated wells or left untreated and seeded into uncoated wells. Following 5 days of stimulation, cells were harvested and analyzed by flow cytometry. Cells were gated on $CD3^{+}CD4^{+}$ surface markers.

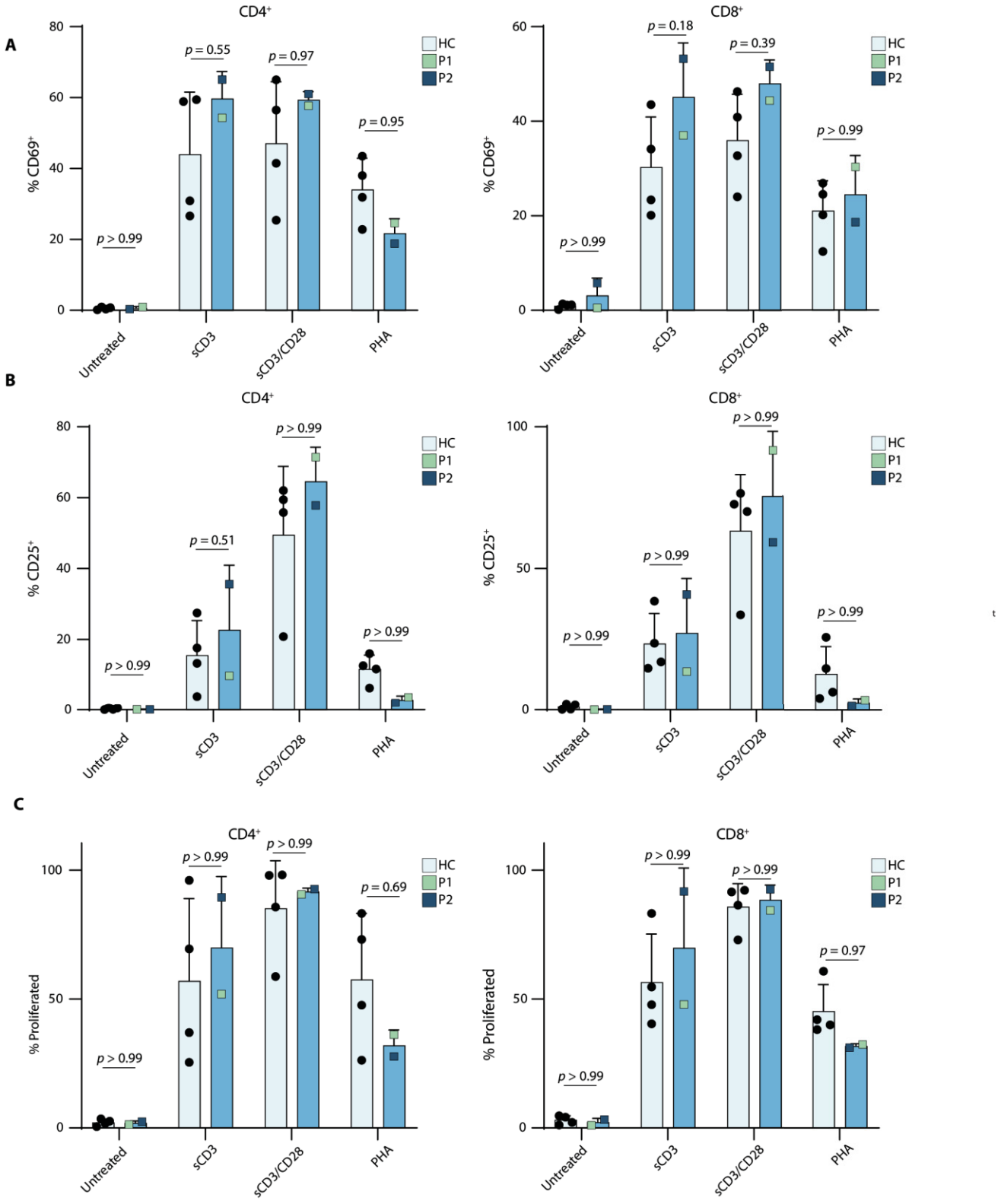

Figure S10. Normal activation and proliferation response in patient T cells.

(**A-B**) PBMCs were stimulated with either anti-CD3 soluble antibody (sCD3), anti-CD3 and anti-CD28 soluble antibody (sCD3/CD28), phytohemagglutinin (PHA) or anti-CD3/CD28 DynaBeads for 24h, and changes in activation markers CD69 (A) and CD25 (B) were assessed on $CD4^+$ and $CD8^+$ T cells. (**C-D**) Corresponding proliferating cells as measured by the dilution of the violet proliferation dye (VPD450) are shown for $CD4^+$ (C) and $CD8^+$ (D) T cells following 4 days of stimulation. The data shown here is from one experiment, representative of *N*=2; HC (n=4), P1 (n=2) and P2 (n=2). Statistical analysis was performed on one of these experiments using two-way analysis of variance (ANOVA) with Bonferroni post hoc test to correct for multiple comparison.

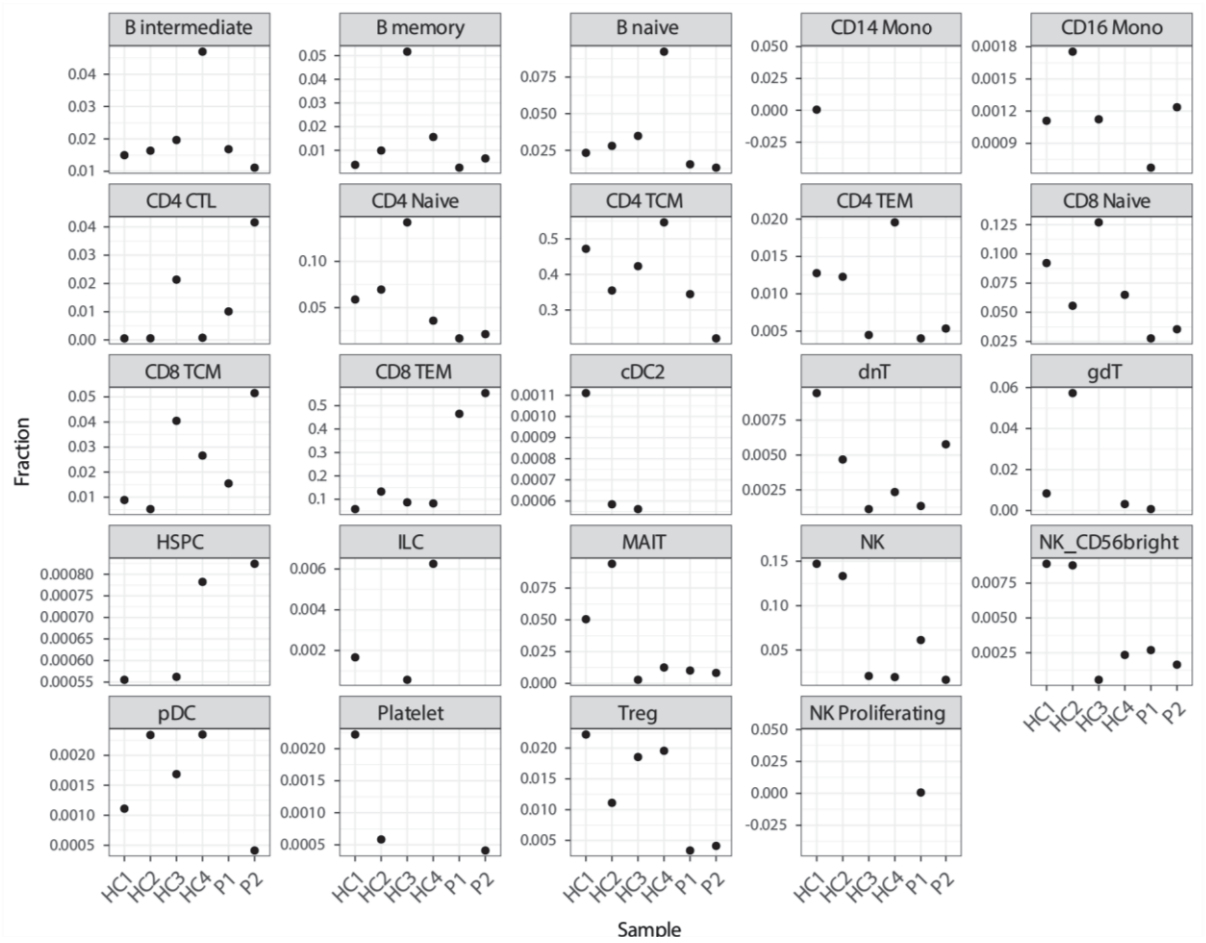

Figure S11. Immune cell type fraction analysis from scRNAseq.

Scatter plots showing proportions of different cell populations within the lymphocytes in the scRNAseq analysis from P1, P2 and four healthy controls.

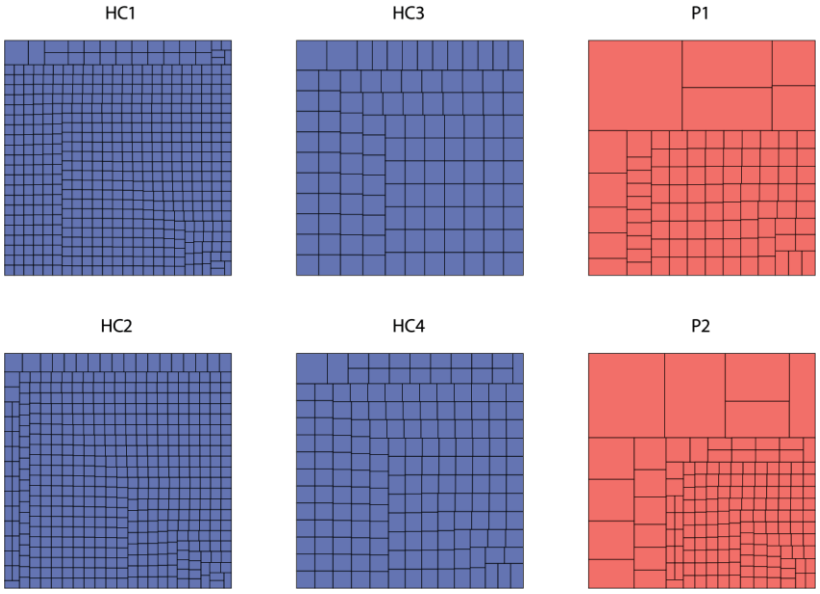

Figure S12. TCR clonality analysis via scRNAseq

Clonality of T cell receptor (TCR) sequences identified in the scRNAseq data of healthy controls (in blue) and P1 and P2 (in red).

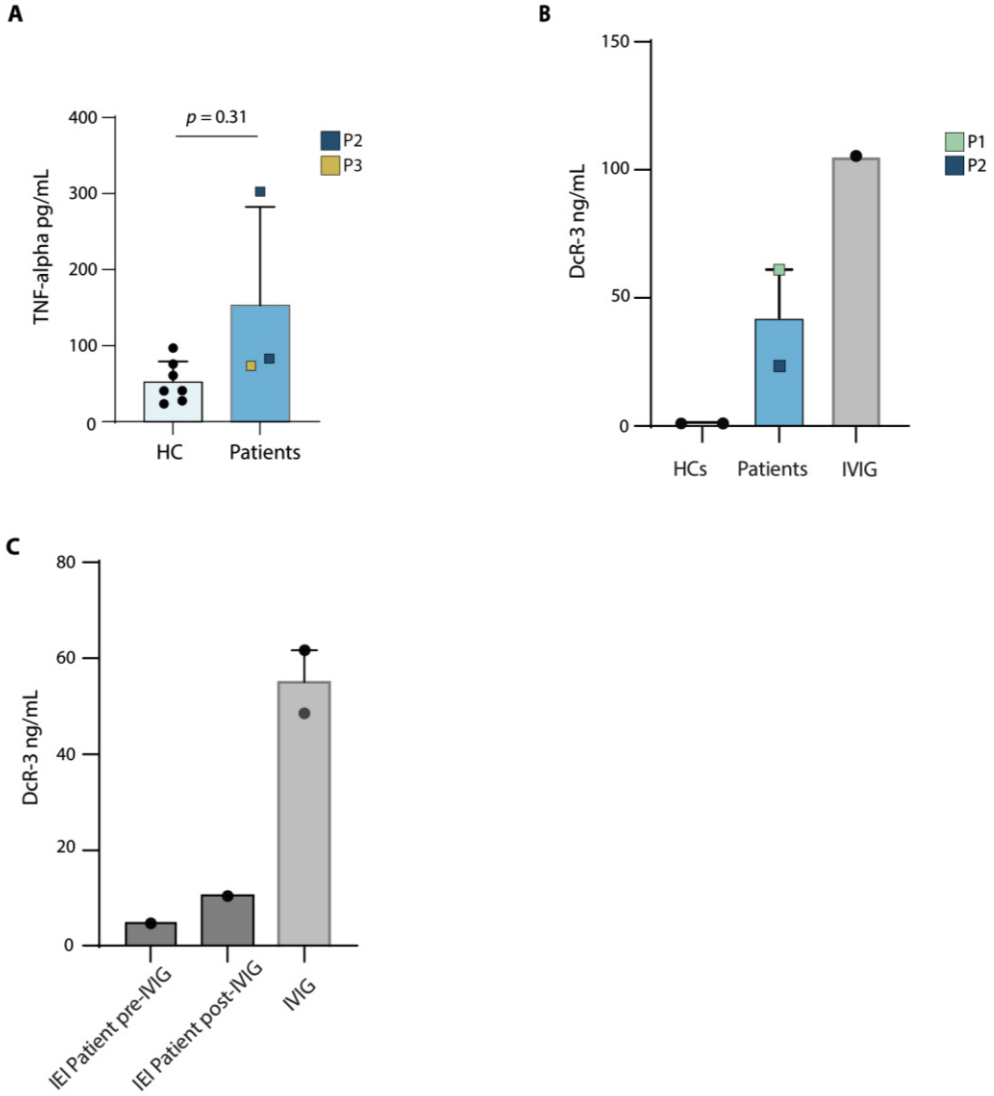

Figure S13. TNF-α and DcR3 ELISA serum measurements

(**A**) ELISA serum analysis for TNF-α. Data from one experiment with HCs (n=7) and from P2 (n=2) and P3 (n=1). Statistical analysis was performed using Unpaired *t* test with Welch's correction. (**B**) Replicate of DcR3 serum analysis via ELISA as depicted in Fig. 4E. Patient samples were taken from a different timepoint. IVIG sample was measured from a different batch. (**C**) ELISA results showing an increase of the serum DcR3 values in an IEI patient following IVIG treatment. Additionally, two different IVIG samples were measured.

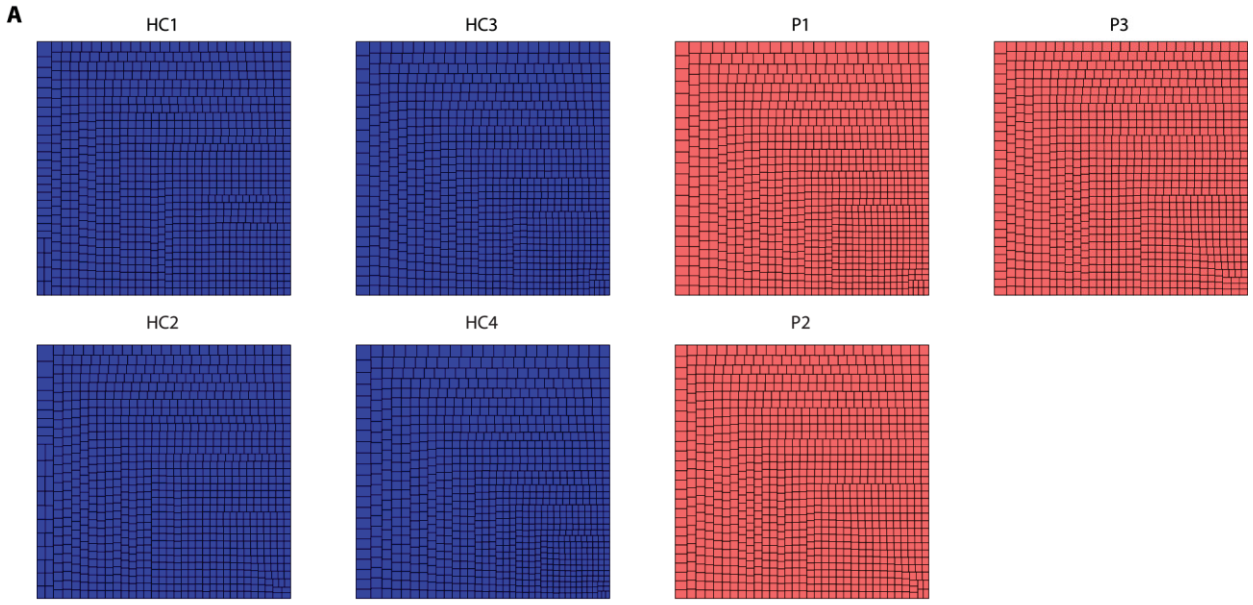
A
HC1
HC3
P1
P3
HC2
HC4
P2

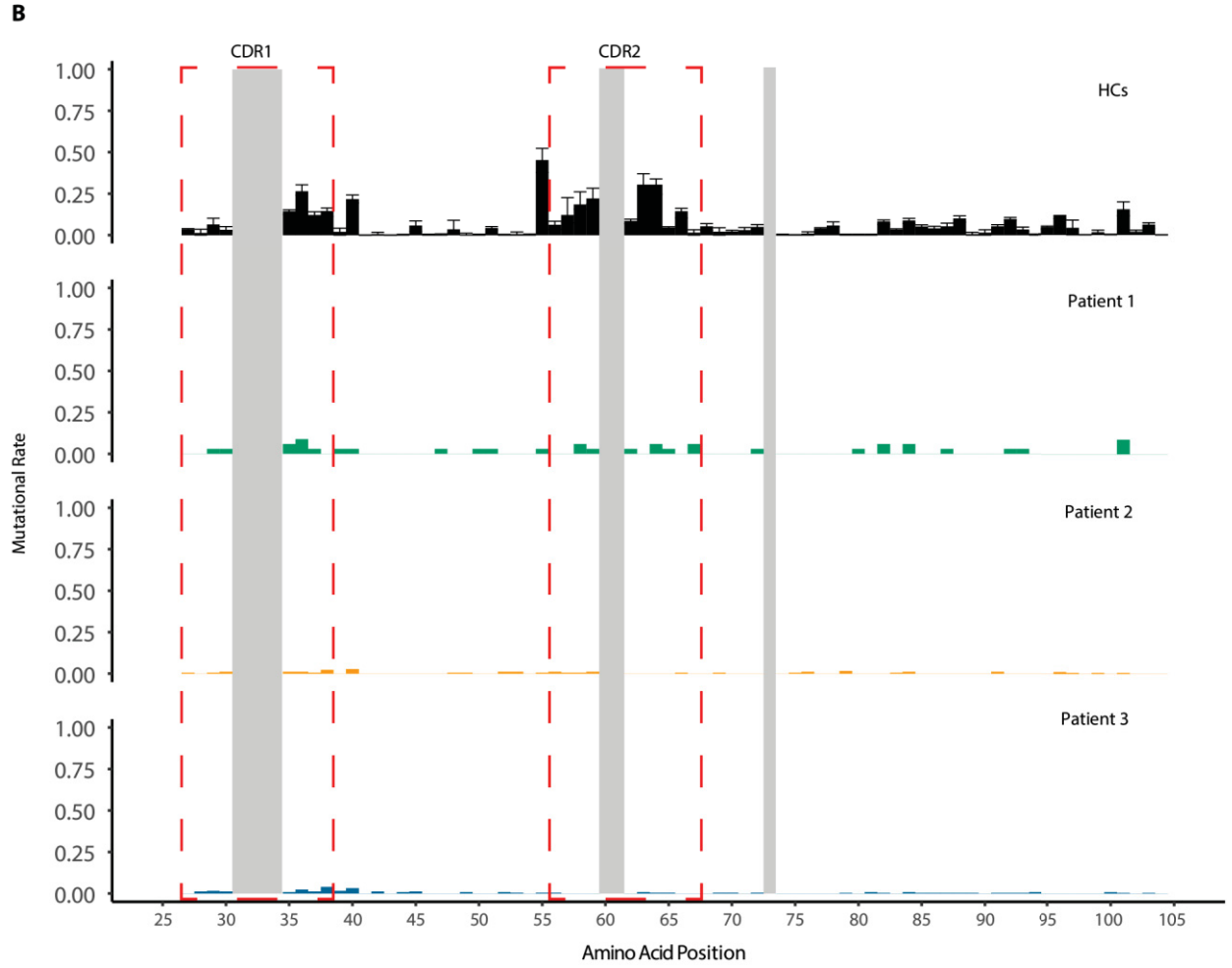
B
CDR1
CDR2
HCs
Patient 1
Patient 2
Patient 3
Mutational Rate
1.00
0.75
0.50
0.25
0.00
25
30
35
40
45
50
55
60
65
70
75
80
85
90
95
100
105
Amino Acid Position

Figure S14. B cell receptor sequencing depicting reduced SHM rate in patients

(**A**) Repertoire diversity plots of the individual clones with productive immunoglobulin heavy-chain (IGH) gene rearrangements. No differences were observed between P1 to P3 (shown in red) and controls (n=4, in blue). (**B**) Rate of somatic hypermutation (SHM) in the *IGHV3-23* region of all productive IGH rearrangements aligned to the IMGT reference. The median and 75th percentile of the mutational rate is shown for controls (in black) and individual bars are shown for each patient at each amino acid position for P1 to P3 in green, orange and blue respectively. Complementarity determining regions (CDR) are marked with dashed red rectangles and grey areas depict positions that correspond to the gaps in the IMGT reference.

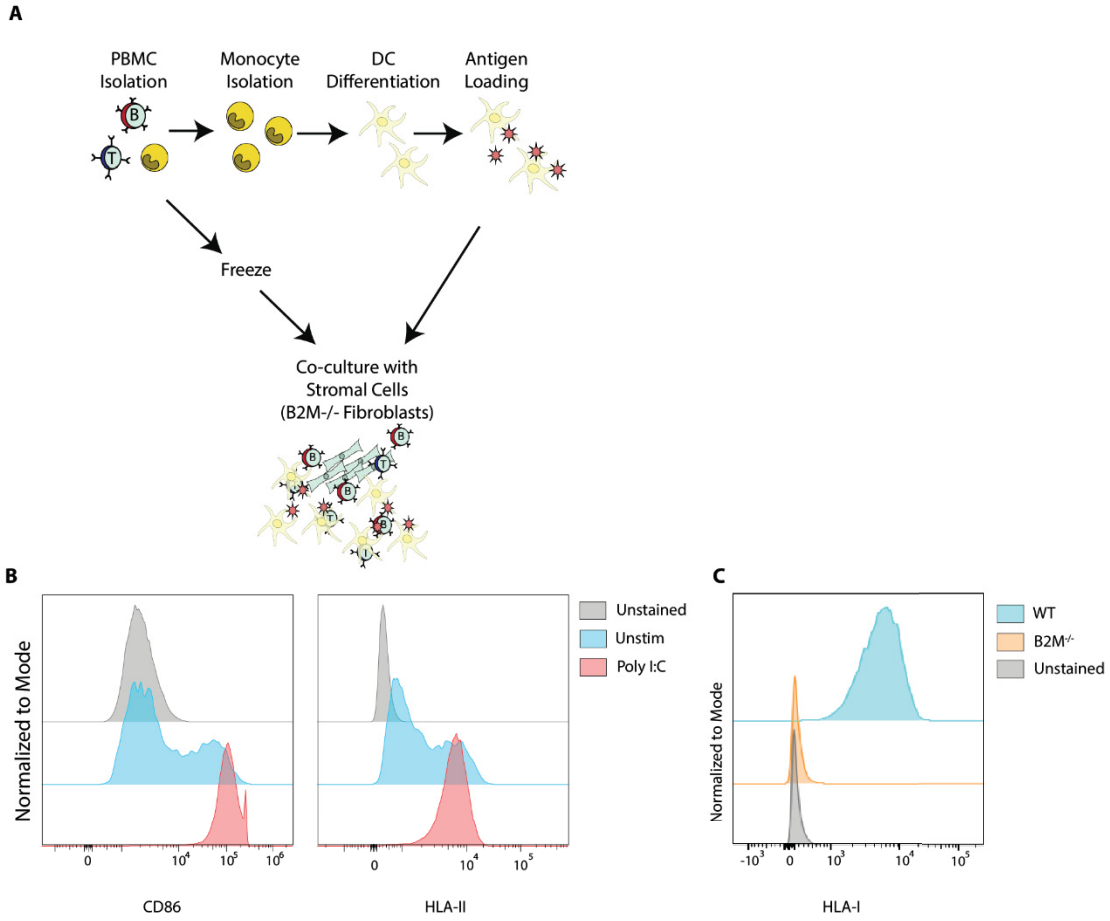

Figure S15. Differentiation of dendritic cells and generation of HLA-I negative fibroblasts

(**A**) Schematic representation of the co-culture assay workflow. $CD14^+$ monocytes were isolated from PBMCs and differentiated over 6 days using GM-CSF+IL-4 into $CD11c^+$ DCs. Following overnight stimulation with Poly I:C, DCs were co-cultured with PBMCs and dermal fibroblasts representing the stromal compartment (SC) from the same donor in a 24-well transwell. For HCs, a dermal fibroblast cell line was used, in which the B2M gene was knocked out using CRISPR-Cas9 to inhibit HLA-I expression and prevent T cell activation due to HLA-I mismatch. BAFF was added to the wells every other day. For further stimulation, some wells were treated once with a measles, mumps and rubella (MMR) vaccine. Detailed method information can be found in the supplementary materials. (**B**) Representative upregulation of the activation markers CD86 and HLA-II in monocyte-derived DCs following overnight stimulation with Poly I:C in cells from HC. (**C**) HLA-I expression in HC dermal fibroblasts compared with B2M CRISPR-Cas9-based knockout fibroblasts from the same HC.

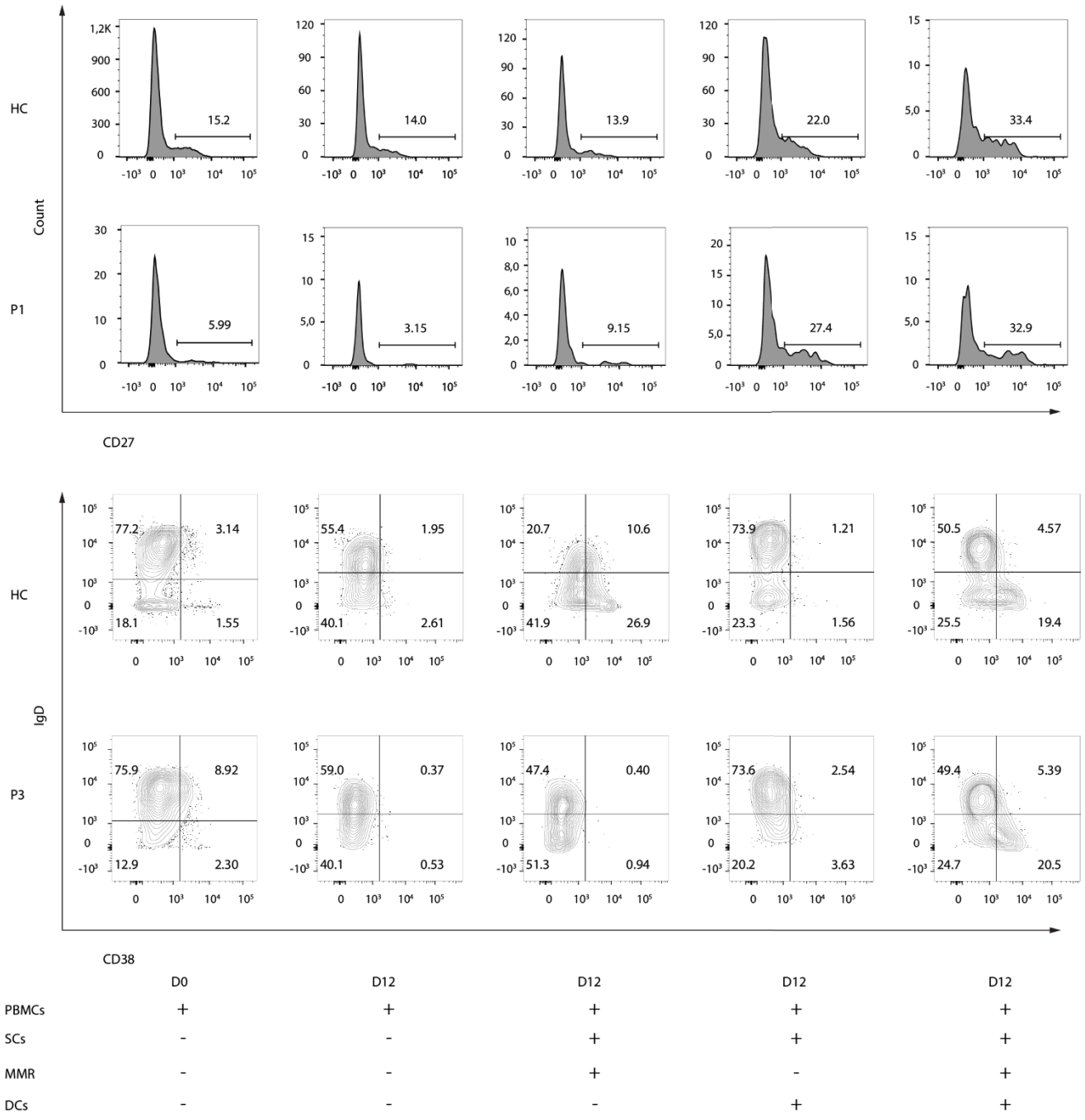

Figure S16. Co-culture for ex vivo B cell maturation in patients and healthy controls

Representative flow cytometry graphs for the quantified data summarized in Fig. 5D showing the upregulation of the memory marker CD27 (Top) and the development of GC-like CD19^{+} B cells (IgD^{-} CD38^{+}, Bottom). Cells were cultured for 12 days under the specified co-culture conditions and compared to Day 0 (first column).

Table S1. Heterozygous Variants in Known IUIS Genes Identified by WES in P2								
Gene	**HGNC_ID**	**Chr**	**Genomic position (hg38)**	**REF/ALT**	**CDS change**	**Amino acid change**	**Allele frequency (gnomAD)**	**CADD score**
THBD	**HGNC:11784**	**chr20**	**23049146**	**C/A**	**ENST00000377103.3:c.359G>T**	**p.Ser120Ile**	**N/A**	**24.2**
POLD2	HGNC:9176	chr7	44116136	T/C	ENST00000610533.6:c.998A>G	p.Gln333Arg	0.00000547	23.2
IL36RN	HGNC:15561	chr2	113060913	C/A	ENST00000393200.7:c.91C>A	p.Leu31Met	0.00001093	21.4
DNASE2	HGNC:2960	chr19	12876153	G/A	ENST00000222219.8:c.920C>T	p.Thr307Ile	N/A	17.46
IRF3	**HGNC:6118**	**chr19**	**49661941**	**C/A**	**ENST00000377139.8:c.982+7G>T**	**N/A**	**N/A**	**3.736**
CSF2RA	HGNC:2435	chrX	1288895	G/A	ENST00000381529.9:c.473+7G>A	N/A	N/A	1.055
DOCK8	HGNC:19191	chr9	432159	G/C	ENST00000432829.7:c.4627-7G>C	N/A	N/A	0.667

Table S1. Heterozygous variants in known IUIS genes identified by WES in P2.

Pre-filtered for variants in genes in the International Union of Immunological Societies (IUIS) classification of 2022 (*9*). In **bold**, those within genes associated with autosomal dominant inheritance. Non-synonymous and splice region variants (+/- 8 bp from the intron/exon boundaries) with MAF < 0.01 and gnomAD AC < 20 are listed and sorted by CADD score. Allele frequencies displayed are derived from the combined gnomAD v2.1.1 and gnomAD v3.1.2 (non-v2) datasets. The variants in *POLD2, IL36N, DNASE2, CSF2RA* and *DOCK8* were not considered pathogenic, because known disease-causing variants in these genes are inherited in an autosomal recessive manner. The variants in *THBD* and *IRF3* were not considered to be disease-causing in the patient given the strongly disparate clinical picture (*82*). No hemizygous or homozygous variants in known IUIS genes remained after filtering. HGNC_ID - HUGO Gene Nomenclature Committee identifier; Chr – Chromosome; REF/ALT - Reference and alternative allele, respectively; CDS - Coding Sequence; CADD - Combined Annotation Dependent Depletion; N/A - not available.

Table S2. Heterozygous Variants in Known IUIS Genes Identified by WES in P3								
Gene	**HGNC_ID**	**Chr**	**Genomic position (hg38)**	**REF/ALT**	**CDS change**	**Amino acid change**	**Allele frequency (gnomAD)**	**CADD score**
ARHGEF1	HGNC:681	chr19	41902334	T/C	ENST00000354532.8:c.1475T>C	p.Ile492Thr	N/A	25.1
PALB2	HGNC:26144	chr16	23636031	G/A	ENST00000261584.9:c.515C>T	p.Ser172Phe	N/A	24.2
PEPD	HGNC:8840	chr19	33401853	C/T	ENST00000244137.12:c.832G>A	p.Gly279Ser	0.00000807[a]	23.6
PMS2	HGNC:9122	chr7	5986766	C/T	ENST00000265849.12:c.1999G>A	p.Glu667Lys	0.00003117	23.1
IL36RN	HGNC:15561	chr2	113060913	C/A	ENST00000393200.7:c.91C>A	p.Leu31Met	0.00001093	21.4
PSMG2	HGNC:24929	chr18	12720595	A/G	ENST00000317615.11:c.493A>G	p.Lys165Glu	N/A	19.41
ORAI1	HGNC:25896	chr12	121626800	G/A	ENST00000617316.2:c.58G>A	p.Gly20Ser	0.00003790[b]	15.18
IFNGR2	HGNC:5440	chr21	33414880	C/T	ENST00000290219.11:c.74-8C>T	N/A	0.00000817[a]	4.101

Table S2. Heterozygous variants in known IUIS genes identified by WES in P3.

Pre-filtered for variants in genes in IUIS classification of 2022 (*9*). Non-synonymous and splice region variants (+/- 8 bp from the intron/exon boundaries) with MAF < 0.01 and gnomAD AC < 20 are listed and sorted by CADD score. Allele frequencies displayed are derived from the combined gnomAD v2.1.1 and gnomAD v3.1.2 (non-v2) datasets for variants present in both of them. Variants only found in one of the datasets are indicated as follows: a) variants only present in v2.1.1, b) variants only present in v3.1.2. None of the variants were considered pathogenic, because known disease-causing variants in these genes are inherited in an autosomal recessive manner. No hemizygous or homozygous variants in known IUIS genes remained after filtering. HGNC_ID - HUGO Gene Nomenclature Committee identifier; Chr – Chromosome; REF/ALT - Reference and alternative allele, respectively; CDS - Coding Sequence; CADD - Combined Annotation Dependent Depletion; N/A - not available.

Table S3. Homozygous and hemizygous variants identified by WES in P2								
Gene	**HGNC_ID**	**Chr**	**Genomic position (hg38)**	**REF/ALT**	**CDS change**	**Amino acid change**	**Allele frequency (gnomAD)**	**CADD score**
Immune-related genes								
LTBR	HGNC:6718	chr12	6384449	C/T	ENST00000228918.9:c.91C>T	p.Gln31Ter	N/A	34
IGFBP2	HGNC:5471	chr2	216633617	G/T	ENST00000233809.9:c.94G>T	p.Gly32Cys	N/A	15.98
Non-immune-related genes								
ZNF384	HGNC:11955	chr12	6673285	G/A	ENST00000683879.1:c.935C>T	p.Ala312Val	0.00003279	22.7
KDM5B	HGNC:18039	chr1	202755359	G/C	ENST00000367265.9:c.1450C>G	p.Leu484Val	0.00000796[a]	17.2
EPHA4	HGNC:3388	chr2	221426474	C/T	ENST00000281821.7:c.2836G>A	p.Val946Met	0.00012160	15.32

Table S3. Homozygous and hemizygous variants identified by WES in P2.

Non-synonymous and splice region variants (+/- 8 bp from the intron/exon boundaries) with MAF < 0.01, gnomAD total number of homozygous/hemizygotes < 5, CADD score > 10 and which were not excluded by segregation analysis are listed. Allele frequencies displayed are derived from the combined gnomAD v2.1.1 and gnomAD v3.1.2 (non-v2) datasets for variants present in both of them. Variants only found in one of the datasets are indicated as follows: a) variants only present in v2.1.1, b) variants only present in v3.1.2. The variant in *IGFBP2* was deprioritized due to low RNA/protein expression in lymphoid tissues and thymus and its absent expression in immune cells, alongside additional literature research undermining the gene's suitability as a candidate. HGNC_ID - HUGO Gene Nomenclature Committee identifier; Chr – Chromosome; REF/ALT - Reference and alternative allele, respectively; CDS - Coding Sequence; CADD - Combined Annotation Dependent Depletion; N/A - not available.

Table S4. Homozygous and hemizygous Variants identified by WES in P3								
Gene	**HGNC_ID**	**Chr**	**Genomic position (hg38)**	**REF/ALT**	**CDS change**	**Amino acid change**	**Allele frequency (gnomAD)**	**CADD score**
Immune-related genes								
LTBR	HGNC:6718	chr12	6385266	G/C	ENST00000228918.9:c.359G>C	p.Arg120Pro	0.00000873[b]	15.28
Non-immune-related genes								
BICD2	HGNC:17208	chr9	92764692	T/G	ENST00000356884.11:c.53>C	p.Gln18Pro	N/A	23
MCM8	HGNC:16147	chr20	5963316	C/T	ENST00000610722.4:c.832C>T	p.Arg278Cys	0.00032217	20.8
FAM47C	HGNC:25301	chrX	37011343	G/GA	ENST00000358047.5:c.2934dup	p.Pro979ThrfsTer5	0.00001098[a]	20.2
TOP2A	HGNC:11989	chr17	40396414	C/G	ENST00000423485.6:c.3589G>C	p.Gly1197Arg	0.00104002	19.84
PTCH1	HGNC:9585	chr9	95468828	G/A	ENST00000331920.11:c.2173C>T	p.Pro725Ser	0.00095361	18.88
DCAF8L1	HGNC:31810	chrX	27980656	G/A	ENST00000441525.4:c.679C>T	p.Arg227Trp	0.00000976[a]	18.29
IARS1	HGNC:5330	chr9	92222663	A/G	ENST00000443024.7:c.3563T>C	p.Met1188Thr	0.00046075	16.96
PHKA1	HGNC:8925	chrX	72603169	T/C	ENST00000373542.9:c.2867A>G	p.Asn956Ser	N/A	12.41
THAP5	HGNC:23188	chr7	108564681	G/A	ENST00000415914.4:c.698C>T	p.Ala233Val	0.00021916	11.87
AKAP11	HGNC:369	chr13	42301454	G/A	ENST00000025301.4:c.2708G>A	p.Arg903His	0.00161323	10.78

Table S4. Homozygous and hemizygous variants identified by WES in P3.

Non-synonymous and splice region variants (+/- 8 bp from the intron/exon boundaries) with MAF < 0.01, gnomAD total number of homozygous/hemizygotes < 5, CADD score > 10 and which were not excluded by segregation analysis are listed. Allele frequencies displayed are derived from the combined gnomAD v2.1.1 and gnomAD v3.1.2 (non-v2) datasets for variants present in both of them. Variants only found in one of the datasets are indicated as follows: a) variants only present in v2.1.1, b) variants only present in v3.1.2. No other rare homozygous variants in immune-related genes were identified. HGNC_ID - HUGO Gene Nomenclature Committee identifier; Chr – Chromosome; REF/ALT - Reference and alternative allele, respectively; CDS - Coding Sequence; CADD - Combined Annotation Dependent Depletion; N/A - not available.

Table S5. Genetic characterization of *LTBR* and the identified variants		
Gene conservation evaluation		
CCDS Size (ENST00000228918.9)	1308	
Loss-of-function Observed/Expected Upper bound Fraction (LOEUF) Score (gnomAD v4)	0.5	
Number of expected and observed pLoF SNVs (gnomAD v4)	48.4 expected, 16 observed	
Missense Z-Score (gnom AD v4)	1.76	
Number of expected and observed missense SNVs (gnomAD v4)	543.7 expected, 431 observed	
Residual Variation Intolerance Score (RVIS) Score of *LTBR* (based on ExAC v2 release 2.0) (*83*)	-0.1434 (42.5611% most intolerant)	
Gene mutation significance cutoff (MSC) for CADD		
Confidence interval	Mutation significance cutoff (MSC)	
99%	1.7	
95%	10.5	
90%	20	
***In silico* pathogenicity assessment of the identified *LTBR* variants**		
Pathogenicity prediction tool	c.91C>T	c.359G>C
CADD score (v1.6) (*65*)	34	15.28
REVEL score (v1.3) (*84*)	N/A	0.546
Evaluation of the identified *LTBR* variants in exome/genome variant databases (last accessed February 2024)		
Source	Present in the database	
	c.91C>T	c.359G>C
125,748 exomes and 15,708 genomes from the Genome Aggregation Database (gnomAD v2.1.1) (*64*)	No	No
56,456 genomes from the Genome Aggregation Database (gnomAD v3.1.2 non-v2 dataset)	No	Yes Allele count: 1 Allele frequency: 0.00000873
150,899 individuals sequenced in NHLBI's TOPMed program (BRAVO, TOPMed Freeze 10 on GRCh38) (*85*)	No	Yes Allele count: 2 (2 heterozygotes) Allele frequency: 0.0000066269
In-house collection of >1,200 individuals (1,140 exomes and 780 targeted enrichment screens)	No	No

Table S5. Genetic characterization of *LTBR* and the identified variants.

Constraint metrics for *LTBR* suggest intolerance to genetic variation, with a lower number of 'observed' compared to 'expected' variants for both missense and pLoF variants. The variant in P1 and P2 (ENST00000228918.9:c.91C>T) is absent from public databases including GnomAD and

BRAVO and has not been previously reported. The variant in P3 (ENST00000228918.9:c.359G>C) is present in GnomAD v3.1.2 and BRAVO at very rare allelic frequencies, with no homozygous individuals observed (last accession date: 27/02/2024). CCDS - Consensus Coding Sequence, pLoF - Predicted loss-of-function, SNV - Single Nucleotide Variant.

Table S6. Differentially expressed genes in scRNAseq CD8 subpopulations					
cell_type	gene	logFC	logCPM	PValue	FDR
CD8 Naïve					
CD8 Naïve	*HMGB2*	-2,085	7,570	2,25E-07	7,24E-04
CD8 Naïve	*CCDC57*	-2,037	6,668	9,02E-07	0,0015
CD8 Naïve	*CDKN2D*	-2,243	6,822	8,20E-06	0,0088
CD8 Naïve	*FTH1*	-1,617	11,288	2,41E-05	0,0194
CD8 Naïve	*ANXA1*	-3,356	6,726	0,0001	0,0372
CD8 TCM					
CD8 TCM	*PFDN2*	-1,978	8,024	1,86E-05	0,0066
CD8 TCM	*CD6*	-1,794	8,435	3,52E-05	0,0066
CD8 TCM	*IL32*	3,378	9,897	3,38E-05	0,0066
CD8 TCM	*CXCR3*	-2,401	7,862	9,22E-06	0,0066
CD8 TCM	*HMGB2*	-1,688	8,815	6,69E-05	0,0100
CD8 TCM	*FAM177A1*	-1,983	8,772	8,04E-05	0,0100
CD8 TCM	*GNLY*	-2,068	8,040	1,45E-04	0,0155
CD8 TCM	*CD52*	2,486	10,286	2,16E-04	0,0160
CD8 TCM	*SPOCK2*	-1,526	9,162	2,00E-04	0,0160
CD8 TCM	*CIB1*	-1,682	8,707	2,35E-04	0,0160
CD8 TCM	*P2RY8*	-1,533	8,171	1,93E-04	0,0160
CD8 TCM	*RAC2*	3,204	8,711	3,32E-04	0,0207
CD8 TCM	*S100A4*	2,810	9,827	4,98E-04	0,0283
CD8 TCM	*ABLIM1*	-1,640	8,541	5,67E-04	0,0283
CD8 TCM	*EMD*	-1,545	7,984	5,39E-04	0,0283
CD8 TEM					
CD8 TEM	*KIR3DL2*	-3,456	6,706	2,03E-16	8,32E-13
CD8 TEM	*IFITM3*	7,007	6,212	1,41E-10	2,89E-07
CD8 TEM	*TRAF4*	-4,993	5,210	5,55E-10	7,61E-07
CD8 TEM	*SNHG7*	-2,280	6,154	5,24E-09	5,38E-06
CD8 TEM	*LTB*	2,578	7,016	5,80E-08	4,77E-05
CD8 TEM	*FOS*	2,564	9,292	1,35E-07	9,23E-05
CD8 TEM	*AUTS2*	-1,893	6,310	1,73E-07	1,02E-04
CD8 TEM	*RASGRP2*	1,587	6,408	3,85E-07	1,98E-04
CD8 TEM	*FERMT3*	1,737	6,388	6,72E-07	3,07E-04
CD8 TEM	*SKIL*	-2,231	6,356	9,24E-07	3,63E-04
CD8 TEM	*DBNL*	2,153	5,933	1,06E-06	3,63E-04
CD8 TEM	*RGS19*	2,051	5,522	1,01E-06	3,63E-04

CD8 TEM	*KIR2DL3*	-2,954	6,841	1,33E-06	4,22E-04
CD8 TEM	*BTG2*	1,724	7,905	1,85E-06	5,14E-04
CD8 TEM	*VCL*	2,610	5,209	1,88E-06	5,14E-04
CD8 TEM	*NR4A2*	1,776	7,390	2,04E-06	5,18E-04
CD8 TEM	*GABARAPL2*	1,531	6,749	2,14E-06	5,18E-04
CD8 TEM	*NORAD*	1,639	6,350	2,40E-06	5,48E-04
CD8 TEM	*TFG*	-1,835	5,671	3,05E-06	6,59E-04
CD8 TEM	*C6orf89*	-1,723	6,020	3,44E-06	7,06E-04
CD8 TEM	*VAMP2*	-1,369	9,649	3,63E-06	7,11E-04
CD8 TEM	*ZBP1*	-2,136	7,589	4,31E-06	8,05E-04
CD8 TEM	*PRDX2*	2,045	6,228	5,19E-06	9,26E-04
CD8 TEM	*CHMP4A*	1,673	6,115	8,69E-06	0,0015
CD8 TEM	*EIF4EBP1*	-1,855	5,930	1,00E-05	0,0016
CD8 TEM	*TALDO1*	1,767	5,595	1,22E-05	0,0019
CD8 TEM	*FLI1*	2,680	5,890	1,34E-05	0,0020
CD8 TEM	*TRBV5-1*	5,274	5,891	1,81E-05	0,0027
CD8 TEM	*MT2A*	1,565	7,889	2,14E-05	0,0030
CD8 TEM	*HCG18*	2,486	4,896	2,23E-05	0,0031
CD8 TEM	*RNASEH2C*	2,202	5,274	2,89E-05	0,0038
CD8 TEM	*GPR183*	3,099	4,632	3,03E-05	0,0039
CD8 TEM	*PPTC7*	-2,186	5,217	3,41E-05	0,0042
CD8 TEM	*VASP*	1,605	5,728	3,49E-05	0,0042
CD8 TEM	*SELL*	3,724	6,370	3,71E-05	0,0044
CD8 TEM	*AGTRAP*	2,819	5,091	4,85E-05	0,0055
CD8 TEM	*LDLRAP1*	1,829	5,137	6,26E-05	0,0063
CD8 TEM	*MYO1G*	1,458	7,158	6,28E-05	0,0063
CD8 TEM	*FAM111A*	1,879	5,078	6,17E-05	0,0063
CD8 TEM	*DCXR*	-1,370	6,949	6,03E-05	0,0063
CD8 TEM	*SLA2*	-1,712	7,576	5,78E-05	0,0063
CD8 TEM	*PFDN2*	-1,572	7,523	7,39E-05	0,0066
CD8 TEM	*PRDX6*	-1,380	8,076	6,87E-05	0,0066
CD8 TEM	*TBCA*	1,405	6,513	7,42E-05	0,0066
CD8 TEM	*TMEM141*	3,185	4,236	6,95E-05	0,0066
CD8 TEM	*LAIR2*	-1,759	5,898	7,27E-05	0,0066
CD8 TEM	*KLRC4*	1,637	6,584	7,60E-05	0,0066
CD8 TEM	*STMN1*	2,332	4,738	8,69E-05	0,0072

CD8 TEM	*ZNRD1*	-1,353	6,689	8,55E-05	0,0072
CD8 TEM	*M6PR*	1,109	6,741	8,77E-05	0,0072
CD8 TEM	*DERL1*	-1,234	6,541	9,31E-05	0,0072
CD8 TEM	*LINC00861*	2,340	6,443	9,03E-05	0,0072
CD8 TEM	*PTGDR*	1,926	5,519	9,17E-05	0,0072
CD8 TEM	*XPO1*	-1,359	6,786	9,92E-05	0,0073
CD8 TEM	*TRIM69*	3,371	3,965	9,73E-05	0,0073
CD8 TEM	*PLSCR3*	1,889	5,730	9,83E-05	0,0073
CD8 TEM	*TPST2*	1,515	7,090	1,02E-04	0,0074
CD8 TEM	*PARP10*	1,676	5,256	1,08E-04	0,0076
CD8 TEM	*ILF3-DT*	1,508	5,498	1,18E-04	0,0082
CD8 TEM	*NRDC*	1,586	5,659	1,24E-04	0,0085
CD8 TEM	*NDUFB5*	2,850	4,616	1,30E-04	0,0088
CD8 TEM	*MVP*	1,524	5,618	1,42E-04	0,0093
CD8 TEM	*PARVG*	1,441	5,814	1,43E-04	0,0093
CD8 TEM	*RASSF7*	2,547	4,545	1,51E-04	0,0096
CD8 TEM	*TPI1*	1,364	7,554	1,52E-04	0,0096
CD8 TEM	*STK38*	1,409	6,563	1,57E-04	0,0098
CD8 TEM	*DUSP1*	2,199	9,458	1,66E-04	0,0101
CD8 TEM	*LYN*	-1,850	5,555	1,67E-04	0,0101
CD8 TEM	*MARCKSL1*	1,881	4,764	1,79E-04	0,0102
CD8 TEM	*DHX36*	-1,183	7,175	1,80E-04	0,0102
CD8 TEM	*ABCB1*	-1,236	6,346	1,75E-04	0,0102
CD8 TEM	*PHPT1*	2,064	5,058	1,81E-04	0,0102
CD8 TEM	*SLC7A5*	-1,317	6,052	1,72E-04	0,0102
CD8 TEM	*CYBC1*	2,733	5,669	1,90E-04	0,0105
CD8 TEM	*THEMIS*	2,835	6,272	2,09E-04	0,0114
CD8 TEM	*AC119396,1*	3,051	4,794	2,11E-04	0,0114
CD8 TEM	*MXD4*	-1,607	5,672	2,21E-04	0,0118
CD8 TEM	*IMPDH2*	1,750	5,336	2,29E-04	0,0121
CD8 TEM	*MYO9A*	2,142	4,565	2,39E-04	0,0124
CD8 TEM	*TMEM230*	1,777	5,804	2,41E-04	0,0124
CD8 TEM	*TRAT1*	1,980	4,905	2,56E-04	0,0130
CD8 TEM	*GIMAP1*	1,706	6,108	2,59E-04	0,0130
CD8 TEM	*PRR5L*	2,636	4,508	2,63E-04	0,0130
CD8 TEM	*KLHL24*	-1,265	6,461	2,73E-04	0,0132

CD8 TEM	*CD27*	3,454	6,324	2,71E-04	0,0132
CD8 TEM	*PRMT1*	1,627	6,031	2,76E-04	0,0132
CD8 TEM	*ITGA5*	-1,674	5,617	2,81E-04	0,0133
CD8 TEM	*ANXA5*	1,519	6,559	2,92E-04	0,0136
CD8 TEM	*TRPV2*	1,874	5,075	3,12E-04	0,0142
CD8 TEM	*ICAM2*	1,415	5,569	3,12E-04	0,0142
CD8 TEM	*SLBP*	-1,270	6,593	3,55E-04	0,0160
CD8 TEM	*POLR2L*	1,282	7,060	3,75E-04	0,0167
CD8 TEM	*IL2RG*	1,855	8,661	3,78E-04	0,0167
CD8 TEM	*GNLY*	-1,425	12,727	3,87E-04	0,0169
CD8 TEM	*ARFRP1*	2,053	4,544	3,97E-04	0,0172
CD8 TEM	*ABRACL*	1,224	6,087	4,27E-04	0,0178
CD8 TEM	*YIF1A*	2,441	4,482	4,21E-04	0,0178
CD8 TEM	*PSME2*	1,409	7,333	4,21E-04	0,0178
CD8 TEM	*EGLN2*	1,490	5,173	4,29E-04	0,0178
CD8 TEM	*TMC6*	1,108	7,014	4,43E-04	0,0182
CD8 TEM	*TTC13*	2,172	4,472	4,76E-04	0,0188
CD8 TEM	*PLEKHA2*	-1,242	6,662	4,69E-04	0,0188
CD8 TEM	*ITGB7*	1,398	6,843	4,74E-04	0,0188
CD8 TEM	*MYO1F*	1,316	7,149	4,75E-04	0,0188
CD8 TEM	*CISD3*	1,977	4,922	5,15E-04	0,0202
CD8 TEM	*NSG1*	2,979	5,003	5,43E-04	0,0202
CD8 TEM	*JAK2*	1,805	4,694	5,46E-04	0,0202
CD8 TEM	*VPS26B*	-1,139	6,499	5,44E-04	0,0202
CD8 TEM	*AC087239,1*	2,486	5,080	5,54E-04	0,0202
CD8 TEM	*BAZ1A*	0,985	6,805	5,36E-04	0,0202
CD8 TEM	*TRADD*	1,901	5,496	5,43E-04	0,0202
CD8 TEM	*RAB37*	2,380	5,273	5,22E-04	0,0202
CD8 TEM	*SCAND1*	-1,021	8,040	5,55E-04	0,0202
CD8 TEM	*ARHGAP15*	1,078	7,046	5,66E-04	0,0202
CD8 TEM	*FAM177A1*	-1,203	7,506	5,65E-04	0,0202
CD8 TEM	*PLEK*	1,442	7,890	5,89E-04	0,0208
CD8 TEM	*ZNF507*	-1,488	5,458	5,92E-04	0,0208
CD8 TEM	*TSTD1*	1,336	6,280	6,17E-04	0,0211
CD8 TEM	*TIGIT*	1,563	5,713	6,21E-04	0,0211
CD8 TEM	*CD69*	1,251	8,337	6,22E-04	0,0211

CD8 TEM	*TMOD3*	1,060	6,228	6,18E-04	0,0211
CD8 TEM	*SPN*	1,846	7,112	6,26E-04	0,0211
CD8 TEM	*STX10*	1,466	5,247	6,77E-04	0,0226
CD8 TEM	*XAF1*	1,249	5,681	6,87E-04	0,0228
CD8 TEM	*MADD*	-1,309	6,247	6,93E-04	0,0228
CD8 TEM	*ST6GAL1*	2,337	4,672	7,04E-04	0,0229
CD8 TEM	*RAC2*	2,109	8,878	7,07E-04	0,0229
CD8 TEM	*SYTL3*	-1,329	8,015	7,23E-04	0,0231
CD8 TEM	*GABPB1-IT1*	1,624	5,194	7,26E-04	0,0231
CD8 TEM	*EPHA4*	-1,830	5,283	7,51E-04	0,0236
CD8 TEM	*UBE2F*	-1,132	6,785	7,52E-04	0,0236
CD8 TEM	*SLA*	-1,195	6,744	7,63E-04	0,0236
CD8 TEM	*NOL11*	-1,487	5,905	7,60E-04	0,0236
CD8 TEM	*SVBP*	-1,381	5,746	7,94E-04	0,0244
CD8 TEM	*HMGB2*	-1,343	8,240	8,43E-04	0,0253
CD8 TEM	*PTPRE*	-1,206	7,088	8,41E-04	0,0253
CD8 TEM	*LAT*	1,240	7,702	8,45E-04	0,0253
CD8 TEM	*RSU1*	1,666	5,283	8,99E-04	0,0258
CD8 TEM	*DPF2*	-1,391	5,404	8,78E-04	0,0258
CD8 TEM	*MRPL51*	1,476	5,360	8,87E-04	0,0258
CD8 TEM	*SUPT20H*	1,353	5,784	8,98E-04	0,0258
CD8 TEM	*HAGH*	1,908	4,873	8,91E-04	0,0258
CD8 TEM	*CFDP1*	1,295	5,415	8,72E-04	0,0258
CD8 TEM	*CAPN1*	1,501	5,538	9,50E-04	0,0271
CD8 TEM	*PYCARD*	1,930	5,166	9,90E-04	0,0281
CD8 TEM	*ACTR3*	1,529	7,609	0,0010	0,0295
CD8 TEM	*DUSP23*	1,583	5,013	0,0011	0,0303
CD8 TEM	*CCAR2*	-1,399	5,994	0,0011	0,0305
CD8 TEM	*RNASEH1*	-1,067	6,122	0,0011	0,0306
CD8 TEM	*STIM1*	1,405	5,211	0,0011	0,0309
CD8 TEM	*PFN1*	1,256	10,983	0,0011	0,0311
CD8 TEM	*ANXA4*	3,146	3,964	0,0012	0,0312
CD8 TEM	*LARP1*	1,794	4,754	0,0012	0,0312
CD8 TEM	*ANAPC16*	1,579	7,072	0,0012	0,0312
CD8 TEM	*ITGAE*	-1,432	6,289	0,0012	0,0312
CD8 TEM	*SMAD7*	-1,427	6,182	0,0012	0,0312

CD8 TEM	*XAB2*	-1,074	6,210	0,0012	0,0312
CD8 TEM	*NOSIP*	1,329	6,586	0,0012	0,0312
CD8 TEM	*RFFL*	-1,352	5,913	0,0012	0,0313
CD8 TEM	*TSPO*	1,489	6,808	0,0013	0,0323
CD8 TEM	*E2F3*	2,462	4,711	0,0013	0,0323
CD8 TEM	*UBASH3A*	1,705	4,689	0,0013	0,0326
CD8 TEM	*KCNAB2*	1,046	6,347	0,0013	0,0327
CD8 TEM	*PHF12*	-1,248	5,928	0,0013	0,0335
CD8 TEM	*AP1S2*	1,702	4,698	0,0014	0,0341
CD8 TEM	*MRPL10*	-1,152	7,529	0,0014	0,0343
CD8 TEM	*IL32*	2,584	10,284	0,0014	0,0348
CD8 TEM	*PFDN6*	1,534	5,075	0,0014	0,0353
CD8 TEM	*NT5C*	1,161	5,740	0,0015	0,0361
CD8 TEM	*TLN1*	1,924	6,939	0,0016	0,0382
CD8 TEM	*RAB4B*	1,676	5,055	0,0016	0,0382
CD8 TEM	*PYCR2*	1,734	5,253	0,0016	0,0382
CD8 TEM	*FGR*	2,056	5,781	0,0016	0,0388
CD8 TEM	*HACD4*	1,102	5,989	0,0016	0,0388
CD8 TEM	*TUFM*	0,891	7,156	0,0017	0,0388
CD8 TEM	*POLR2E*	1,036	6,111	0,0017	0,0388
CD8 TEM	*PGLS*	1,068	6,426	0,0017	0,0388
CD8 TEM	*RPS19BP1*	-0,967	7,110	0,0017	0,0394
CD8 TEM	*GIMAP6*	2,082	4,388	0,0017	0,0398
CD8 TEM	*CLEC2D*	1,607	7,110	0,0017	0,0398
CD8 TEM	*SLC6A6*	-1,646	5,405	0,0018	0,0402
CD8 TEM	*FGD3*	0,966	6,469	0,0018	0,0402
CD8 TEM	*ITGB1*	1,685	8,055	0,0019	0,0427
CD8 TEM	*MT-ND6*	0,929	8,874	0,0019	0,0427
CD8 TEM	*NCOA7*	-1,173	6,780	0,0020	0,0435
CD8 TEM	*CXCR3*	-1,267	6,921	0,0020	0,0435
CD8 TEM	*EEA1*	1,651	4,700	0,0020	0,0439
CD8 TEM	*UGP2*	1,046	5,906	0,0020	0,0441
CD8 TEM	*DAD1*	1,381	6,777	0,0020	0,0445
CD8 TEM	*ITGB1BP1*	0,935	6,221	0,0021	0,0447
CD8 TEM	*CX3CR1*	2,040	5,479	0,0021	0,0447
CD8 TEM	*IL7R*	2,054	8,816	0,0021	0,0447

CD8 TEM	*WASHC3*	1,430	5,023	0,0021	0,0447
CD8 TEM	*RRAGA*	-1,258	5,555	0,0022	0,0458
CD8 TEM	*ARRDC3*	-0,874	6,734	0,0022	0,0463
CD8 TEM	*NDUFA3*	1,197	7,320	0,0022	0,0463
CD8 TEM	*LARS*	2,487	4,954	0,0022	0,0466
CD8 TEM	*HNRNPA2B1*	1,167	9,182	0,0024	0,0494
CD8 TEM	*RAB27B*	-1,274	5,756	0,0024	0,0495

Table S6. Differentially expressed genes in scRNAseq in CD8 subpopulations.

Table S7. Sanger sequencing primers for validation and segregation of the *LTBR* variants identified in the patients and their family members			
Exon/Intron # (Patient #)	Variant	Forward Primer Sequence (5‘-3‘)	Reverse Primer Sequence (5‘-3‘)
Exon 1 (P1 and P2)	ENST00000228918.9: c.91C>T	CGATCGGGCTTCCGAAGAA	GGTTCTCCGACGCATATGGA
Exon 4 (P3)	ENST00000228918.9: c.359G>C	TTACCTCACTGAGAGGGAGCC	CTGTCCCAGTTCCATGTCCCA

Table S7. Sanger sequencing primers for validation and segregation of the LTBR variants identified in the patients and their family members

Table S8. Guide and ssODN template design for CRISPR/Cas9 Editing			
Target gene	Exon	sgRNA sequence	ssODN
LTBR	Exon 1	CCUGGCAGCAUCGCAGCCCU	GGGGGCCTCTGGTGCTGGGCCTCTTCGGGCTCCT GGCAGCATCGCAGCCCCAAGCGGTGAGGAAGGGGC CTGGTAGGAGTGGGCGAGGGTGGGCAAGAGGG
LTBR	Exon 4	UGGCAGCGGCACUGGGUCUU	GATGGGCCTCGAGGAGATTGCCCCCTGCAC AAGCAAACGGAAGACCCAGTGCCGCTGCCA GCCGGGAATGTTCTGTGCTGCCTGGGCCCT
B2M	Exon 1	GAGUAGCGCGAGCACAGCUA	

Table S8. Guide and ssODN template design for CRISPR/Cas9 Editing

Table S9. List of antibodies used in this work		
Antibody-Fluorophore	**Clone**	**Manufacturer**
CD3-FITC	SK7	BD Biosciences
CD3-APC	SK7	BD Biosciences
CD3-APCH7	SK7	BD Biosciences
CD4-PE-Cy7	SFCI12T4D11	Beckman Coulter
CD4-PerCpCy5.5	RPA-T4	Invitrogen
CD4-BV605	RPA-T4	BD Biosciences
CD8-PE-Cy7	SFCI21Thy2D3	Beckman Coulter
CD8 FITC	HIT8a	BD Biosciences
CD8-V500	RPA-T8	BD Biosciences
CD10-APC	SN5c	Invitrogen
CD11c-eFluor450	3.9	Invitrogen
CD14-PC7	RMO52	Beckman Coulter
CD19-PE-Cy7	J3-119	Beckman Coulter
CD19-BV510	SJ25C1	BD Biosciences
CD19-APC-Cy7	SJ25C1	BD Biosciences
CD19-PerCpCy5.5	HIB19	Invitrogen
CD20-FITC	2H7	BD Biosciences
CD21-PE	HB5	BD Biosciences
CD25 APC	M-A251	BD Biosciences
CD25-BV605	2A3	BD Biosciences
CD25-PE	MA-A251	BD Biosciences
CD27-BV421	M-T271	BD Biosciences
CD27-PE-Cy7	M-T271	BD Biosciences
CD28 APC	CD28.2	Invitrogen
CD31-APC	WM-59	Invitrogen
CD38-BV711	HIT2	BD Biosciences
CD45RA-AF700	HI100	BD Biosciences
CD47-BV421	CC2C6	Biolegend
CD57 PE	TB01	Invitrogen
CD62L-FITC	DREG-56	Invitrogen
CD69-PE	L78	BD Biosciences
CD86-FITC	2331 (FUN-1)	BD Biosciences
CD95/Fas-PE-Cy7	DX2	BD Biosciences
CD120a/TNFR-1-PE-Vio 770	REA252	Miltenyi Biotec
CD127-FITC	eBioRDR5	Invitrogen
CD138-BV605	281-2	BioLegend
CD197/CCR7-PE-CF594	150503	BD Biosciences

CD279-BV605	EH12.1	BD Biosciences
AID-AF647	EK2-5G9	BD Biosciences
CCR6-BV605	G034E3	BioLegend
CXCR5-BV421	RF8B2	BD Biosciences
FOXP3-APC	236A/E7	Invitrogen
HLA-I (ABC)-APC	W6/32	BD Biosciences
HLA-II-(DR)-APC	G46-6	BD Biosciences
IFNγ-FITC	4S.B3	Biolegend
IgA-APC	IS11-8E10	Miltenyi Biotec
IgA-PE	IS11-8E10	Miltenyi Biotec
IgD-PE-TR	IA6-2	BD Biosciences
IgG-APC	IS11-3B2.2.3	Miltenyi Biotec
IgM-APC-Cy7	MHM-88	Biolegend
IgM-FITC	G20-127	BD Biosciences
IL-4-APC	MP4-25D2	BD Biosciences
IL-17A-eFluor450	eBio64DEC17	Invitrogen
LTβR-PE	551503	BD Biosciences
Tbet-BV421	4B10	Biolegend
TCRab FITC	WT31	BD Biosciences
TCRgd-PE	11F2	BD Biosciences
Mouse monoclonal anti-IκBα	L35A5)	Cell Signaling
Rabbit polyclonal anti-NF-κB2 p100/p52		Cell Signaling
Rabbit monoclonal anti-Phospho-NF-κB p65	93H1	Cell Signaling
Mouse monoclonal anti-HSP90α/β	F-8	Santa Cruz

Table S9. List of antibodies used in this work

3. DISCUSSION

3.1 General Discussion

3.1.1 The role of LTβR in lymphoid organogenesis

The importance of lymphotoxin signaling for adaptive immunity was discovered more than 30 years ago, following the identification of lymphotoxin-deficient mice presenting with extensive disruptions in the secondary lymphoid organs (De Togni *et al*, 1994). Pharmacological inhibition of LTβR in pregnant mice, using an LTβR–immunoglobulin fusion protein, revealed the order and time point of lymph node development (Rennert *et al*, 1996). By varying the gestational day of the LTβR-Ig injection, the genesis of lymph nodes was shown to begin with the mesenteric, followed sequentially by the brachial, axillary, inguinal, and finally popliteal lymph nodes. Discontinuation of the treatment did not result in a late development of the lymph nodes, revealing that dysfunctional LTβR signaling during fetal development had irreversible consequences. Our understanding of the molecular mechanisms involved in lymph node organogenesis has immensely advanced in the three decades since, especially due to the utilization of *Ltbr*$^{-/-}$ mice, but how this translates to human biology has so far been unknown.

This is of particular importance, as both *Tnfsf11*$^{-/-}$ and *Tnfrsf11a*$^{-/-}$ mice (lacking the ligand RANKL and its receptor RANK, respectively) display absent peripheral lymph nodes (Yy *et al*, 1999), but this observation has not been reported in RANK (Guerrini *et al*, 2008) and RANKL (Sobacchi *et al*, 2007) deficient patients who display a milder immune phenotype than mice. The LTβR-deficient patients in our studies not only recapitulated the aberrations in lymph node development reported from *Ltbr*$^{-/-}$ mice but displayed an even more pronounced defect in lymph node organogenesis. Whereas mice lacking LTβR do not express peripheral lymph nodes and Peyer's patches, they still form nasopharyngeal-associated lymphoid tissue (NALT) (Fukuyama *et al*, 2002). Subsequent investigation of P1 and P2, after our study had been published, revealed that they not only lacked tonsils, which are part of the NALT, but that endoscopic rhinoscopy showed no signs of NALT in the nasal cavity or nasopharynx of these patients. Results like this highlight again the differences between human and rodent biology and the importance of IEI studies to understand the human immune system.

3.1.2 The role of LTβR in establishing tolerance

Recent studies uncovered the mechanism behind the autoimmune phenotype of *Ltbr*$^{-/-}$ mice, described as massive infiltrations of CD4^{+} T cells and B220^{+} B cells around perivascular areas in lungs, liver, pancreas, submandibular glands, the fatty tissue of the mediastinum, mesenterium, cortex of the suprarenal glands, and kidney (Fütterer *et al*, 1998) as well as the development of autoantibodies against multiple tissues and organs such as the lung, pancreas, liver, and salivary glands (Boehm *et al.*, 2003). While initial studies proposed that lymphotoxin signaling promotes the expression of the transcription factor Autoimmune Regulator (AIRE) (Chin *et al*, 2003), subsequent investigations contradicted these findings and suggested that AIRE expression occurs independently of lymphotoxin signal (Martins *et al*, 2008). It was then discovered that LTβR signaling is required for upregulating the transcription factor Fezf2, which, similar to AIRE, regulates tissue-restricted antigen (TRA) expression on medullary thymic epithelial cells (mTECs) (Takaba *et al*, 2015). Surprisingly, LTβR knockout specifically in thymic epithelial cells resulted only in a mild form of autoimmunity (Wu *et al*, 2017). Finally, the underlying mechanism was shown to involve a subset of thymic medullary fibroblasts that depend on LTβR signaling, inducing the expression of fibroblast-specific antigens, thereby contributing to the establishment of central tolerance mediated by AIRE- and Fezf2-expressing thymic epithelial cells (Figure 7) (Nitta *et al*, 2020). These findings are part of a growing body of evidence highlighting that the role of fibroblasts in immune regulation is more significant than previously appreciated (Krausgruber *et al*, 2020).

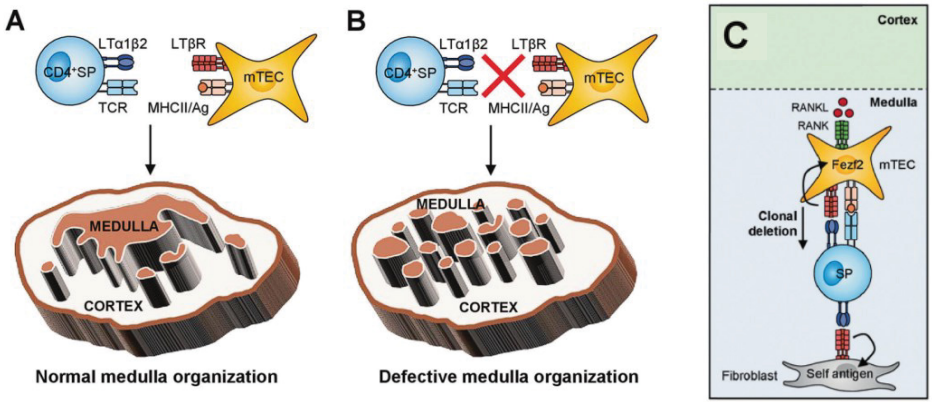

Figure 1. Contributions of LTβR signaling to thymic tolerance

*(**A**) Lymphotoxin expressed by T cells binds to LTβR expressed by thymic stromal cells, particularly medullary fibroblasts and thymic epithelial cells. (**B**) Defects in thymic LTβR signaling result in defective cellular organization in the medullary thymus. (**C**) LTβR activation upregulated Fezf2, which drives the expression of AIRE-independent tissue-restricted antigens, contributing to clonal deletion of autoreactive T cells and establishing tolerance. Figure adapted from* (Borelli & Irla, 2021) *and used with permission of Springer Nature BV conveyed through Copyright Clearance Center, Inc.*

Interestingly, none of the three LTβR-deficient patients showed any clinical signs of autoimmunity, despite reduced numbers of T_{regs}. This came as a surprise, not only because of the findings from the mouse model, but because many IEIs caused by mutations in the non-canonical NF-κB pathway present with autoimmunity, including mutations in RelB (Sharfe *et al*, 2023), NIK deficiency (Le Voyer *et al*, 2023), and NF-κB2 deficiency (Klemann *et al*, 2019). While the proposed mechanism for the autoimmune phenotype in the patients with incomplete RelB variants was suggested to be the result of compromised RelB-mediated inhibition of RelA-induced pro-inflammatory transcriptional activity (Sharfe *et al*, 2023), recent findings have shown the formation of neutralizing autoantibodies against type I interferons (IFNs) in patients with complete RelB deficiency, NIK deficiency, and NF-κB2 deficiency (Le Voyer *et al*, 2023). Based on previous mouse studies mentioned previously, the authors propose the underlying mechanism to be impaired development of *AIRE*-expressing medullary thymic epithelial cells (mTECs) due to aberrant non-canonical NF-κB signaling. However, we were not able to detect any autoantibodies against type I IFNs in serum from P3.

3.1.3 Potential contributing factors for absent clinical autoimmunity in LTβR-deficient patients

While it is impossible to definitively exclude the future development of clinical signs of autoimmunity in our LTβR-deficient patients or in additional cases, we propose several potential mechanisms that may contribute to preventing or delaying its onset. One possibility is that LTβR signaling plays a more redundant role in establishing central tolerance in the human thymus compared to mice. As noted above, one of the key reasons for studying IEIs is to uncover species-specific differences in immune physiology, which are often revealed by the divergent phenotypes observed in generated mouse models and human patients (Medetgul-Ernar & Davis, 2022).

Additionally, we propose that the defects in SLOs in these patients may paradoxically protect these patients from developing and sustaining an autoimmune phenotype. As detailed above, SLOs provide the confined microenvironment required for antigen-specific lymphocytes to interact and initiate the adaptive immune response (van de Pavert & Mebius, 2010). Without SLOs, self-reactive T cells have a lower likelihood of encountering relevant autoantigens presented in a pro-inflammatory context by APCs. Correspondingly, these autoreactive T lymphocytes are less likely to interact with B cells capable of binding the presented autoantigen. It is reasonable to speculate that even in the unlikely event that these cells encounter each other in these patients, due to the defects in the SLOs, their lymphocytes lack the environment to initiate the GC process. This could ultimately have the beneficial effect of limiting the development of a sustained autoimmune response, which is dependent on the generation of long-living plasma cells and memory B cells in the GC (DeFranco, 2016). In line with this reasoning, LTβR signaling has also been shown to be critical for the formation of tertiary lymphoid structures (TLS), ectopic structures that resemble SLOs in their organization and function (Tang *et al*, 2017). TLS arise transiently near sites of chronic inflammation and are associated with autoimmunity, correlating with pathological conditions and a more severe disease course (Sato *et al*, 2023).

Another theory that we propose could contribute to the absence of clinical autoimmunity in these LTβR-deficient patients is the continuous immunoglobulin since their early childhood. Notably, immunoglobulins are not only used as immunoglobulin substitution in antibody deficient patients, but are also employed as an immunomodulatory and immunosuppressive drug in various autoimmune and inflammatory diseases, such as multiple sclerosis (MS), idiopathic

thrombocytopenic purpura, Guillain–Barré syndrome, chronic inflammatory demyelinating polyneuropathy, myasthenia gravis (MG), systemic lupus erythematosus (SLE), corticosteroid-resistant dermatomyositis, Kawasaki syndrome, as well as in the prevention of graft-versus-host disease (GvHD) following HSCT. (Fazekas *et al*, 1997; Kazatchkine & Kaveri, 2001; Nieto-Aristizábal *et al*, 2019). Several mechanisms have been described that could contribute to the beneficial effect of IVIG in autoimmune and inflammatory diseases. For instance, immunoglobulin concentrates contain a substantial amount of idiotypic antibodies that recognize and bind to other antibodies, particularly potentially pathogenic autoantibodies, which are then neutralized and subsequently degraded (Dalakas, 2020). Supplementation with immunoglobulins increases the catabolism speed of pathogenic endogenous IgG by saturating the recycling process. IgG is constantly taken up by cells through pinocytosis and then either transported back to the cell surface to re-enter circulation or sent to the lysosome for degradation (Dalakas & Spaeth, 2021). Additionally, immunoglobulins have also been shown to affect cytokine levels, with a suppressing effect on the levels of pro-inflammatory cytokines such as tumor necrosis factor-alpha (TNFα), while promoting anti-inflammatory cytokines like IL-4 and IL-10 (Zhu *et al*, 2006). Finally, pharmaceutical immunoglobulins also have a direct effect on various immune cell types. Treatment with immunoglobulins has been shown to modulate monocytes (Abe *et al*, 2005), macrophages (Guo *et al*, 2020) and DCs (Wiedeman *et al*, 2013), as well as to expand and enhance Tregs (Xu *et al*, 2020), and inhibit NK cells (Ruiz *et al*, 1996) and neutrophils (Uozumi *et al*, 2020).

3.1.3 Neutralization of LIGHT and FAS via DcR3

Interestingly, immunoglobulins also affect structural cells such as fibroblasts, epithelial, and endothelial cells (Bayry *et al*, 2023). Patients with toxic epidermal necrolysis, a severe drug-induced skin disorder characterized by extensive apoptosis of keratinocytes, have benefited from treatment with immunoglobulins (Paul *et al*, 1996). These patients had increased serum levels of FasL, and administration of immunoglobulins rapidly reversed disease progression, supposedly by blocking Fas-mediated keratinocyte death (Viard *et al*, 1998; Murata *et al*, 2008). Further highlighting the unusual absence of autoimmunity in the LTβR-deficient patients in our study, we detected not only increased serum levels of FasL, but also elevated levels of the TNF superfamily cytokine TNFSF14 known as LIGHT (homologous to **l**ymphotoxin, exhibits **i**nducible expression

and competes with HSV **g**lycoprotein D for binding to **h**erpesvirus entry mediator a receptor expressed on **T** lymphocytes). LIGHT is the second known ligand of LTβR besides lymphotoxin, but it can also bind to the more broadly expressed herpesvirus entry mediator (HVEM) (Mauri *et al*, 1998). It is primarily expressed on activated T cells, capable of reverse signaling and inducing a pro-inflammatory response (Lee *et al*, 2019). LIGHT exists in both membrane-bound and soluble forms, the latter resulting from proteolytic shedding and retaining its ability to engage HVEM and LTβR. Noteworthy, elevated serum levels of LIGHT have been observed in patients with Crohn's disease (Cardinale *et al*, 2023), ulcerative colitis (Moraes *et al*, 2020), type 2 diabetes (Halvorsen *et al*, 2016) and in patients hospitalized with COVID-19 (Arunachalam *et al*, 2020), with subsequent studies demonstrating a correlation between LIGHT levels and clinical severity (Perlin *et al*, 2022).

We detected increased serum levels of decoy receptor 3 (DcR-3), a soluble member of the tumor necrosis factor receptor superfamily, that can bind and neutralize FasL, LIGHT, and TNF-like ligand 1A (TL1A) (Pitti *et al*, 1998). The functions of these ligands vary depending on the cellular context and environment, but are generally considered pro-inflammatory, and binding to their receptors can even result in the induction of apoptosis. All three of these proteins have been implicated to contribute to pathogenesis in various autoimmune diseases such as rheumatoid arthritis (Edwards *et al*, 2006; Palao *et al*, 2006; Bamias *et al*, 2008) and inflammatory bowel disease (Ueyama *et al*, 1998; Wang & Fu, 2005; Bamias *et al*, 2010). Furthermore, genetic variants in their respective genes have been identified in genome-wide association studies (GWAS) of IBD (Rivas *et al*, 2011; Demir *et al*, 2020).

DcR-3 levels are increased in pathological conditions such as cancer, autoimmune and inflammatory diseases (Lin & Hsieh, 2011). Variants in TNFRSF6B encoding for DcR-3 have been found in GWAS studies of pediatric IBD cases (Anderson *et al*, 2011) and missense mutations leading to reduced DcR-3 secretion were discovered in pediatric cases of Crohn's disease and ulcerative colitis (Cardinale *et al*, 2013). Due to its neutralizing effects on FasL, LIGHT, and TL1A, DcR-3 can be defined as an immunomodulator, but it has also been shown to function via "non-decoy" activities (Lin & Hsieh, 2011), presumably by binding and cross-linking heparan sulfate proteoglycans (You *et al*, 2008). We were able to show that treatment with DcR-3 ameliorated activation-induced cell death (AICD) in expanded T cells, as well as reduced their killing capacity

in a concentration-dependent manner. Additionally, we detected DcR-3 in multiple intravenous immunoglobulin (IVIG) products tested and observed an increase in serum DcR-3 levels in a different IEI patient following IVIG substitution. However, the levels did not reach the much higher concentrations that we detected in serum from the LTβR-deficient patients across multiple timepoints. The presence of DcR-3 in IVIG, along with its ability to neutralize FasL, may contribute to the beneficial effects of IVIG treatment observed in patients with toxic epidermal necrolysis, as mentioned above.

Therefore, IvRT could be a contributing factor to the increased DcR-3 levels in the LTβR-deficient patients, as well as the imbalance in the LTβR network. While it was previously known that epithelial cells and innate T cells can secrete DcR-3 in response to inflammatory signals (Kim et al., 2005; Kim et al., 2012), the molecular mechanisms were not entirely understood. We demonstrated for the first time that fibroblasts are capable of secreting DcR3 upon stimulation with TNF-α, TNF-β/LTα3, and the two isoforms of lymphotoxin, LTα1β2 and LTα2β1. This response was dependent on the expression of TNFR1 and LTβR, with TNFR1 stimulation appearing to induce higher levels of DcR3 production. One could speculate that the absence of LTβR leads to increased availability and binding of lymphotoxin ligands to TNFR1, thereby enhancing DcR3 expression (Figure 8).

The elevated levels and immunosuppressive function of DcR-3 could explain the lack of clinical autoimmunity in the LTβR-deficient patients in contrast to findings from mouse studies, as there is no ortholog of DCR3 in the rodent genome (Cardinale *et al*, 2013). However, whether increased DcR3 expression or other factors suggested in this study help prevent autoimmunity in the LTβR-deficient individuals is still not entirely clear. Further research and the identification of additional patients with LTβR deficiency are warranted to answer this question.

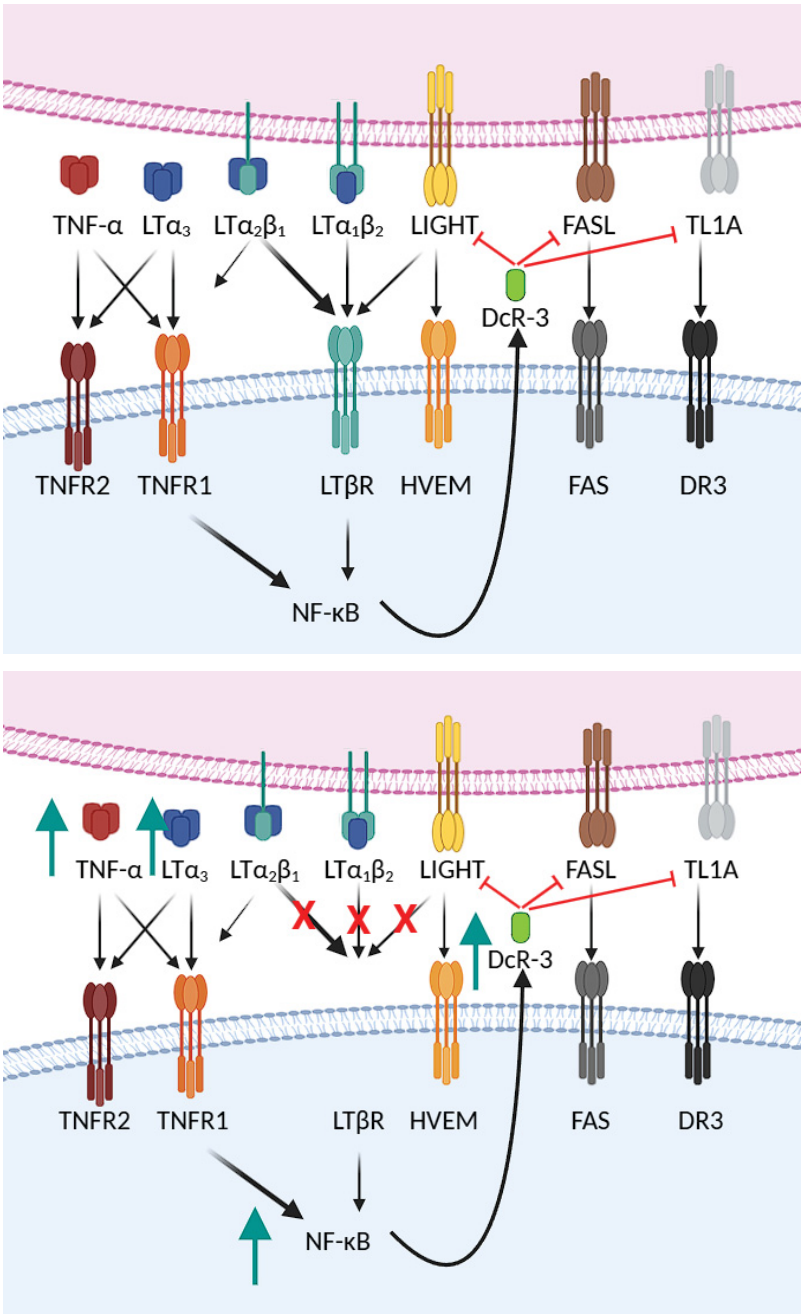

Figure 2. The lymphotoxin signaling network

*(**Top image**) The lymphotoxin network under physiological conditions: LTβR and its known ligands, lymphotoxin and LIGHT, are part of a large complex signaling network. Results from our study suggest that the less-characterized and expressed isoform of*

*lymphotoxin, composed of two LTα subunits and one LTβ subunit ($LT\alpha_2\beta_1$), is also capable of activating the TNFR receptor, similar to TNF-β/$LT\alpha_3$, the soluble homotrimer of the LTα subunit. (**Bottom image**) Proposed hypothesis of aberrations in the system resulting from lack of LTβR expression: We have detected increased levels of LTα and TNF-α in the patients, which could be the consequence of the missing binding of LTβR and unknown feedback loops. This results in increased TNFR activation, possibly explaining the increased levels of DcR-3 in the serum of these patients. DcR-3 binds and neutralizes the pro-inflammatory cytokines LIGHT, FasL, and TL1A. Figure created with BioRender.com.*

3.2 Outlook

3.2.1 Pharmacological modulation of LTβR signaling

While primary and secondary lymphoid organs are part of the physiological embryonic development, lymphoid organ-like structures can develop temporarily (Pitzalis *et al*, 2014). These so-called tertiary lymphoid structures (TLS) or tertiary lymphoid organs (TLOs) form close to sites of prolonged inflammation and typically resolve once the inflammatory stimulus subsides. As such, the formation of TLOs has a strong influence on the course of diseases such as infection, autoimmune diseases, and cancer. Whereas recent studies have shown a positive effect TLOs in several types of cancers (Cabrita *et al*, 2020; Helmink *et al*, 2020), the opposite seems to be the case in autoimmune diseases, where the number of TLOs correlates with increased disease activity and more severe tissue damage (Sato *et al*, 2023). Thus, both the pharmacological promotion and inhibition of TLO formation may be therapeutically desirable, depending on the disease context. Similar to the development of SLOs, LTβR signaling has been identified as a central pathway driving TLO formation (Tang *et al*, 2017). Whereas enhancement of LIGHT signaling has recently been explored as a strategy to improve CAR T-cell efficacy (Zhang *et al*, 2023; Cai *et al*, 2024), agonistic LTβR antibodies are being investigated to modulate the tumour microenvironment and induce TLO formation (An *et al*, 2024).

While therapeutic promotion of LTβR signaling is still in an early development, its inhibition has advanced further, due to early discoveries of increased LTβR activity in antibody driven autoimmune diseases such as Sjögren's syndrome (Shen *et al*, 2010) and rheumatoid arthritis

(Hirose *et al*, 2018), and the positive effect of LTβR inhibition being demonstrated in various mouse models of autoimmunity (Gommerman & Browning, 2003). This led to the development of the monoclonal antibodies Baminercept, which blocks LTβR, and Pateclizumab, which targets LTα. However, despite the promising preclinical data, Baminercept was unsuccessful in a randomized, double-blind and placebo-controlled phase II trial for Sjögren's syndrome (St Clair *et al*, 2018), as was Pateclizumab in a phase II trial for the treatment of rheumatoid arthritis (Kennedy *et al*, 2014). Based on our co-culturing experiments, which demonstrated successful B cell differentiation even in the absence of LTβR-expressing cells, we proposed that the failure of these clinical trials may be due to the redundancy of LTβR signaling once a TLO is already established. In this context, inhibiting LTβR signaling alone and for a short duration might be insufficient to halt the ongoing germinal center reaction and the generation of autoantibody-secreting plasma cells supported by these structures.

This could potentially provide an explanation for the failed clinical trials, as these included primarily patients with advanced stages of disease. Additionally, a recent study using a mouse model of Sjögren's syndrome showed that blockade of LTα or LTβR had a beneficial effect only when administered during the early phase of disease (Jacob *et al*, 2022). Therefore, LTβR-inhibiting therapies may still hold potential in autoimmune disease if they are applied during the early stage of disease or for a prolonged time in combination with other interventions. The investigation of our as well as potential future patients with LTβR deficiency may provide valuable insights into the physiological consequences and potential side effects of long-term LTβR inhibition, ultimately guiding safer and more effective therapeutic strategies.

3.2.2 Conclusion and therapeutic outlook for LTβR-deficient patients

In summary, we identified and characterized the first patients with disease-causing mutations in *LTBR*, resulting in a combined immunodeficiency. Both homozygous mutations led to the complete loss of the encoded protein LTβR. The patients present with a remarkable phenotype of absent lymph nodes, most prominently absent tonsils, despite normal B cell counts. We could show that the significant reduction of class-switched and differentiated memory B cells is due to the absence of the microenvironment usually established in the secondary lymphoid organs. The results from our self-developed and sophisticated co-culturing model have shown that even in

the absence of LTβR on patient cells, the B cells are able to interact with other cell types and differentiate into GC-like and memory B cells.

These results, coupled with functional ex vivo assays that we performed, strongly suggest that the lymphocytes in these patients are functional and only lack the microenvironment provided in SLOs, which are formed in cooperation with stromal cells (Onder & Ludewig, 2018). While LTβR is also expressed in myeloid cells (Upadhyay & Fu, 2013), we were not able to detect any functional defects in monocytes or monocyte-derived dendritic cells. Notably, wildtype bone marrow transfer studies in *Ltβr*$^{-/-}$ mice have shown that the absence of lymph nodes was irreversible after birth (Wege *et al*, 2014). This was also the case in *Ltβ*$^{-/-}$ mice, where the genetic defect affected only the lymphocytes (Müller *et al*, 1996).

This is highly important for the therapeutic decisions made for these and potential future LTβR-deficient patients, as these patients are unlikely to benefit from HSCT. Instead, IgRT and antibiotic prophylaxis have proven to be an effective and sufficient treatment for these patients, as all three are doing well, with two having already reached adulthood. However, early diagnosis and intervention are crucial, as it is highly likely that the undiagnosed sibling of P3, who died at a young age from infection, was also affected by the same genetic defect.

Finally, we proposed several mechanisms that could contribute to the absence of clinical autoimmunity in LTβR-deficient patients, despite the low number of regulatory T cells and the phenotype reported in *Ltβr*$^{-/-}$ mice. Nevertheless, close monitoring of autoimmunity is warranted in these patients as well as potential future patients with genetic aberrations in *LTβR* or its ligands.

4. MATERIALS AND METHODS

The corresponding materials and methods are described in detail in the published manuscript included in Chapter 2.

REFERENCES

Abe J, Jibiki T, Noma S, Nakajima T, Saito H & Terai M (2005) Gene expression profiling of the effect of high-dose intravenous Ig in patients with Kawasaki disease. *J Immunol* 174: 5837–5845

Abolhassani H, Hammarström L & Cunningham-Rundles C (2020) Current genetic landscape in common variable immune deficiency. *Blood* 135: 656–667

Akalu YT & Bogunovic D (2024) Inborn errors of immunity: an expanding universe of disease and genetic architecture. *Nat Rev Genet* 25: 184–195

Akkaya M, Kwak K & Pierce SK (2020) B cell memory: building two walls of protection against pathogens. *Nat Rev Immunol* 20: 229–238

Alonso N, Wani S, Rose L, van't Hof RJ, Ralston SH & Albagha OME (2021) Insertion Mutation in Tnfrsf11a Causes a Paget's Disease–Like Phenotype in Heterozygous Mice and Osteopetrosis in Homozygous Mice. *Journal of Bone and Mineral Research* 36: 1376–1386

Alosaimi MF, Hoenig M, Jaber F, Platt CD, Jones J, Wallace J, Debatin K-M, Schulz A, Jacobsen E, Möller P, *et al* (2019) Immunodeficiency and EBV-induced lymphoproliferation caused by 4-1BB deficiency. *J Allergy Clin Immunol* 144: 574-583.e5

An D, Chen G, Cheng W-Y, Mohrs K, Adler C, Gupta NT, Atwal GS, DiLillo DJ, Daly C, Lin JC, *et al* (2024) LTβR Agonism Promotes Antitumor Immune Responses via Modulation of the Tumor Microenvironment. *Cancer Research* 84: 3984–4001

Anderson CA, Boucher G, Lees CW, Franke A, D'Amato M, Taylor KD, Lee JC, Goyette P, Imielinski M, Latiano A, *et al* (2011) Meta-analysis identifies 29 additional ulcerative colitis risk loci, increasing the number of confirmed associations to 47. *Nat Genet* 43: 246–252

Aqdas M & Sung M-H (2023) NF-κB dynamics in the language of immune cells. *Trends Immunol* 44: 32–43

Arunachalam PS, Wimmers F, Mok CKP, Perera RAPM, Scott M, Hagan T, Sigal N, Feng Y, Bristow L, Tak-Yin Tsang O, *et al* (2020) Systems biological assessment of immunity to mild versus severe COVID-19 infection in humans. *Science* 369: 1210–1220

Bamias G, Kaltsa G, Siakavellas SI, Papaxoinis K, Zampeli E, Michopoulos S, Zouboulis-Vafiadis I & Ladas SD (2010) High intestinal and systemic levels of decoy receptor

3 (DcR3) and its ligand TL1A in active ulcerative colitis. *Clin Immunol* 137: 242–249

Bamias G, Siakavellas SI, Stamatelopoulos KS, Chryssochoou E, Papamichael C & Sfikakis PP (2008) Circulating levels of TNF-like cytokine 1A (TL1A) and its decoy receptor 3 (DcR3) in rheumatoid arthritis. *Clin Immunol* 129: 249–255

Banchereau J & Steinman RM (1998) Dendritic cells and the control of immunity. *Nature* 392: 245–252

Banday AZ, Nisar R, Patra PK, Kaur A, Sadanand R, Chaudhry C, Bukhari STA, Banday SZ, Bhattarai D & Notarangelo LD (2023) Clinical and Immunological Features, Genetic Variants, and Outcomes of Patients with CD40 Deficiency. *J Clin Immunol* 44: 17

Barker AF (2002) Bronchiectasis. *New England Journal of Medicine* 346: 1383–1393

Basu S, Rosenzweig KR, Youmell M & Price BD (1998) The DNA-dependent protein kinase participates in the activation of NF kappa B following DNA damage. *Biochem Biophys Res Commun* 247: 79–83

Bauernfeind FG, Horvath G, Stutz A, Alnemri ES, MacDonald K, Speert D, Fernandes-Alnemri T, Wu J, Monks BG, Fitzgerald KA, *et al* (2009) Cutting edge: NF-kappaB activating pattern recognition and cytokine receptors license NLRP3 inflammasome activation by regulating NLRP3 expression. *J Immunol* 183: 787–791

Bayry J, Ahmed EA, Toscano-Rivero D, Vonniessen N, Genest G, Cohen CG, Dembele M, Kaveri SV & Mazer BD (2023) Intravenous Immunoglobulin: Mechanism of Action in Autoimmune and Inflammatory Conditions. *The Journal of Allergy and Clinical Immunology: In Practice* 11: 1688–1697

Beinke S & Ley SC (2004) Functions of NF-kappaB1 and NF-kappaB2 in immune cell biology. *Biochem J* 382: 393–409

Béziat V, Rapaport F, Hu J, Titeux M, Bonnet des Claustres M, Bourgey M, Griffin H, Bandet É, Ma CS, Sherkat R, *et al* (2021) Humans with inherited T cell CD28 deficiency are susceptible to skin papillomaviruses but are otherwise healthy. *Cell* 184: 3812-3828.e30

Bleesing J (2022) Gain-of-function defects in toll-like receptor 8 shed light on the interface between immune system and bone marrow failure disorders. *Front Immunol* 13

Boehm T, Scheu S, Pfeffer K & Bleul CC (2003) Thymic medullary epithelial cell differentiation, thymocyte emigration, and the control of autoimmunity require lympho-epithelial cross talk via LTbetaR. *J Exp Med* 198: 757–769

Bonthron DT, Markham AF, Ginsburg D & Orkin SH (1985) Identification of a point mutation in the adenosine deaminase gene responsible for immunodeficiency. *J Clin Invest* 76: 894–897

Borelli A & Irla M (2021) Lymphotoxin: from the physiology to the regeneration of the thymic function. *Cell Death Differ* 28: 2305–2314

Bousfiha AA, Jeddane L, Ailal F, Al Herz W, Conley ME, Cunningham-Rundles C, Etzioni A, Fischer A, Franco JL, Geha RS, *et al* (2013) A Phenotypic Approach for IUIS PID Classification and Diagnosis: Guidelines for Clinicians at the Bedside. *J Clin Immunol* 33: 1078–1087

Brown GC (2024) Cell death by phagocytosis. *Nat Rev Immunol* 24: 91–102

Buchan SL, Rogel A & Al-Shamkhani A (2018) The immunobiology of CD27 and OX40 and their potential as targets for cancer immunotherapy. *Blood* 131: 39–48

Byun M, Ma CS, Akçay A, Pedergnana V, Palendira U, Myoung J, Avery DT, Liu Y, Abhyankar A, Lorenzo L, *et al* (2013) Inherited human OX40 deficiency underlying classic Kaposi sarcoma of childhood. *J Exp Med* 210: 1743–1759

Cabrita R, Lauss M, Sanna A, Donia M, Skaarup Larsen M, Mitra S, Johansson I, Phung B, Harbst K, Vallon-Christersson J, *et al* (2020) Tertiary lymphoid structures improve immunotherapy and survival in melanoma. *Nature* 577: 561–565

Cai W, Tanaka K, Mi X, Rajasekhar VK, Khan JF, Yoo S, de Stanchina E, Rahman J, Mathew S, Abrahimi P, *et al* (2024) Augmenting CAR T-cell Functions with LIGHT. *Cancer Immunol Res* 12: 1361–1379

Cao Z, Xiong J, Takeuchi M, Kurama T & Goeddel DV (1996) TRAF6 is a signal transducer for interleukin-1. *Nature* 383: 443–446

Capitani M, Al-Shaibi AA, Pandey S, Gartner L, Taylor H, Hubrack SZ, Agrebi N, Al-Mohannadi MJ, Al Kaabi S, Vogl T, *et al* (2023) Biallelic TLR4 deficiency in humans. *Journal of Allergy and Clinical Immunology* 151: 783-790.e5

Cardinale CJ, Abrams DJ, Mentch FD, Cardinale JA, Wang X, Kao C, Sleiman PMA & Hakonarson H (2023) Elevated Levels of the Cytokine LIGHT in Pediatric Crohn's Disease. *J Immunol* 210: 590–594

Cardinale CJ, Wei Z, Panossian S, Wang F, Kim CE, Mentch FD, Chiavacci RM, Kachelries KE, Pandey R, Grant SFA, *et al* (2013) Targeted resequencing identifies defective variants of decoy receptor 3 in pediatric-onset inflammatory bowel disease. *Genes Immun* 14: 447–452

Carroll MC & Isenman DE (2012) Regulation of humoral immunity by complement. *Immunity* 37: 199–207

Casrouge A, Zhang S-Y, Eidenschenk C, Jouanguy E, Puel A, Yang K, Alcais A, Picard C, Mahfoufi N, Nicolas N, *et al* (2006) Herpes Simplex Virus Encephalitis in Human UNC-93B Deficiency. *Science* 314: 308–312

Castigli E, Wilson SA, Garibyan L, Rachid R, Bonilla F, Schneider L & Geha RS (2005) TACI is mutant in common variable immunodeficiency and IgA deficiency. *Nat Genet* 37: 829–834

Chan TD, Gatto D, Wood K, Camidge T, Basten A & Brink R (2009) Antigen affinity controls rapid T-dependent antibody production by driving the expansion rather than the differentiation or extrafollicular migration of early plasmablasts. *J Immunol* 183: 3139–3149

Chang Y, Cesarman E, Pessin MS, Lee F, Culpepper J, Knowles DM & Moore PS (1994) Identification of Herpesvirus-Like DNA Sequences in AIDS-Sssociated Kaposi's Sarcoma. *Science* 266: 1865–1869

Chen K, Coonrod EM, Kumánovics A, Franks ZF, Durtschi JD, Margraf RL, Wu W, Heikal NM, Augustine NH, Ridge PG, *et al* (2013) Germline mutations in NFKB2 implicate the noncanonical NF-κB pathway in the pathogenesis of common variable immunodeficiency. *Am J Hum Genet* 93: 812–824

Chin RK, Lo JC, Kim O, Blink SE, Christiansen PA, Peterson P, Wang Y, Ware C & Fu Y-X (2003) Lymphotoxin pathway directs thymic Aire expression. *Nat Immunol* 4: 1121–1127

Cudrici C, Deuitch N & Aksentijevich I (2020) Revisiting TNF Receptor-Associated Periodic Syndrome (TRAPS): Current Perspectives. *Int J Mol Sci* 21: 3263

Dabbah-Krancher G & Snow AL (2023) Mistuned NF-κB signaling in lymphocytes: lessons from relevant inborn errors of immunity. *Clinical and Experimental Immunology* 212: 117–128

Dalakas MC (2020) Progress in the therapy of myasthenia gravis: getting closer to effective targeted immunotherapies. *Curr Opin Neurol* 33: 545–552

Dalakas MC & Spaeth PJ (2021) The importance of FcRn in neuro-immunotherapies: From IgG catabolism, FCGRT gene polymorphisms, IVIg dosing and efficiency to specific FcRn inhibitors. *Ther Adv Neurol Disord* 14: 1756286421997381

De Togni P, Goellner J, Ruddle NH, Streeter PR, Fick A, Mariathasan S, Smith SC, Carlson R, Shornick LP & Strauss-Schoenberger J (1994) Abnormal development of peripheral lymphoid organs in mice deficient in lymphotoxin. *Science* 264: 703–707

DeFranco AL (2016) Germinal centers and autoimmune disease in humans and mice. *Immunol Cell Biol* 94: 918–924

Demir A, Kahraman R, Candan G & Ergen A (2020) The role of FAS gene variants in inflammatory bowel disease. *Turk J Gastroenterol* 31: 356–361

Denton AE & Linterman MA (2017) Stromal networking: cellular connections in the germinal centre. *Current Opinion in Immunology* 45: 103–111

de Diego RP, Sancho-Shimizu V, Lorenzo L, Puel A, Plancoulaine S, Picard C, Herman M, Cardon A, Durandy A, Bustamante J, *et al* (2010) Human TRAF3 adaptor molecule deficiency leads to impaired Toll-like receptor 3 response and susceptibility to herpes simplex encephalitis. *Immunity* 33: 400–411

Dougall WC, Glaccum M, Charrier K, Rohrbach K, Brasel K, Smedt TD, Daro E, Smith J, Tometsko ME, Maliszewski CR, *et al* (1999) RANK is essential for osteoclast and lymph node development. *Genes Dev* 13: 2412–2424

Edwards JR, Sun SG, Locklin R, Shipman CM, Adamopoulos IE, Athanasou NA & Sabokbar A (2006) LIGHT (TNFSF14), a novel mediator of bone resorption, is elevated in rheumatoid arthritis. *Arthritis Rheum* 54: 1451–1462

Elgueta R, Benson MJ, de Vries VC, Wasiuk A, Guo Y & Noelle RJ (2009) Molecular mechanism and function of CD40/CD40L engagement in the immune system. *Immunol Rev* 229: 10.1111/j.1600-065X.2009.00782.x

Fathi N, Nirouei M, Salimian Rizi Z, Fekrvand S, Abolhassani H, Salami F, Ketabforoush AHME, Azizi G, Saghazadeh A, Esmaeili M, *et al* (2024) Clinical, Immunological, and Genetic Features in Patients with NFKB1 and NFKB2 Mutations: a Systematic Review. *J Clin Immunol* 44: 160

Fazekas F, Deisenhammer F, Strasser-Fuchs S, Nahler G & Mamoli B (1997) Randomised placebo-controlled trial of monthly intravenous immunoglobulin therapy in relapsing-remitting multiple sclerosis. Austrian Immunoglobulin in Multiple Sclerosis Study Group. *Lancet* 349: 589–593

Ferrari S, Giliani S, Insalaco A, Al-Ghonaium A, Soresina AR, Loubser M, Avanzini MA, Marconi M, Badolato R, Ugazio AG, *et al* (2001) Mutations of CD40 gene cause an autosomal recessive form of immunodeficiency with hyper IgM. *Proceedings of the National Academy of Sciences* 98: 12614–12619

Fitzgerald DC, Meade KG, McEvoy AN, Lillis L, Murphy EP, MacHugh DE & Baird AW (2007) Tumour necrosis factor-alpha (TNF-alpha) increases nuclear factor kappaB (NFkappaB) activity in and interleukin-8 (IL-8) release from bovine mammary epithelial cells. *Vet Immunol Immunopathol* 116: 59–68

Fliegauf M, Bryant VL, Frede N, Slade C, Woon S-T, Lehnert K, Winzer S, Bulashevska A, Scerri T, Leung E, *et al* (2015) Haploinsufficiency of the NF-κB1 Subunit p50 in Common Variable Immunodeficiency. *Am J Hum Genet* 97: 389–403

Fliegauf M, Kinnunen M, Posadas-Cantera S, Camacho-Ordonez N, Abolhassani H, Alsina L, Atschekzei F, Bogaert DJ, Burns SO, Church JA, *et al* (2022) Detrimental NFKB1 missense variants affecting the Rel-homology domain of p105/p50. *Front Immunol* 13: 965326

Foy TM, Laman JD, Ledbetter JA, Aruffo A, Claassen E & Noelle RJ (1994) gp39-CD40 interactions are essential for germinal center formation and the development of B cell memory. *J Exp Med* 180: 157–163

Fukuyama S, Hiroi T, Yokota Y, Rennert PD, Yanagita M, Kinoshita N, Terawaki S, Shikina T, Yamamoto M, Kurono Y, *et al* (2002) Initiation of NALT Organogenesis Is Independent of the IL-7R, LTβR, and NIK Signaling Pathways but Requires the Id2 Gene and CD3−CD4+CD45+ Cells. *Immunity* 17: 31–40

Fütterer A, Mink K, Luz A, Kosco-Vilbois MH & Pfeffer K (1998) The Lymphotoxin β Receptor Controls Organogenesis and Affinity Maturation in Peripheral Lymphoid Tissues. *Immunity* 9: 59–70

Garside P, Ingulli E, Merica RR, Johnson JG, Noelle RJ & Jenkins MK (1998) Visualization of specific B and T lymphocyte interactions in the lymph node. *Science* 281: 96–99

Goldstein DB, Allen A, Keebler J, Margulies EH, Petrou S, Petrovski S & Sunyaev S (2013) Sequencing studies in human genetics: design and interpretation. *Nat Rev Genet* 14: 460–470

Gommerman JL & Browning JL (2003) Lymphotoxin/light, lymphoid microenvironments and autoimmune disease. *Nat Rev Immunol* 3: 642–655

Gretz JE, Anderson AO & Shaw S (1997) Cords, channels, corridors and conduits: critical architectural elements facilitating cell interactions in the lymph node cortex. *Immunol Rev* 156: 11–24

Gruber CN, Calis JJA, Buta S, Evrony G, Martin JC, Uhl SA, Caron R, Jarchin L, Dunkin D, Phelps R, *et al* (2020) Complex Autoinflammatory Syndrome Unveils Fundamental Principles of JAK1 Kinase Transcriptional and Biochemical Function. *Immunity* 53: 672-684.e11

Grumach AS & Goudouris ES (2021) Inborn Errors of Immunity: how to diagnose them? *J Pediatr (Rio J)* 97: S84–S90

Guerrini MM, Sobacchi C, Cassani B, Abinun M, Kilic SS, Pangrazio A, Moratto D, Mazzolari E, Clayton-Smith J, Orchard P, *et al* (2008) Human osteoclast-poor osteopetrosis with hypogammaglobulinemia due to TNFRSF11A (RANK) mutations. *Am J Hum Genet* 83: 64–76

Guo L, Elcioglu NH, Karalar OK, Topkar MO, Wang Z, Sakamoto Y, Matsumoto N, Miyake N, Nishimura G & Ikegawa S (2018) Dysosteosclerosis is also caused by TNFRSF11A mutation. *J Hum Genet* 63: 769–774

Guo MM-H, Chang L-S, Huang Y-H, Wang F-S & Kuo H-C (2020) Epigenetic Regulation of Macrophage Marker Expression Profiles in Kawasaki Disease. *Front Pediatr* 8: 129

Guo Q, Jin Y, Chen X, Ye X, Shen X, Lin M, Zeng C, Zhou T & Zhang J (2024) NF-κB in biology and targeted therapy: new insights and translational implications. *Sig Transduct Target Ther* 9: 1–37

Halvorsen B, Santilli F, Scholz H, Sahraoui A, Gulseth HL, Wium C, Lattanzio S, Formoso G, Di Fulvio P, Otterdal K, *et al* (2016) LIGHT/TNFSF14 is increased in patients with type 2 diabetes mellitus and promotes islet cell dysfunction and endothelial cell inflammation in vitro. *Diabetologia* 59: 2134–2144

Hay M, Thomas DW, Craighead JL, Economides C & Rosenthal J (2014) Clinical development success rates for investigational drugs. *Nat Biotechnol* 32: 40–51

Heesters BA, Myers RC & Carroll MC (2014) Follicular dendritic cells: dynamic antigen libraries. *Nat Rev Immunol* 14: 495–504

Helmink BA, Reddy SM, Gao J, Zhang S, Basar R, Thakur R, Yizhak K, Sade-Feldman M, Blando J, Han G, *et al* (2020) B cells and tertiary lymphoid structures promote immunotherapy response. *Nature* 577: 549–555

Hirose T, Fukuma Y, Takeshita A & Nishida K (2018) The role of lymphotoxin-α in rheumatoid arthritis. *Inflamm Res* 67: 495–501

Hogquist KA, Baldwin TA & Jameson SC (2005) Central tolerance: learning self-control in the thymus. *Nat Rev Immunol* 5: 772–782

Hughes AE, Ralston SH, Marken J, Bell C, MacPherson H, Wallace RG, van Hul W, Whyte MP, Nakatsuka K, Hovy L, *et al* (2000) Mutations in TNFRSF11A, affecting the signal peptide of RANK, cause familial expansile osteolysis. *Nat Genet* 24: 45–48

Itano AA & Jenkins MK (2003) Antigen presentation to naive CD4 T cells in the lymph node. *Nat Immunol* 4: 733–739

Iwasaki A & Medzhitov R (2015) Control of adaptive immunity by the innate immune system. *Nat Immunol* 16: 343–353

Jacob A, Shen L, He J, Nealon K, Alexander JJ & Ambrus JL (2022) Effect of lymphotoxin blockage on different stages of Sjogren's syndrome in an animal model. *Rheumatology & Autoimmunity* 2: 76–81

Jin J, Hu H, Li HS, Yu J, Xiao Y, Brittain GC, Zou Q, Cheng X, Mallette FA, Watowich SS, *et al* (2014) Noncanonical NF-κB Pathway Controls the Production of Type I Interferons in Antiviral Innate Immunity. *Immunity* 40: 342–354

Kaustio M, Haapaniemi E, Göös H, Hautala T, Park G, Syrjänen J, Einarsdottir E, Sahu B, Kilpinen S, Rounioja S, *et al* (2017) Damaging heterozygous mutations in NFKB1 lead to diverse immunologic phenotypes. *J Allergy Clin Immunol* 140: 782–796

Kawai T, Ikegawa M, Ori D & Akira S (2024) Decoding Toll-like receptors: Recent insights and perspectives in innate immunity. *Immunity* 57: 649–673

Kazatchkine MD & Kaveri SV (2001) Immunomodulation of Autoimmune and Inflammatory Diseases with Intravenous Immune Globulin. *New England Journal of Medicine* 345: 747–755

Kennedy WP, Simon JA, Offutt C, Horn P, Herman A, Townsend MJ, Tang MT, Grogan JL, Hsieh F & Davis JC (2014) Efficacy and safety of pateclizumab (anti-lymphotoxin-α) compared to adalimumab in rheumatoid arthritis: a head-to-head phase 2 randomized controlled study (The ALTARA Study). *Arthritis Res Ther* 16: 467

Kırkgöz T, Özkan B, Hazan F, Acar S, Nalbantoğlu Ö, Özkaya B, Kulalı MA, Gürsoy S, Ikegawa S & Guo L (2022) A Null Mutation of TNFRSF11A Causes Dysosteosclerosis, Not Osteopetrosis. *Front Genet* 13

Kleinnijenhuis J, Quintin J, Preijers F, Joosten LAB, Ifrim DC, Saeed S, Jacobs C, van Loenhout J, de Jong D, Stunnenberg HG, *et al* (2012) Bacille Calmette-Guerin induces NOD2-dependent nonspecific protection from reinfection via epigenetic reprogramming of monocytes. *Proc Natl Acad Sci U S A* 109: 17537–17542

Kleinnijenhuis J, Quintin J, Preijers F, Joosten LAB, Jacobs C, Xavier RJ, van der Meer JWM, van Crevel R & Netea MG (2014) BCG-induced trained immunity in NK cells: Role for non-specific protection to infection. *Clin Immunol* 155: 213–219

Klemann C, Camacho-Ordonez N, Yang L, Eskandarian Z, Rojas-Restrepo JL, Frede N, Bulashevska A, Heeg M, Al-Ddafari MS, Premm J, *et al* (2019) Clinical and Immunological Phenotype of Patients With Primary Immunodeficiency Due to Damaging Mutations in NFKB2. *Front Immunol* 10

Krausgruber T, Fortelny N, Fife-Gernedl V, Senekowitsch M, Schuster LC, Lercher A, Nemc A, Schmidl C, Rendeiro AF, Bergthaler A, *et al* (2020) Structural cells are key regulators of organ-specific immune response. *Nature* 583: 296–302

Kuehn HS, Ouyang W, Lo B, Deenick EK, Niemela JE, Avery DT, Schickel J-N, Tran DQ, Stoddard J, Zhang Y, *et al* (2014) Immune dysregulation in human subjects with heterozygous germline mutations in CTLA4. *Science* 345: 1623–1627

Kumar BV, Connors T & Farber DL (2018) Human T cell development, localization, and function throughout life. *Immunity* 48: 202–213

Le Voyer T, Parent AV, Liu X, Cederholm A, Gervais A, Rosain J, Nguyen T, Perez Lorenzo M, Rackaityte E, Rinchai D, *et al* (2023) Autoantibodies against type I IFNs in humans with alternative NF-κB pathway deficiency. *Nature* 623: 803–813

Lee W-H, Seo D, Lim S-G & Suk K (2019) Reverse Signaling of Tumor Necrosis Factor Superfamily Proteins in Macrophages and Microglia: Superfamily Portrait in the Neuroimmune Interface. *Front Immunol* 10

Li Y, Yu Z, Schenk M, Lagovsky I, Illig D, Walz C, Rohlfs M, Conca R, Muise AM, Snapper SB, *et al* (2023) Human MD2 deficiency-an inborn error of immunity with pleiotropic features. *J Allergy Clin Immunol* 151: 791-796.e7

Lim HK, Seppänen M, Hautala T, Ciancanelli MJ, Itan Y, Lafaille FG, Dell W, Lorenzo L, Byun M, Pauwels E, *et al* (2014) TLR3 deficiency in herpes simplex encephalitis. *Neurology* 83: 1888–1897

Lin W-W & Hsieh S-L (2011) Decoy receptor 3: a pleiotropic immunomodulator and biomarker for inflammatory diseases, autoimmune diseases and cancer. *Biochem Pharmacol* 81: 838–847

Liu T, Zhang L, Joo D & Sun S-C (2017) NF-κB signaling in inflammation. *Sig Transduct Target Ther* 2: 1–9

Lorenzini T, Fliegauf M, Klammer N, Frede N, Proietti M, Bulashevska A, Camacho-Ordonez N, Varjosalo M, Kinnunen M, Vries E de, *et al* (2020) Characterization of the clinical and immunologic phenotype and management of 157 individuals with 56 distinct heterozygous NFKB1 mutations. *Journal of Allergy and Clinical Immunology* 146: 901–911

van der Made CI, Simons A, Schuurs-Hoeijmakers J, van den Heuvel G, Mantere T, Kersten S, van Deuren RC, Steehouwer M, van Reijmersdal SV, Jaeger M, *et al* (2020) Presence of Genetic Variants Among Young Men With Severe COVID-19. *JAMA* 324: 663–673

Mahlaoui N, Minard-Colin V, Picard C, Bolze A, Ku C-L, Tournilhac O, Gilbert-Dussardier B, Pautard B, Durand P, Devictor D, *et al* (2011) Isolated congenital asplenia: a French nationwide retrospective survey of 20 cases. *J Pediatr* 158: 142–148, 148.e1

Martins VC, Boehm T & Bleul CC (2008) Ltbetar signaling does not regulate Aire-dependent transcripts in medullary thymic epithelial cells. *J Immunol* 181: 400–407

Mastellos DC, Hajishengallis G & Lambris JD (2024) A guide to complement biology, pathology and therapeutic opportunity. *Nat Rev Immunol* 24: 118–141

Mauri DN, Ebner R, Montgomery RI, Kochel KD, Cheung TC, Yu GL, Ruben S, Murphy M, Eisenberg RJ, Cohen GH, *et al* (1998) LIGHT, a new member of the TNF superfamily, and lymphotoxin alpha are ligands for herpesvirus entry mediator. *Immunity* 8: 21–30

May MJ (2006) A Nuclear Factor in B Cells and Beyond. *The Journal of Immunology* 177: 7483–7484

McDermott MF, Aksentijevich I, Galon J, McDermott EM, Ogunkolade BW, Centola M, Mansfield E, Gadina M, Karenko L, Pettersson T, *et al* (1999) Germline mutations in the extracellular domains of the 55 kDa TNF receptor, TNFR1, define a family of dominantly inherited autoinflammatory syndromes. *Cell* 97: 133–144

Mebius RE & Kraal G (2005) Structure and function of the spleen. *Nat Rev Immunol* 5: 606–616

Medetgul-Ernar K & Davis MM (2022) Standing on the shoulders of Mice. *Immunity* 55: 1343–1353

Miller JFAP (1961) IMMUNOLOGICAL FUNCTION OF THE THYMUS. *The Lancet* 278: 748–749

Moraes L, Magnusson MK, Mavroudis G, Polster A, Jonefjäll B, Törnblom H, Sundin J, Simrén M, Strid H & Öhman L (2020) Systemic Inflammatory Protein Profiles Distinguish Irritable Bowel Syndrome (IBS) and Ulcerative Colitis, Irrespective of Inflammation or IBS-Like Symptoms. *Inflamm Bowel Dis* 26: 874–884

Morgan NV, Goddard S, Cardno TS, McDonald D, Rahman F, Barge D, Ciupek A, Straatman-Iwanowska A, Pasha S, Guckian M, *et al* (2011) Mutation in the TCRα subunit constant gene (TRAC) leads to a human immunodeficiency disorder characterized by a lack of TCRαβ+ T cells. *J Clin Invest* 121: 695–702

Morita CT, Beckman EM, Bukowski JF, Tanaka Y, Band H, Bloom BR, Golan DE & Brenner MB (1995) Direct presentation of nonpeptide prenyl pyrophosphate antigens to human gamma delta T cells. *Immunity* 3: 495–507

Mosser DM & Edwards JP (2008) Exploring the full spectrum of macrophage activation. *Nat Rev Immunol* 8: 958–969

Müller M, Eugster H-P, Le Hir M, Shakhov A, Di Padova F, Maurer C, Quesniaux VFJ & Ryffel B (1996) Correction or Transfer of Immunodeficiency Due to TNF-LTα Deletion by Bone Marrow Transplantation. *Mol Med* 2: 247–255

Muramatsu M, Kinoshita K, Fagarasan S, Yamada S, Shinkai Y & Honjo T (2000) Class switch recombination and hypermutation require activation-induced cytidine deaminase (AID), a potential RNA editing enzyme. *Cell* 102: 553–563

Murata J, Abe R & Shimizu H (2008) Increased soluble Fas ligand levels in patients with Stevens-Johnson syndrome and toxic epidermal necrolysis preceding skin detachment. *J Allergy Clin Immunol* 122: 992–1000

Murphy K & Weaver C (2016) Janeway's Immunobiology. 9th ed. Garland Science

Ng SB, Turner EH, Robertson PD, Flygare SD, Bigham AW, Lee C, Shaffer T, Wong M, Bhattacharjee A, Eichler EE, *et al* (2009) Targeted capture and massively parallel sequencing of 12 human exomes. *Nature* 461: 272–276

Nieto-Aristizábal I, Martínez T, Urbano M-A, Posso-Osorio I, Plata IF, Garcia-Robledo JE, Aragón CC, Santos VA & Tobón GJ (2019) Treatment with intravenous immunoglobulins in systemic lupus erythematosus: a single-center experience with 63 patients. *Lupus* 28: 1566–1570

Nikolich-Zugich J, Slifka MK & Messaoudi I (2004) The many important facets of T-cell repertoire diversity. *Nat Rev Immunol* 4: 123–132

Nitta T, Tsutsumi M, Nitta S, Muro R, Suzuki EC, Nakano K, Tomofuji Y, Sawa S, Okamura T, Penninger JM, *et al* (2020) Fibroblasts as a source of self-antigens for central immune tolerance. *Nat Immunol* 21: 1172–1180

Ochando J, Mulder WJM, Madsen JC, Netea MG & Duivenvoorden R (2023) Trained immunity — basic concepts and contributions to immunopathology. *Nat Rev Nephrol* 19: 23–37

Ogishi M, Yang R, Aytekin C, Langlais D, Bourgey M, Khan T, Ali FA, Rahman M, Delmonte OM, Chrabieh M, *et al* (2021) Inherited PD-1 deficiency underlies tuberculosis and autoimmunity in a child. *Nat Med* 27: 1646–1654

Oh H & Ghosh S (2013) NF-κB: roles and regulation in different CD4(+) T-cell subsets. *Immunol Rev* 252: 41–51

Onder L & Ludewig B (2018) A Fresh View on Lymph Node Organogenesis. *Trends Immunol* 39: 775–787

Palao G, Santiago B, Galindo MA, Rullas JN, Alcamí J, Ramirez JC & Pablos JL (2006) Fas activation of a proinflammatory program in rheumatoid synoviocytes and its regulation by FLIP and caspase 8 signaling. *Arthritis Rheum* 54: 1473–1481

Paludan SR, Pradeu T, Masters SL & Mogensen TH (2021) Constitutive immune mechanisms: mediators of host defence and immune regulation. *Nat Rev Immunol* 21: 137–150

Parra D, Rieger AM, Li J, Zhang Y-A, Randall LM, Hunter CA, Barreda DR & Sunyer JO (2012) Pivotal Advance: Peritoneal cavity B-1 B cells have phagocytic and microbicidal capacities and present phagocytosed antigen to CD4+ T cells. *J Leukoc Biol* 91: 525–536

Paskiewicz A, Niu J & Chang C (2023) Autoimmune lymphoproliferative syndrome: A disorder of immune dysregulation. *Autoimmun Rev* 22: 103442

Paul C, Wolkenstein P, Adle H, Wechsler J, Garchon HJ, Revuz J & Roujeau JC (1996) Apoptosis as a mechanism of keratinocyte death in toxic epidermal necrolysis. *Br J Dermatol* 134: 710–714

van de Pavert SA & Mebius RE (2010) New insights into the development of lymphoid tissues. *Nat Rev Immunol* 10: 664–674

Pedersen FK (1983) Postsplenectomy infections in Danish children splenectomized 1969-1978. *Acta Paediatr Scand* 72: 589–595

Perlin DS, Neil GA, Anderson C, Zafir-Lavie I, Raines S, Ware CF & Wilkins HJ (2022) Randomized, double-blind, controlled trial of human anti-LIGHT monoclonal antibody in COVID-19 acute respiratory distress syndrome. *J Clin Invest* 132

Pieper K, Grimbacher B & Eibel H (2013) B-cell biology and development. *Journal of Allergy and Clinical Immunology* 131: 959–971

Pillai S & Cariappa A (2009) The follicular versus marginal zone B lymphocyte cell fate decision. *Nat Rev Immunol* 9: 767–777

Pitti RM, Marsters SA, Lawrence DA, Roy M, Kischkel FC, Dowd P, Huang A, Donahue CJ, Sherwood SW, Baldwin DT, *et al* (1998) Genomic amplification of a decoy receptor for Fas ligand in lung and colon cancer. *Nature* 396: 699–703

Pitzalis C, Jones GW, Bombardieri M & Jones SA (2014) Ectopic lymphoid-like structures in infection, cancer and autoimmunity. *Nat Rev Immunol* 14: 447–462

Poli CM, Aksentijevich I, Bousfiha A, Cunningham-Rundles C, Hambleton S, Klein C, Morio T, Picard C, Puel A, Rezaei N, *et al* (2025) Human inborn errors of immunity: 2024 Update on the classification from the International Union of Immunological Societies Expert Committee.

Pone EJ, Zhang J, Mai T, White CA, Li G, Sakakura JK, Patel PJ, Al-Qahtani A, Zan H, Xu Z, *et al* (2012) BCR-signalling synergizes with TLR-signalling for induction of AID and immunoglobulin class-switching through the non-canonical NF-κB pathway. *Nat Commun* 3: 767

Rapaport F, Boisson B, Gregor A, Béziat V, Boisson-Dupuis S, Bustamante J, Jouanguy E, Puel A, Rosain J, Zhang Q, *et al* (2021) Negative selection on human genes underlying inborn errors depends on disease outcome and both the mode and mechanism of inheritance. *Proc Natl Acad Sci U S A* 118: e2001248118

Régnier CH, Song HY, Gao X, Goeddel DV, Cao Z & Rothe M (1997) Identification and Characterization of an IκB Kinase. *Cell* 90: 373–383

Rennert PD, Browning JL, Mebius R, Mackay F & Hochman PS (1996) Surface lymphotoxin alpha/beta complex is required for the development of peripheral lymphoid organs. *J Exp Med* 184: 1999–2006

Rennie D (1985) 'Bubble Boy'. *JAMA* 253: 78–80

Revy P, Muto T, Levy Y, Geissmann F, Plebani A, Sanal O, Catalan N, Forveille M, Dufourcq-Labelouse R, Gennery A, *et al* (2000) Activation-induced cytidine deaminase (AID) deficiency causes the autosomal recessive form of the Hyper-IgM syndrome (HIGM2). *Cell* 102: 565–575

Ricklin D, Hajishengallis G, Yang K & Lambris JD (2010) Complement: a key system for immune surveillance and homeostasis. *Nat Immunol* 11: 785–797

Rider NL, Truxton A, Ohrt T, Margolin-Katz I, Horan M, Shin H, Davila R, Tenembaum V, Quinn J, Modell V, *et al* (2024) Validating inborn error of immunity prevalence and risk with nationally representative electronic health record data. *J Allergy Clin Immunol* 153: 1704–1710

Rieux-Laucat F, Le Deist F, Hivroz C, Roberts IA, Debatin KM, Fischer A & de Villartay JP (1995) Mutations in Fas associated with human lymphoproliferative syndrome and autoimmunity. *Science* 268: 1347–1349

Riordan JR, Rommens JM, Kerem B-S, Alon N, Rozmahel R, Grzelczak Z, Zielenski J, Lok S, Plavsic N, Chou J-L, *et al* (1989) Identification of the Cystic Fibrosis Gene: Cloning and Characterization of Complementary DNA. *Science* 245: 1066–1073

Rivas MA, Beaudoin M, Gardet A, Stevens C, Sharma Y, Zhang CK, Boucher G, Ripke S, Ellinghaus D, Burtt N, *et al* (2011) Deep resequencing of GWAS loci identifies independent rare variants associated with inflammatory bowel disease. *Nat Genet* 43: 1066–1073

Robinette CD & Fraumeni J (1977) SPLENECTOMY AND SUBSEQUENT MORTALITY IN VETERANS OF THE 1939-45 WAR. *The Lancet* 310: 127–129

Ruiz JE, Kwak JY, Baum L, Gilman-Sachs A, Beaman KD, Kim YB & Beer AE (1996) Intravenous immunoglobulin inhibits natural killer cell activity in vivo in women with recurrent spontaneous abortion. *Am J Reprod Immunol* 35: 370–375

Sagar & Ehl S (2025) γδ T Cells and Inborn Errors of Immunity. *Eur J Immunol* 55: e51457

Salzer U & Grimbacher B (2021) TACI deficiency — a complex system out of balance. *Current Opinion in Immunology* 71: 81–88

Sancho-Shimizu V, Pérez de Diego R, Lorenzo L, Halwani R, Alangari A, Israelsson E, Fabrega S, Cardon A, Maluenda J, Tatematsu M, *et al* (2011) Herpes simplex encephalitis in children with autosomal recessive and dominant TRIF deficiency. *J Clin Invest* 121: 4889–4902

Sato Y, Silina K, van den Broek M, Hirahara K & Yanagita M (2023) The roles of tertiary lymphoid structures in chronic diseases. *Nat Rev Nephrol* 19: 525–537

Schnappauf O & Aksentijevich I (2020) Mendelian diseases of dysregulated canonical NF-κB signaling: From immunodeficiency to inflammation. *J Leukoc Biol* 108: 573–589

Sen R & Baltimore D (1986) Multiple nuclear factors interact with the immunoglobulin enhancer sequences. *Cell* 46: 705–716

Sevdali E, Block Saldana V, Speletas M & Eibel H (2021) BAFF receptor polymorphisms and deficiency in humans. *Current Opinion in Immunology* 71: 103–110

Sharfe N, Dalal I, Naghdi Z, Lefaudeux D, Vong L, Dadi H, Navarro H, Tasher D, Ovadia A, Zangen T, *et al* (2023) NFκB pathway dysregulation due to reduced RelB expression leads to severe autoimmune disorders and declining immunity. *J Autoimmun* 137: 102946

Shay T, Jojic V, Zuk O, Rothamel K, Puyraimond-Zemmour D, Feng T, Wakamatsu E, Benoist C, Koller D, Regev A, *et al* (2013) Conservation and divergence in the transcriptional programs of the human and mouse immune systems. *Proc Natl Acad Sci U S A* 110: 2946–2951

Shen K, Wang J, Zhou K, Mu W, Zhang M, Deng X, Cai H, Zhang W, Huang W & Xiao M (2023) CD137 deficiency because of two novel biallelic TNFRSF9 mutations in a patient presenting with severe EBV-associated lymphoproliferative disease. *Clinical & Translational Immunology* 12: e1448

Shen L, Suresh L, Wu J, Xuan J, Li H, Zhang C, Pankewycz O & Ambrus JL (2010) A role for lymphotoxin in primary Sjogren's disease. *J Immunol* 185: 6355–6363

Sobacchi C, Frattini A, Guerrini MM, Abinun M, Pangrazio A, Susani L, Bredius R, Mancini G, Cant A, Bishop N, *et al* (2007) Osteoclast-poor human osteopetrosis due to mutations in the gene encoding RANKL. *Nat Genet* 39: 960–962

Somekh I, Thian M, Medgyesi D, Gülez N, Magg T, Gallón Duque A, Stauber T, Lev A, Genel F, Unal E, *et al* (2019) CD137 deficiency causes immune dysregulation with predisposition to lymphomagenesis. *Blood* 134: 1510–1516

St Clair EW, Baer AN, Wei C, Noaiseh G, Parke A, Coca A, Utset TO, Genovese MC, Wallace DJ, McNamara J, *et al* (2018) Clinical Efficacy and Safety of Baminercept, a Lymphotoxin β Receptor Fusion Protein, in Primary Sjögren's Syndrome: Results From a Phase II Randomized, Double-Blind, Placebo-Controlled Trial. *Arthritis Rheumatol* 70: 1470–1480

Stebegg M, Kumar SD, Silva-Cayetano A, Fonseca VR, Linterman MA & Graca L (2018) Regulation of the Germinal Center Response. *Front Immunol* 9

Stiehm ER (2012) Joseph A. Bellanti (ed) immunology IV: clinical applications in health and disease. *J Clin Immunol* 32: 647

Sun S-C (2011) Non-canonical NF-κB signaling pathway. *Cell Res* 21: 71–85

Sun S-C (2017) The non-canonical NF-κB pathway in immunity and inflammation. *Nat Rev Immunol* 17: 545–558

Suwara MI, Green NJ, Borthwick LA, Mann J, Mayer-Barber KD, Barron L, Corris PA, Farrow SN, Wynn TA, Fisher AJ, *et al* (2014) IL-1α released from damaged epithelial cells is sufficient and essential to trigger inflammatory responses in human lung fibroblasts. *Mucosal Immunol* 7: 684–693

Takaba H, Morishita Y, Tomofuji Y, Danks L, Nitta T, Komatsu N, Kodama T & Takayanagi H (2015) Fezf2 Orchestrates a Thymic Program of Self-Antigen Expression for Immune Tolerance. *Cell* 163: 975–987

Tang H, Zhu M, Qiao J & Fu Y-X (2017) Lymphotoxin signalling in tertiary lymphoid structures and immunotherapy. *Cell Mol Immunol* 14: 809–818

Tangye SG, Al-Herz W, Bousfiha A, Chatila T, Cunningham-Rundles C, Etzioni A, Franco JL, Holland SM, Klein C, Morio T, *et al* (2020) Human Inborn Errors of Immunity: 2019 Update on the Classification from the International Union of Immunological Societies Expert Committee. *J Clin Immunol* 40: 24–64

Tangye SG, Al-Herz W, Bousfiha A, Cunningham-Rundles C, Franco JL, Holland SM, Klein C, Morio T, Oksenhendler E, Picard C, *et al* (2022) Human Inborn Errors of Immunity: 2022 Update on the Classification from the International Union of Immunological Societies Expert Committee. *J Clin Immunol* 42: 1473–1507

Thalhammer J, Kindle G, Nieters A, Rusch S, Seppänen MRJ, Fischer A, Grimbacher B, Edgar D, Buckland M, Mahlaoui N, *et al* (2021) Initial presenting manifestations in 16,486 patients with inborn errors of immunity include infections and noninfectious manifestations. *J Allergy Clin Immunol* 148: 1332-1341.e5

Tuijnenburg P, Lango Allen H, Burns SO, Greene D, Jansen MH, Staples E, Stephens J, Carss KJ, Biasci D, Baxendale H, *et al* (2018) Loss-of-function nuclear factor κB subunit 1 (NFKB1) variants are the most common monogenic cause of common variable immunodeficiency in Europeans. *J Allergy Clin Immunol* 142: 1285–1296

Ueyama H, Kiyohara T, Sawada N, Isozaki K, Kitamura S, Kondo S, Miyagawa J, Kanayama S, Shinomura Y, Ishikawa H, *et al* (1998) High Fas ligand expression on lymphocytes in lesions of ulcerative colitis. *Gut* 43: 48–55

Uozumi R, Iguchi R, Masuda S, Nishibata Y, Nakazawa D, Tomaru U & Ishizu A (2020) Pharmaceutical immunoglobulins reduce neutrophil extracellular trap formation and ameliorate the development of MPO-ANCA-associated vasculitis. *Mod Rheumatol* 30: 544–550

Upadhyay V & Fu Y-X (2013) Lymphotoxin signalling in immune homeostasis and the control of microorganisms. *Nat Rev Immunol* 13: 270–279

Uranues S & Kilic YA (2008) Injuries to the Spleen. *Eur J Trauma Emerg Surg* 34: 355

Viard I, Wehrli P, Bullani R, Schneider P, Holler N, Salomon D, Hunziker T, Saurat J-H, Tschopp J & French LE (1998) Inhibition of Toxic Epidermal Necrolysis by Blockade of CD95 with Human Intravenous Immunoglobulin. *Science* 282: 490–493

Victora GD & Nussenzweig MC (2022) Germinal Centers. *Annu Rev Immunol* 40: 413–442

de Villartay J-P, Poinsignon C, de Chasseval R, Buck D, Le Guyader G & Villey I (2003) Human and animal models of V(D)J recombination deficiency. *Curr Opin Immunol* 15: 592–598

Voskoboinik I, Whisstock JC & Trapani JA (2015) Perforin and granzymes: function, dysfunction and human pathology. *Nat Rev Immunol* 15: 388–400

Walsh MC & Choi Y (2014) Biology of the RANKL–RANK–OPG System in Immunity, Bone, and Beyond. *Front Immunol* 5

Wang J & Fu Y-X (2005) Tumor necrosis factor family members and inflammatory bowel disease. *Immunol Rev* 204: 144–155

Wang N, Liang H & Zen K (2014) Molecular mechanisms that influence the macrophage m1-m2 polarization balance. *Front Immunol* 5: 614

Wang Z, Chai Q & Zhu M (2018) Differential Roles of LTβR in Endothelial Cell Subsets for Lymph Node Organogenesis and Maturation. *J Immunol* 201: 69–76

Warnatz K, Salzer U, Rizzi M, Fischer B, Gutenberger S, Böhm J, Kienzler A-K, Pan-Hammarström Q, Hammarström L, Rakhmanov M, *et al* (2009) B-cell activating factor receptor deficiency is associated with an adult-onset antibody deficiency syndrome in humans. *Proc Natl Acad Sci U S A* 106: 13945–13950

Wege AK, Huber B, Wimmer N, Männel DN & Hehlgans T (2014) LTβR expression on hematopoietic cells regulates acute inflammation and influences maturation of myeloid subpopulations. *Innate Immun* 20: 461–470

Wheeler DA, Srinivasan M, Egholm M, Shen Y, Chen L, McGuire A, He W, Chen Y-J, Makhijani V, Roth GT, *et al* (2008) The complete genome of an individual by massively parallel DNA sequencing. *Nature* 452: 872–876

White A, Carragher D, Parnell S, Msaki A, Perkins N, Lane P, Jenkinson E, Anderson G & Caamaño JH (2007) Lymphotoxin a-dependent and -independent signals regulate stromal organizer cell homeostasis during lymph node organogenesis. *Blood* 110: 1950–1959

Wiedeman AE, Santer DM, Yan W, Miescher S, Käsermann F & Elkon KB (2013) Contrasting mechanisms of interferon-α inhibition by intravenous immunoglobulin after induction by immune complexes versus Toll-like receptor agonists. *Arthritis Rheum* 65: 2713–2723

Wong CH, Siah KW & Lo AW (2019) Estimation of clinical trial success rates and related parameters. *Biostatistics* 20: 273–286

Wozniak W, Sechet E, Kwon Y-J, Aulner N, Navarro L & Sperandio B (2024) Identification of human host factors required for beta-defensin-2 expression in intestinal epithelial cells upon a bacterial challenge. *Sci Rep* 14: 15442

Wu W, Shi Y, Xia H, Chai Q, Jin C, Ren B & Zhu M (2017) Epithelial LTβR signaling controls the population size of the progenitors of medullary thymic epithelial cells in neonatal mice. *Sci Rep* 7: 44481

Xiao G, Harhaj EW & Sun S-C (2001) NF-κB-Inducing Kinase Regulates the Processing of NF-κB2 p100. *Molecular Cell* 7: 401–409

Xu W, Ren M, Ghosh S, Qian K, Luo Z, Zhang A, Zhang C & Cui J (2020) Defects of CTLA-4 Are Associated with Regulatory T Cells in Myasthenia Gravis Implicated by Intravenous Immunoglobulin Therapy. *Mediators Inflamm* 2020: 3645157

Yang C, McCoy K, Davis JL, Schmidt-Supprian M, Sasaki Y, Faccio R & Novack DV (2010) NIK stabilization in osteoclasts results in osteoporosis and enhanced inflammatory osteolysis. *PLoS One* 5: e15383

Yoshida H, Naito A, Inoue J-I, Satoh M, Santee-Cooper SM, Ware CF, Togawa A, Nishikawa S & Nishikawa S-I (2002) Different cytokines induce surface lymphotoxin-alphabeta on IL-7 receptor-alpha cells that differentially engender lymph nodes and Peyer's patches. *Immunity* 17: 823–833

You R-I, Chang Y-C, Chen P-M, Wang W-S, Hsu T-L, Yang C-Y, Lee C-T & Hsieh S-L (2008) Apoptosis of dendritic cells induced by decoy receptor 3 (DcR3). *Blood* 111: 1480–1488

Yy K, H Y, I S, Hl T, E T, C C, S M, Aj O-S, G V, A I, *et al* (1999) OPGL is a key regulator of osteoclastogenesis, lymphocyte development and lymph-node organogenesis. *Nature* 397

Zarnegar BJ, Wang Y, Mahoney DJ, Dempsey PW, Cheung HH, He J, Shiba T, Yang X, Yeh W, Mak TW, *et al* (2008) Activation of noncanonical NF-κB requires coordinated assembly of a regulatory complex of the adaptors cIAP1, cIAP2, TRAF2, TRAF3 and the kinase NIK. *Nat Immunol* 9: 1371–1378

Zhang F, Xia Y, Su J, Quan F, Zhou H, Li Q, Feng Q, Lin C, Wang D & Jiang Z (2024) Neutrophil diversity and function in health and disease. *Sig Transduct Target Ther* 9: 1–49

Zhang N, Liu X, Qin J, Sun Y, Xiong H, Lin B, Liu K, Tan B, Zhang C, Huang C, *et al* (2023) LIGHT/TNFSF14 promotes CAR-T cell trafficking and cytotoxicity through reversing immunosuppressive tumor microenvironment. *Mol Ther* 31: 2575–2590

Zhang Q, Lenardo MJ & Baltimore D (2017) 30 Years of NF-κB: A Blossoming of Relevance to Human Pathobiology. *Cell* 168: 37–57

Zhang S-Y, Jouanguy E, Ugolini S, Smahi A, Elain G, Romero P, Segal D, Sancho-Shimizu V, Lorenzo L, Puel A, *et al* (2007) TLR3 deficiency in patients with herpes simplex encephalitis. *Science* 317: 1522–1527

Zhu K-Y, Feferman T, Maiti PK, Souroujon MC & Fuchs S (2006) Intravenous immunoglobulin suppresses experimental myasthenia gravis: immunological mechanisms. *J Neuroimmunol* 176: 187–197

Zinkernagel RM & Doherty PC (1974) Restriction of in vitro T cell-mediated cytotoxicity in lymphocytic choriomeningitis within a syngeneic or semiallogeneic system. *Nature* 248: 701–702

LIST OF ALGORITHMS

APPENDIX

Licenses

Figure 2 – Nature Reviews Immunology, License 1615576-1 (Springer Nature BV)

Figure 3 – Journal of Clinical Immunology, License ID 1615576-2 (Springer Nature BV)

Figure 4 – Signal Transduction and Targeted Therapy, License ID 1615576-3 (Springer Nature BV)

Figure 5 – Immunity, License ID 1640139-1 (Elsevier Science & Technology Journals)

Figure 6 – Trends in Immunology, License ID 1615576-4 (Elsevier Science & Technology Journals)

Results – Science Immunology, License ID 1615605-1 (American Association for the Advancement of Science)

Figure 7 – Cell Death and Differentiation, License ID 1615576-5 (Springer Nature BV)

Curriculum Vitae

EDUCATION

09/2018-07/2025 (Expected) **PhD studies in Immunology** at the Medical University of Vienna (Austria).

10/2011-07/2018 **Doctor of General Medicine** (Dr.med.univ., Doctor medicinae universae), Medical University of Vienna (Austria). Thesis: Optogenetic activation of growth factor signaling in a Parkinson's disease cell model**.**

EMPLOYMENT

10/2018-12/2024 **PhD** in the group of **Prof. Kaan Boztug** at St. Anna Children's Cancer Research Institute (CCRI) and CeMM Research Center for Molecular Medicine (CeMM) in Vienna, Austria.
Main lab focus: Genetic diagnosis and description of rare and novel inborn errors of immunity, Paediatric cancer predisposition, development of targeted therapy approaches for immune and haematological childhood disorders.

04/2020-11/2020 **Freelance Contract** to establish and maintain a SARS-CoV-2 Testing pipeline at CeMM.

06/2017-04/2018 **Medical Internships** at Allgemeines Krankenhaus Wien (Austria) in the department of Neurology, Spital Affoltern (Switzerland) in the department of Internal Medicine, Jikei University Hospital (Japan) in the department of Neurosurgery and Royal Melbourne Hospital (Australia) in the department of Neurosurgery.

03/2015-09/2015 **Student Internship,** Institute of Science and Technology Austria (ISTA), Group **Prof. Harald Janovjak,**

08/2011-08/2016 Volunteer at the Red Cross Purkersdorf (Austria) as a paramedic.

01/2011-07/2011 Compulsory military service, trained as a paramedic.

ACHIEVEMENTS- AWARDS, GRANTS

08/2025 International congress of immunology by the International Union of Immunological Societies (IUIS), Vienna (Austria), **Oral Presentation.**

07/2025 Selected for the 2nd European **B Cell Summer School** organized by the European B Cell Network (EBCnet).

02/2025 Keystone Symposia - B Cells: Multifaceted Functions and Dysfunctions, Monte Carlo (Monaco), **Poster** Presentation.

10/2024 European Society for Immunodeficiencies (ESID), Marseille (France), **Oral Presentation**.

01/2023 Contribution to **successful Grant** from the Austrian Science Fund (FWF), Project: Molecular Mechanisms of Non-Coding RNA Dysregulation in Immune Diseases.

11/2022 Undiagnosed Diseases Network International (UDNI), Vienna (Austria) **Poster Presentation**.

04/2022 **Winter School** Writing Retreat and Communication Skills for Research.

05/2020 **Fellowship awarded** from the Austrian Research Promotion Agency (FFG) for the duration of four years.

PUBLICATIONS

1. **B. Ransmayr**, SK. Bal, M. Thian, M. Svaton, C. van de Wetering, C. Hafemeister, A. Segarra-Roca, J. Block, A. Frohne, A. Krolo, MY Altunbas, S. Bilgic-Eltan, A. Kıykım, O. Aydiner, S. Kesim, S. Inanir, E. Karakoc-Aydiner, A. Ozen, Ü. Aba, A. Çomak, G. D. Tuğcu, R. Pazdzior, B. Huber, M. Farlik, S. Kubicek, H. von Bernuth, I. Simonitsch-Klupp, M. Rizzi, F. Halbritter, A. V. Tumanov, M. J. Kraakman, A. Metin, I. Castanon, B. Erman, S. Baris, K. Boztug. LTβR deficiency causes lymph node aplasia and impaired B cell differentiation.
   Sci Immunol. 2024 Nov 22;9(101) PMID: 39576873.

2. SK. Bal, S. Giuliani, J. Block, P. Repiscak, C. Hafemeister, T. Shahin, N. Kasap, **B. Ransmayr**, Y. Miao, C. van de Wetering, A. Frohne, R. Jimenez Heredia, M. Schuster, S. Zoghi, V. Hertlein, M. Thian, A. Bykov, R. Babayeva, S. Bilgic Eltan, E. Karakoc-Aydiner, L. E. Shaw, I. Chowdhury, M. Varjosalo, R. J. Argüello, M. Farlik, A. Ozen, E. Serfling, L. Dupré, C. Bock, F. Halbritter, J. T. Hannich, I. Castanon, M. J. Kraakman, S. Baris, K. Boztug. Biallelic NFATC1 mutations cause an inborn error of immunity with impaired CD8+ T-cell function and perturbed glycolysis.
   Blood. 2023 Aug 31;142(9) PMID: 37249233.

3. J. Block, C. Rashkova, I. Castanon, S. Zoghi, J. Platon, R. C. Ardy, M. Fujiwara, B. Chaves, R. Schoppmeyer, C. I. van der Made, R. Jimenez Heredia, F. L. Harms, S. Alavi, L. Alsina, P. Sanchez Moreno, R. Ávila Polo, R. Cabrera-Pérez, S. Kostel Bal, L. Pfajfer, **B. Ransmayr**, A.-K. Mautner, R. Kondo, A. Tinnacher, M. Caldera, M. Schuster, C. Domínguez Conde, R. Platzer, E. Salzer, T. Boyer, H. G. Brunner, J. E. Nooitgedagt-Frons, E. Iglesias, A. Deyà-Martinez, M. Camacho-Lovillo, J. Menche, C. Bock, J. B. Huppa, W. F. Pickl, M. Distel, J. A. Yoder, D. Traver, K. R. Engelhardt, T. Linden, L. Kager, J. T. Hannich, A. Hoischen, S. Hambleton, S. Illsinger, L. Da Costa, K. Kutsche, Z. Chavoshzadeh, J. D. van Buul, J. Antón, J. Calzada-Hernández, O. Neth, J. Viaud, A. Nishikimi, L. Dupré, K. Boztug. Systemic Inflammation and Normocytic Anemia in DOCK11 Deficiency.
   N Engl J Med. 2023 Aug 10;389(6) PMID: 37342957.

4. SK. Bal, S. Haskoloğlu, **B. Ransmayr**, S. Sevinç, C. İslamoğlu, K. Baskın, B. Savaş, S. Fitöz, A. Küpesiz, T. Kendirli, K. Boztuğ, F. Doğu, A. İkincioğulları. Long term outcome of bone marrow transplantation in NIK Deficiency: Non redundant Role of Non-canonical NF-κB Signaling in Thymic Reconstitution and Secondary Lymphoid Organ Development. ***J. Clin. Immunol.*** (Submitted)

RESEARCH SKILLS

Cell Biology - Isolation and maintenance of primary human cells (monocytes, lymphocytes, fibroblasts); culture and expansion of primary T cells; immortalization of B-LCLs; iPSC culture and differentiation into monocytes and dendritic cells; generation of knock-out and knock-in cells using CRISPR/Cas9.

Cellular Assays –Multicolor flow cytometry and compensation strategies; cell activation, proliferation, apoptosis, and cell cycle assays; cytotoxicity and target cell killing assays; transwell migration assays; design and execution of small-scale drug screens.

Molecular Biology – Isolation and analysis of DNA and RNA from cells and tissues; primer and probe design; PCR, qPCR; molecular cloning, plasmid construction, and DNA sequence analysis.

Biochemistry – Western blotting, gel filtration chromatography; ELISA; multiplex assays including Luminex and Legendplex.

Teamwork – Contributed to numerous published and ongoing research projects in collaborative, interdisciplinary teams.

Organisation – Leadership of an internal taskforce for the genetic investigation of a cohort of patients with early-onset inflammatory bowel disease, tasks included workflow organization and task distribution as well as regular communication and meetings with the treating clinicians.

Presentation and Writing - Regularly presented research at lab meetings, institutional seminars, and high-profile conferences; writing of scientific publications; attended a winter school focused on communication and writing skills for researchers.

Teaching and Supervision – Supervised two visiting graduate students, providing guidance on experimental design, data analysis, and scientific presentation.

Funding Acquisition – Successfully secured a fellowship awarded by the Austrian Research Promotion Agency (FFG); contributed to the development and writing of multiple competitive grant applications.

LANGUAGES AND IT SKILLS

Languages	German – Native Language
	English – Highly proficient; acquired through years of working in English-speaking environments and several international internships
	Spanish – Basic knowledge
IT	Microsoft Office, GraphPad/Prism, Adobe Illustrator, Flowjo. Basic programming skills using Python.